

**WestminsterResearch**

<http://www.westminster.ac.uk/westminsterresearch>

**An In Vitro 3D Model to Evaluate Behaviour of Breast Cancer  
Cells and Response to Treatment**

**Azimi, T.**

This is an electronic version of a PhD thesis awarded by the University of Westminster.  
© Miss Tayebah Azimi, 2019.

---

The WestminsterResearch online digital archive at the University of Westminster aims to make the research output of the University available to a wider audience. Copyright and Moral Rights remain with the authors and/or copyright owners.

---

Whilst further distribution of specific materials from within this archive is forbidden, you may freely distribute the URL of WestminsterResearch: (<http://westminsterresearch.wmin.ac.uk/>).

In case of abuse or copyright appearing without permission e-mail [repository@westminster.ac.uk](mailto:repository@westminster.ac.uk)

**AN IN VITRO 3D MODEL TO EVALUATE  
BEHAVIOUR OF BREAST CANCER CELLS AND  
RESPONSE TO TREATMENT**

**TAYEBEH AZIMI**

A thesis submitted in partial fulfilment of the requirements of the  
University of Westminster for the degree of Doctor of Philosophy

May 2019

## **Author's declaration**

I declare that the work presented was carried out in accordance with the guidelines and regulations of the University of Westminster. The work is original except where indicated by reference in the text.

The submission as a whole or part is not substantially the same as any that I previously or am currently making, whether in published or unpublished form, for a degree, diploma or similar qualification at any university or similar institution.

Until the outcome of the current application to the University of Westminster is known, the work will not be submitted for any such qualification at another university or similar institution.

Any views expressed in this work are those of the author and in no way represent those of the University of Westminster.

**Signed**

**Date: 27<sup>th</sup> May 2019**

## Abstract

The field of 3D culture models of disease has started to move towards systems that aim to recapitulate the complexity of human tissues. However, despite recent improvements, current 3D systems remain overly simplistic, lacking the biophysical characteristics and diverse structures found in most organs.

In this project, the cellular behaviour of breast cancer and their responsiveness to chemotherapeutic agents were evaluated under different 3D cell culture conditions. MDA-MB231 and SKBR3 cells were prepared as spheroids using ultra-low attachment plates and as 'artificial cancer masses' (ACM) by embedding cells in a dense collagen type-I. The ACMs were maintained under flow (150  $\mu\text{L}/\text{min}$ ) and flow/pressure (550  $\mu\text{L}/\text{min}$ ,  $\sim 19$  mmHg) conditions. A significant reduction in cell viability was observed when cancer cells were grown as ACM compared to 2D culture. Cell viability also declined significantly when ACMs were maintained in flow/pressure condition compared to static condition. Similarly, an increase in the expression levels of markers of EMT was observed when cells were cultured as ACM. However, compared to static 3D incorporation of flow and pressure was associated with decreased expression levels of vimentin, HIF1- $\alpha$ , whilst MMP14 expression increased and snail remained unchanged. HER2 levels were increased in SKBR3 when the cells were cultured under flow/pressure (1.5 fold) compared to static condition. Overall, cells cultured as ACMs exhibited reduced responsiveness to doxorubicin compared to those grown in the conventional 2D culture. A decrease sensitivity was also observed in 3D/flow/pressure and 3D/flow compared to 3D/static condition.

The results obtained in this study show that cancer cell behaviour and their response to therapeutic agents are affected by different microenvironments. Therefore, a new generation of 3D in vitro models need to be developed as pre-clinical drug testing platforms.

**Dedicated**

**To**

My Beloved Parents

## Acknowledgments

First and foremost, I would like to thank my supervisor Dr Miriam Dwek for her undivided support. Miriam, I will never forget the first exciting moments you were talking about this project and I was seeing my dreams coming true. Thank you for giving me this opportunity to work on this project. I would also like to thank my second supervisor Dr Anatoliy Markiv for his helpful guidance and support.

I would like to extend my gratitude to the UCL team for the assistance and their support during challenging times, in particular Professor Marilena Loizidou who was always there to encourage me and guide me in the right direction. Special thanks also to Katerina Stamati and Judith Pape for welcoming me into their team and offering me their technical experiences and knowledge.

A very special thanks to Dr Hazel Welch for kindly providing fibroblast cells.

I would also like to thank my lab partners, Dr Carlos Balcazar Lopez and Dr Diluka Peiris who supported me at the beginning of my time at the university. Carlos, thank you for being so supportive and for your helpful feedback on my thesis. I am extremely grateful to Dr Louise Usher who always gave me helpful advice and kindly reviewed my thesis. Special thanks to Nasrin Nuri A. Berruien for her help in qPCR troubleshooting.

I highly appreciate the support from Cavendish Research Scholarship for giving me this golden opportunity to embark on a PhD.

A very special thanks to Professor Tajali Keshavarz for inspiring me as a scientist and for supporting me in all stages of my PhD.

Finally, I would like to thank my partner and sisters for encouraging me to successfully finish this research.

## List of abbreviations

ACM	artificial cancer mass
ATCC	American Type Culture Collection
AR	Androgen receptor
CAFs	cancer associated fibroblasts
CAM	cell adhesion molecule
ECM	extracellular matrix
EGFR	epidermal growth factor receptor
EMT	epithelial mesenchymal transition
ER	oestrogen receptor
FSP1	fibroblast-specific protein 1
HER2	human epidermal growth factor receptor 2
IAPs	inhibitor of apoptosis proteins
IHC	immuno-histochemistry
IF	intermediate filament
IFF	interstitial fluid flow
IFP	interstitial fluid pressure
MET	mesenchymal epithelial transition
MMP	matrix metalloprotease
MT1-MMP	membrane type 1 matrix metalloprotease
NF	normal fibroblast
PDX	patient-derived tumour xenografts
PR	progesterone receptor
qRT-PCR	quantitative real time polymerase chain reaction
RGD	tripeptide Arg-Gly-Asp
RTK	receptor tyrosine kinases
TAMs	tumour-associated macrophages

TGF- $\beta$	tumour growth factor $\beta$
TNBC	triple negative breast cancer
TUNEL	terminal nucleotidyl transferase-mediated nick end labeling
TSA	tumour specific antigen
VE-cadherin	vascular endothelial cadherin

## Table of contents

Abstract.....	i
Dedicated.....	ii
Acknowledgments.....	iii
List of abbreviations .....	iv
List of figures.....	x
List of tables.....	xvi
1    CHAPTER 1 INTRODUCTION .....	1
1.1    Breast Cancer Epidemiology .....	2
1.2    Breast cancer subtypes .....	2
1.2.1    Luminal tumours .....	4
1.2.2    HER2 over-expressing breast tumours.....	4
1.2.3    Triple negative breast cancer subtype .....	5
1.3    Breast cancer hallmarks, biomarkers and subtypes .....	6
1.3.1    Genome instability and gene mutation.....	7
1.3.2    Supporting proliferative signalling .....	8
1.3.3    Invasion and metastasis .....	10
1.3.4    Detachment of cancer cells from the primary tumour.....	10
1.3.5    Epithelial mesenchymal transition (EMT).....	13
1.3.6    Hypoxia and EMT .....	19
1.3.7    Tumour cell invasion into the surrounding tissue .....	19
1.3.8    Resistance to cell death.....	21
1.4    Tumour microenvironment.....	22
1.4.1    Biochemical phase of the tumour microenvironment .....	23
1.4.2    Interstitial fluid flow and pressure.....	26
1.4.3    Interstitial flow and progression of cancer.....	31
1.5 <i>In vivo</i> models of breast cancer .....	32
1.6 <i>In vitro</i> tissue culture models of breast cancer .....	34
1.7    Naturally derived matrix materials.....	36
1.8    Doxorubicin and resistance to therapy.....	38
1.9    Aims and objectives .....	41
2    CHAPTER 2 MATERIAL AND METHODS .....	42

2.1	Materials and equipment.....	43
2.1.1	General reagents, buffers and other chemicals .....	43
2.1.2	Media, buffers, reagents and consumables used in cell culture, cell harvest and cell lysate processes .....	43
2.1.3	Kits.....	43
2.1.4	Electrophoresis buffers and reagents .....	44
2.1.5	Western blotting reagents.....	45
2.1.6	Antibodies.....	45
2.1.7	Doxorubicin.....	46
2.2	Methods.....	46
2.2.1	Cell culture.....	46
2.2.2	Immunostaining .....	53
2.2.3	Harvesting cancer cells for gene and protein analysis.....	55
2.2.4	Cell lysate preparation for SDS-PAGE.....	56
2.2.5	Bicinchoninic acid (BCA) Protein assay.....	56
2.2.6	SDS polyacrylamide gel electrophoresis (PAGE) .....	57
2.2.7	Coomassie Brilliant Blue staining of protein gels .....	58
2.2.8	Western Blotting (wet blot).....	59
2.2.9	Gene expression analysis.....	60
2.2.10	Alamar blue cell viability assay .....	64
2.2.11	Drug treatment in 2D and 3D.....	66
2.3	Statistical Tests.....	66
CHAPTER 3 RESULT.....		67
3.1	Viability of cancer cells cultured in 2D and 3D .....	68
3.2	Ki67 mRNA expression in 2D and 3D cell culture.....	71
3.3	Investigating hypoxia status by measuring HIF-1 $\alpha$ mRNA expression .....	72
3.3	EMT mRNA expression levels in MDA-MB231 .....	74
3.4	Western blot analysis and immunostaining for vimentin protein in MDA-MB231 cells.....	75
3.5	Expression of HER2 in SKBR3 cells cultured in 2D and 3D .....	78
3.6	Western blot analysis and immunostaining of HER2 protein in SKBR3 cells.....	79
3.7	mRNA expression of apoptosis-related genes.....	81
3.8	Efficacy of doxorubicin in 2D and 3D culture.....	83
3.9	Cell aggregates and invasion bodies formed in static and flow/pressure conditions.....	85
3.10	Comparing cell viability of cancer cells in static and flow/ pressure.....	88

3.11	Ki67 mRNA expression level in the cancer cells cultured in static and dynamic conditions .....	90
3.12	Hypoxia status of the cells grown in 3D/static and 3D/dynamic conditions.....	92
3.13	EMT marker expression in MDA-MB231 cultured in static and dynamic conditions .....	94
3.14	Western blot and immunostaining of vimentin protein in MDA-MB231 cells cultured in static and flow/pressure condition .....	96
3.15	Expression of HER2 in SKBR3 cells cultured in 3D/static and 3D/flow/pressure conditions.....	98
3.16	Immunostaining of SKBR3 cells against HER2 antibody .....	99
3.17	mRNA expression of apoptosis-related genes in breast cancer cells cultured in 3D/static and 3D/dynamic conditions .....	99
3.18	Sensitivity to doxorubicin in breast cancer cells cultured in 3D/static and 3D/dynamic conditions.....	102
3.19	Expression of EMT markers in presence of flow and normal fibroblasts .....	104
3.20	MDA-MB231 invasion in ACMs with and without normal fibroblasts .....	106
CHAPTER 4 DISCUSSION.....		108
4.1	Breast cancer cell viability, proliferation and apoptosis.....	109
4.1.1.	Cellular viability in 3D cell culture compared with conventional 2D cell culture.....	109
4.1.2.	Cellular viability and colony morphologies of the cells grown in 3D culture and in the presence of fluid flow.....	112
4.2.	Epithelial mesenchymal transition (EMT) of breast cancer cells grown under different conditions.....	116
4.2.1.	EMT of breast cancer cells maintained in 3D cell cultures compared with conventional 2D cell culture.....	116
4.2.2.	EMT of 3D cell cultures in the presence of fluid flow .....	120
4.3.	The effect of cell culture conditions on HIF-1 $\alpha$ expression levels in breast cancer .....	122
4.3.1.	HIF-1 $\alpha$ expression of breast cancer cells in 3D cell culture .....	123
4.3.2.	HIF-1 $\alpha$ expression of 3D cell cultures in the presence of fluid flow	123
4.4.	The effect of culture conditions on HER2 expression of SKBR3 cells .....	124
4.4.1.	HER2 expression of breast cancer cells in 3D cell culture.....	125
4.5.	Efficacy of doxorubicin under different culture conditions .....	127
4.5.1.	Efficacy of doxorubicin when breast cancer cells are cultured in 3D	128

4.5.2. Efficacy of doxorubicin when breast cancer cells were cultured in the presence of fluid flow .....	130
4.6. Addition of fibroblasts to breast cancer cell cultures .....	132
Future perspectives .....	134
Conclusion .....	136
References.....	137
Appendices .....	157

## List of figures

- Figure 1.** Schematic view of the main steps of the metastatic process (Reymond et al., 2013). Step 1: Tumour cells lose their adherent traits and gain mesenchymal invasive phenotype. Step 2: Tumour cells enter the blood circulatory system through intravasation reaching capillaries or vasculature. Step 3: Cells disseminate systemically throughout the body through the circulatory system blood and are arrested at the capillaries at the organ of the site of the distant metastasis. Step 4: Tumour cells cross the endothelial barrier at the organ through a process of extravasation. Step 5: Cancer cells undergo mesenchymal epithelial transition (MET) in a tissue which is appropriate for their growth. .... 12
- Figure 2.** Schematic diagram showing changes in cellular structure accompanying the epithelial-mesenchymal transition (EMT). Left to right: epithelial cells lose their characteristic cuboidal shape and adopt a fibroblast-like structure. EMT is accompanied by a loss of adherent traits and a gain in markers and phenotype that facilitate cellular migration. Expression levels of the underlined markers were studied in this project..... 18
- Figure 3.** Figure 3. Biochemical and biomechanical components of the tumour microenvironment exert effects on the cancer cells and influence the behaviour of other infiltrating and tissue-resident cells. The role of tissue flow and interstitial fluid pressure on cellular behaviour is less well understood but indicated in the figure. Adapted from (Leyva-Illades et al., 2012) and modified by the author. .... 25
- Figure 4.** Interstitial fluid pressure (IFP) in human tumours and normal tissues. Previous studies indicated significant increase in IFP level in the solid tumours. The data were aggregated from previous studies (Goel et al., 2011). .... 29
- Figure 5.** Co-clinical trial paradigm (Nardella et al., 2011). .... 33
- Figure 6.** The components of the tumour microenvironment contribute to environment-mediated drug resistance. A fraction of tumour cells which interact with microenvironmental factors, survive treatment. These cells remain as minimal residual disease (not shown). Over time, more mutations occur, resulting in more complicated and a diverse resistance-acquired phenotype which ultimately results in disease recurrence with lower chance of response to therapy. Therefore, developing therapeutic agents that disrupt the interaction between cancer cells and microenvironmental factors can reduce the chance of cancer recurrence. .... 40
- Figure 7.** The preparation of the 3D ‘artificial cancer mass’ (ACM) used in this study. Panel A: Breast cancer cells were mixed with rat tail type-I collagen. To provide a dense ‘cancer mass’ the RAFT system (Lonza, U.K.) was used to absorb significant, reproducible, quantities of liquid away from the cell culture/collagen mixture. This enabled the formation of a dense cancer mass (RAFT gel). The

RAFT gel was then embedded in a cell-free looser rat tail type-I collagen matrix and absorbers were applied to remove further liquid resulting in a final thickness ACM of 100  $\mu\text{m}$ . Panel B: Fibroblasts were embedded in rat tail type-I collagen in a 24-well plate format. After the gel had solidified, an absorber was applied to remove the liquid. The system is based on Nyga et al., 2013. .... 49

**Figure 8.** The flow system developed and utilised in this project. Panel A: schematic view of the Quasi Vivo QV500 with implementation of the flow restrictors enabling an increase in the fluid pressure. Panel B: the bioreactor with artificial cancer masses, ACM, in each of the chambers, a pressure of 1.6 mm Hg was generated by use of the Masterflex peristaltic pump housed at 37°C, in a humidified 5% v/v CO<sub>2</sub>, atmosphere..... 52

**Figure 9.** Phenotype of MDA-MB231 and SKBR3 breast cancer cells grown in 2D monolayer and 3D. The artificial cancer mass (ACM) was prepared using collagen type-I with the RAFT system. The ACM was imaged on the first day, after seeding with cells, using the inverted light microscope. The images show that although MDA-MB231 and SKBR3 have different phenotypes in 2D culture: MDA-MB231 cells, panel a) are more spindle and SKBR3 cells, panel b) are more rounded; they adopt a similar phenotype, panel c) and panel d) both rounded when grown in a 10% dense collagen type-I as ACM. However, as can be observed in panel e) MDA-MB231 cells of ACM regain a spindle-like phenotype when they invade towards acellular collagen (surrounding stroma), image was taken on day 14..... 69

**Figure 10.** reduction of alamar blue reagent indicating the metabolic activity of MDA-MB231 and SKBR3 cells grown over a 7-day period in 2D or in 3D (ACM). Overall, the rate of increase in metabolic activity reduced in both cells grown in 3D compared to 2D. Mean average values  $\pm$  SD (n=3)..... 70

**Figure 11.** Quantification of Ki67 mRNA expression level in MDA-MB231 and SKBR3 cells cultured in 3D (ACM) and 3D (spheroid) relative to 2D culture. Ki67 mRNA level increased significantly when cells were cultured as spheroids compared to 2D culture. However, its expression decreased significantly when cells were grown in collagen matrix (ACM). The experiment was performed using quantitative real time PCR technique and mRNA expression levels were normalised with GAPDH as reference  $\Delta\Delta\text{CT}$  was calculated by subtracting  $\Delta\text{CT}$  2D culture (control) from  $\Delta\text{CT}$  of each culture condition.  $R = 2^{-\Delta\Delta\text{CT}}$ , corresponds to the fold change. Data presented is mean average  $\pm$  SD (n = 3). Asterisks denote significant differences in gene expression, paired Student's t-test; \*P < 0.05; \*\*P < 0.01; \*\*\*P < 0.001..... 72

**Figure 12.** Quantification of HIF-1 $\alpha$  mRNA expression levels in MDA-MB231 and SKBR3 cells cultured in ACM and spheroid relative to its level in 2D culture after a week. HIF-1 $\alpha$  mRNA expression level increased significantly when both cells grown in spheroid format

compared to 2D culture. Its expression also increased significantly when SKBR3 cells cultured in collagen matrix. The experiment was performed using quantitative real time PCR technique and mRNA expression levels were normalised with reference to GAPDH.  $\Delta\Delta CT$  was calculated by subtracting  $\Delta CT$  2D culture (control) from  $\Delta CT$  of each culture condition.  $R = 2^{-\Delta\Delta CT}$ , corresponds to the fold change. Data presented are mean average values  $\pm$  SD (n=3). Asterisks denote significant differences in gene expression, paired Student's t-test; \*P <0.05. .... 73

**Figure 13.** Quantification of expression level of the genes involved in EMT in MDA-MB231 cells cultured in 3D (ACM) and 3D (spheroid) relative to 2D culture. The expression levels of MMP14, snail and cadherin 11 increased significantly when cells were grown as spheroid. The mRNA expression of MMP14 and snail 1 also increased in cells grown in collagen matrix while cadherin 11 expression showed a significant reduction compared to 2D condition. Vimentin mRNA expression increased slightly in 3D spheroid and ACM culture compared to 2D condition (non-significant). The experiment was performed using quantitative real time PCR technique and mRNA expression levels were normalised against GAPDH.  $\Delta\Delta CT$  was calculated by subtracting  $\Delta CT$  2D culture (control) from  $\Delta CT$  of each culture condition.  $R = 2^{-\Delta\Delta CT}$ , corresponds to the fold change. Data presented are mean average values  $\pm$  SD (n=3)..... 75

**Figure 14.** Analysis of level of vimentin protein in MDA-MB231 cells grown in 2D and 3D (ACM) culture. Panel a) Western blot analysis of vimentin protein in MDA-MB231 cells grown in 2D and 3D (ACM) cultures. 10  $\mu$ g protein was loaded in each well. GAPDH antibody was used as loading control. Vimentin protein level increased in the presence of collagen compared to 2D. Panel b) Immunofluorescent staining of MDA-MB231 using vimentin antibody. Left panel, taken using confocal microscopy, shows MDA-MB231 cells grown in 2D and stained with To-pro-3 (blue) and vimentin antibody (green). Right panel, taken using fluorescent microscope, shows MDA-MB231 cells grown in ACM and stained with DAPI (blue) and vimentin antibody (green). The cell aggregates formed in collagen expressed almost the same amount of vimentin protein as they do in 2D culture. Representative images taken from n=3 experiments. .... 77

**Figure 15.** Quantification of HER2 mRNA expression in SKBR3 cells cultured as ACM and spheroid relative to its expression in cells grown in 2D condition. HER2 expression increased significantly in cells grown as spheroid and ACM compared to 2D culture. The experiment was performed using quantitative real time PCR and mRNA expression levels normalised against GAPDH.  $\Delta\Delta CT$  was calculated by subtracting  $\Delta CT$  2D culture (control) from  $\Delta CT$  of each culture condition.  $R = 2^{-\Delta\Delta CT}$ , corresponds to the fold change. Data presented: mean average  $\pm$ SD (n=3). .... 78

- Figure 16.** HER2 protein level in SKBR3 cells grown in 2D and 3D (ACM) condition. Panel a) Western blot analysis of HER2 protein in SKBR3 cells grown as 2D or 3D (ACM) cultures. 10 µg protein was loaded in each well. GAPDH antibody was used as loading control. Panel b) Immunofluorescent staining of SKBR3 using HER2 antibody. Left picture, taken using confocal microscopy, shows SKBR3 cells grown in 2D and stained with To-Pro-3 (blue) and HER2 antibody (green). The middle image shows SKBR3 cell aggregates in ACM imaged using confocal microscope. The right image, taken using Zeiss Apo Tom 0.2 fluorescent microscope, shows SKBR3 cells grown in ACM and stained with DAPI (blue) and anti-HER2 antibody (green). The images indicated the presence of HER2 protein in SKBR3 cells cultured in 2D and 3D collagen matrix. Representative images taken from n=2 experiments imaged in triplicate..... 80
- Figure 17.** Relative quantification of apoptosis related genes in MDA-MB231 and SKBR3 cells cultured in 2D and 3D. The results indicated that BCL2 anti-apoptotic gene was upregulated in both cells when they were grown in 3D (ACM) condition compared to 2D condition. Transcriptional expression of indicated genes was measured by real-time qPCR. mRNA expression levels were normalised against GAPDH.  $\Delta\Delta CT$  was calculated by subtracting  $\Delta CT$  2D culture (control) from  $\Delta CT$  of each culture condition.  $R = 2^{-\Delta\Delta CT}$ , corresponds to the fold change. Data were presented as mean average  $\pm$  SD (n=3)..... 82
- Figure 18.** The cytotoxic effect of doxorubicin on MDA-MB231 and SKBR3 cells cultured in 2D and 3D. Both cell types showed less sensitivity to specific concentrations of doxorubicin when they were grown in 3D collagen matrix (ACM) compared to 2D condition. Three wells were assessed for each concentration. Data were presented as mean  $\pm$  SD (n = 3)..... 84
- Figure 19.** Microscopic images of the aggregates of MDA-MB231 (left panel) and SKBR3 (right panel) cells cultured in 3D (ACM) and maintained in static (top panel) and flow/pressure (bottom panel) for 2 weeks (MDA-MB231) and 1 week (SKBR3) using Apo Tom 0.2 microscope..... 86
- Figure 20.** Nuclei of MDA-MB231 cells in ACM stained with DAPI. ACMs were maintained for a month under static and flow/conditions. Four images were taken of each quarter using the 2.5x objective of the Apo Tom 0.2 microscope. These images were then used to create the collages above. MDA-MB231 cells were dispersed more evenly over the ACM area while the shape of the invasion bodies was more organised in static conditions. There was no significant difference between distribution of SKBR3 cells in both conditions..... 87
- Figure 21.** The effect of fluid flow and pressure on cell viability when cells are grown in 3D under static and flow conditions, measured by Alamar blue assay. Upper graph, MDA-MB231 cells grown over a 14-day, bottom graph, SKBR3 grown over a 7-day period. Both cell types were less metabolically active in the presence of flow and

pressure compared to static condition. Data presented are mean average  $\pm$  SD (n=3). ..... 89

**Figure 22.** Relative quantification of Ki67 gene expression levels in MDA-MB231 and SKBR3 cells cultured in static and flow/pressure conditions. Ki67 mRNA level of both cell types increased significantly in the presence of flow and pressure compared to static condition.  $\Delta\Delta CT$  was calculated by subtracting  $\Delta CT$  2D culture (control) from  $\Delta CT$  of each culture condition.  $R = 2^{-\Delta\Delta CT}$ , corresponds to the fold change. Data is mean average  $\pm$  SD (n=3). ..... 91

**Figure 23.** Relative quantification of HIF-1 $\alpha$  mRNA expression levels in MDA-MB231 cells cultured in 3D static, 3D flow and 3D flow + pressure after 2 weeks. HIF-1 $\alpha$  expression increased significantly in flow condition compared to static condition however it remained unchanged in flow + pressure. The experiment was performed using quantitative real time PCR and mRNA expression levels were normalised against GAPDH.  $\Delta\Delta CT$  was calculated by subtracting  $\Delta CT$  static culture (control) from  $\Delta CT$  of the other culture conditions.  $R = 2^{-\Delta\Delta CT}$ , corresponds to the fold change. Data presented are mean average  $\pm$  SD (n = 3). ..... 93

**Figure 24.** Relative quantification of vimentin, MMP14 and snail1 mRNA expression levels in MDA-MB231 cells cultured in 3D/static, 3D/flow and 3D/flow/pressure after 2 weeks. The experiment was performed using quantitative real time PCR technique and mRNA expression levels were normalised against GAPDH.  $\Delta\Delta CT$  was calculated by subtracting  $\Delta CT$  of static culture (control) from  $\Delta CT$  of each culture condition.  $R = 2^{-\Delta\Delta CT}$ , corresponds to the fold change. Data is mean average  $\pm$  SD (n=3). ..... 95

**Figure 25.** Expression of vimentin protein in MDA-MB231 cell maintained in static and flow + pressure conditions for two weeks. a) Western blot analysis of vimentin protein in MDA-MB231 cells grown in 3D (ACM) and maintained in static and flow + pressure conditions. 10  $\mu$ g protein was loaded in each well. GAPDH antibody was used as loading control. Vimentin protein expression reduced significantly in the presence of flow and pressure compared to static and 2D conditions. b) Immunofluorescent staining of MDA-MB231 grown in ACM using Vimentin antibody (green). Left panel; the edges of ACMs and right panel; the centre the ACMs maintained in static and flow + pressure. The nuclei were stained with DAPI (blue). Images show a significant reduction in Vimentin protein level both at the edge and centre of the ACMs when the cells maintained under flow and pressure condition. Representative images taken from n=2 experiment..... 97

**Figure 26.** Relative quantification of HER2 mRNA expression levels in SKBR3 cells cultured in 3D static and 3D flow + pressure system after a week. The results indicated that HER2 expression upregulated in the presence of flow and pressure compared to static condition. The experiment was performed using quantitative real

time PCR technique and mRNA expression levels were normalised against GAPDH.  $\Delta\Delta CT$  was calculated by subtracting  $\Delta CT$  static condition (control) from  $\Delta CT$  of each culture condition.  $R = 2^{-\Delta\Delta CT}$ , corresponds to the fold change. Data were presented as mean  $\pm$  SD (n = 3). ..... 98

**Figure 27.** Immunofluorescent staining of HER2 proteins in SKBR3 cells grown in different microenvironments: from left to right: 2D, 3D static and 3D flow + pressure. The images show that HER2 protein level remained unchanged in all three conditions. The nuclei were counter-stained with TO-PRO-3 in the case of 2D and DAPI (blue) in static and flow/pressure. Representative images taken from n=3 experiment..... 100

**Figure 28.** Quantification of apoptosis related genes in MDA-MB231 (top graph) and SKBR3 cells (bottom graph) cultured in flow + pressure condition relative to its level in static condition. Caspase 9 mRNA expression increased and BCL2 decreased in both cell types suggesting induction of apoptosis in the presence of flow and pressure. Transcriptional expression of indicated genes was measured by real-time qPCR. mRNA expression levels were normalised against GAPDH.  $\Delta\Delta CT$  was calculated by subtracting  $\Delta CT$  of static (control) from  $\Delta CT$  of each culture condition.  $R = 2^{-\Delta\Delta CT}$ , corresponds to the fold change. Data were presented as mean  $\pm$  SD (n = 3). ..... 101

**Figure 29.** Comparing the cytotoxic effect of doxorubicin on MDA-MB231 and SKBR3 cells grown in different conditions. a) Viability of MDA-MB231 ACMs maintained in 3D low flow with those in 3D static condition. b) Comparing viability of MDA-MB231 cells grown in flow/pressure with those grown in static. c) SKBR3 responses to doxorubicin treatment in flow + pressure and static conditions. The results indicated that the cells are less sensitive to doxorubicin treatment when they were grown in the dynamic (flow and pressure) condition compared to static condition. Two wells were assessed for each concentration and the result is from three experiments. .... 104

**Figure 30.** Relative quantification of vimentin, MMP14, snail1, cadherin 11 and Ki67 mRNA expression levels in MDA-MB231 cells cultured in 3D flow with and without fibroblasts after a week. MMP14 and snail1 mRNA expression increased in the presence of normal fibroblasts (NFs). The experiment was performed using quantitative real time PCR technique and mRNA expression levels were normalised against GAPDH.  $\Delta\Delta CT$  was calculated by subtracting  $\Delta CT$  of flow culture (control) from  $\Delta CT$  of flow + NF condition.  $R = 2^{-\Delta\Delta CT}$ , corresponds to the fold change. Data is presented as single experiment performed in triplicate. .... 105

**Figure 31.** MDA-MB231 grown as ACM with and without normal fibroblasts in the stroma. The cancer cells are in the centre of the ACM and surrounded with normal fibroblast cells. The images show cancer cells invasion towards stroma increases in the presence of

breast-derived fibroblasts. Blue arrows show normal fibroblasts and red arrows are the cancer cells. Black arrows show the migration distance..... 107

## List of tables

<b>Table 1.</b> The key methods developed for the preparation of cancer cell spheroids.....	35
<b>Table 2.</b> Proportion of reagents used for preparation and construction of ACMs.....	47
<b>Table 3.</b> Specification of Quasi Vivo® system .....	51
<b>Table 4.</b> Antibodies used in immunostaining processes.....	54
<b>Table 5.</b> Quantity of reagents used for SDS-PAGE .....	58
<b>Table 6.</b> Cycling conditions for the qPCR analysis .....	63
<b>Table 7.</b> List of primer sequences used for qRT-PCR.....	64

# **CHAPTER 1**

## **INTRODUCTION**

## 1.1 Breast Cancer Epidemiology

Breast cancer is amongst the most common cancers in women and the incidence is increasing globally. There were an estimated 1.4 million new cases diagnosed worldwide in 2008 and nearly 459,000 breast cancer related deaths worldwide (DeSantis et al., 2014). In 2012, the GLOBOCAN project released statistics showing that 1.7 million women were diagnosed and 522,000 succumbed to breast cancer. According to the American Cancer Society, one in eight women in the United States will be diagnosed with breast cancer in her lifetime (Hortobagyi et al., 2005). Furthermore, it has been estimated that the annual worldwide incidence of female breast cancer will rise to approximately 3.2 million new cases by 2050 (Ma and Jemal, 2013). Even though breast cancer incidence is rising worldwide, the figures for developed countries are higher than those for less developed countries. Conversely, the mortality rate is higher in less developed countries partly due to the lack of screening tests and consequential late stage at diagnosis. These trends demonstrate that breast cancer incidence and its effect on society is a worldwide health problem and new diagnostic and therapeutic measures are needed.

## 1.2 Breast cancer subtypes

In any tumour stratification system, important considerations include the origin and histology of the tumour, in breast cancer this includes ductal or lobular cancer and whether the primary tumour is *in situ* or invasive and the extent of any local-regional or distant metastases. In the clinical setting, breast tumours are initially classed into three main subtypes: tumours expressing oestrogen receptor (ER  $\alpha/\beta$ ) and/or progesterone receptor (PR), generally referred to as hormone receptor-positive [HR-positive] tumours, Erb-B2 amplified also known as human epidermal growth factor receptor 2-amplified [human epidermal growth factor-2; HER2-amplified] breast cancer, and a group which

lack expression of the ERs, PR and HER2 called triple-negative breast cancer (TNBC). Recently, based on the gene expression profile of breast cancer tissues, new molecular classifications have been established: luminal A, luminal B, basal-like, HER2-enriched and unclassified or normal breast (Sotiriou et al., 2003, Prat and Perou, 2011). It has been shown that these different subtypes are associated with different prognostic features such as the frequency of ER/PR/HER2 expression, histological grade, p53 mutation status and varying levels of genes of proliferation (Eroles et al., 2012). In addition, stratification of breast cancer to different subtypes has provided a predictive tool for the response to different therapies (Siow et al., 2018). A number of new prognostic approaches using gene profiling platforms have been developed recently. Among these analyses, Oncotype DX and MammaPrint are the most extensively cited and are tools that are being trialled for determining which subgroups of breast cancer patients will respond to hormonal and/or chemotherapy (Van De Vijver et al., 2002, Kittaneh et al., 2013) with the aim of better targeting the treatments. For example, a recent report of the Oncotype DX system with 10,273 early-stage hormone receptor-positive, HER2-negative and axillary node-negative breast cancer patients, with 7.5 years follow-up, showed that an Oncotype DX recurrence score of 11-25 indicated patients for whom the addition of chemotherapy did not improve disease-free survival; in the presence of hormone therapy. The study also revealed a subgroup of patients who did not benefit from post-operative chemotherapy (Oncology, 2018) illustrating the potential for gene-expression profiling for identifying patients likely to benefit from particular treatment regimens.

### **1.2.1 Luminal tumours**

Luminal-like tumours, the most prevalent breast cancer subtype, are positive for hormone receptors in immunohistochemistry (IHC) assessments. The gene expression patterns of these tumours include expression of luminal breast epithelial cell cytokeratins 8/18, ER and genes associated with ER activation such as *LIV1* and *CCND1* and similar to the luminal epithelial cells of normal healthy breast tissue. Luminal tumours are themselves divided into two subtypes: luminal A and luminal B, both subtypes represent ER+, PR+, HER2- breast cancer in the basic clinical assessment. However, some luminal B tumours have also been reported to be HER2+ (Cheang et al., 2009). A key feature of luminal B tumours is increased expression levels of genes associated with cell proliferation (including *MKI67*) and lower expression levels of ER-related genes compared to luminal A. In general, the luminal breast cancer subtype has a good prognosis compared to the other subtypes. Comparing the two subtypes, luminal B carries significantly worse prognosis than the luminal A (Sorlie et al., 2003). Endocrine therapy has been the approved therapeutic strategy for the treatment of both luminal A and B tumours. However, for the luminal B subtype which has higher cell proliferative activity, a combination of hormone therapy and chemotherapy has been shown to be more beneficial (Dai et al., 2015).

### **1.2.2 HER2 over-expressing breast tumours**

HER2 amplification occurs in approximately 20% of invasive breast cancers and is associated with a poorer prognosis and a reduced overall survival. HER2 has been a target for breast cancer therapy (Sjögren et al., 1998) with Trastuzumab (Herceptin), a humanised recombinant antibody which binds to extracellular domain of HER2, having been shown to benefit HER2+ breast cancer patients in combination with chemotherapy (Vogel et al., 2002). Despite all the benefits of Trastuzumab, many HER2 overexpressing breast tumours do not respond to this therapy (clinical benefit rate: 48%) when used as a

single agent, and both acquired and *de novo* resistance has been identified (Vogel et al., 2002). Lapatinib is a dual tyrosine kinase inhibitor that targets both HER2 and HER1 (EGFR) in breast cancer (Xia and Powell, 2002) and Pertuzumab is a monoclonal antibody that blocks dimerisation of HER2 with other HER family members via binding to the dimerisation domain (domain II) of the HER2 extracellular domain which is different to the binding site of Trastuzumab in domain IV (Franklin et al., 2004). Several clinical studies have suggested that a combination of Trastuzumab with either Pertuzumab and/or Lapatinib might be a valuable choice to avoid insufficient sensitivity or resistance to Trastuzumab (MacFarlane and Gelmon, 2011). In addition to these therapeutic strategies, the combination of Trastuzumab with chemotherapeutic agents enhances overall survival and reduces the risk of recurrence and this is considered the gold standard of care for patients with HER2 amplified breast carcinomas (Hudis, 2007).

### **1.2.3 Triple negative breast cancer subtype**

Triple negative breast cancer (TNBC) refers to breast cancers exhibiting low levels of ER, PR and HER2. Epidemiological studies have shown that approximately 20 percent of all breast cancer patients are diagnosed with TNBC worldwide, accounting for approximately 200,000 new cases diagnosed each year (Swain, 2008). The TNBC subtype is more common in women of African descent compared to Caucasians and is also more common in premenopausal women under 40 years of age (Trivers et al., 2009). Based on gene-expression profile studies, TNBC may be stratified to six subtypes: basal-like 1 (BL1), basal-like 2 (BL2), immunomodulatory (IM), mesenchymal (M), mesenchymal stem cell-like (MSCL) and luminal androgen receptor (LAR) (Lehmann et al., 2011). In most of the literature, the basal-like subtype is identical to TNBC. Basal-like breast tumours express markers for basal-type cells and are defined as ER/PR/HER2 negative, CK5/6 positive, and/or positive for EGFR. Breast cancers that are positive for basal cell markers have

been shown to be associated with a poorer prognosis compared to the other TNBC subtypes. However, when treated with adjuvant chemotherapy, patients with basal like breast cancers had improved disease free survival compared to TNBC as a whole (Choi et al., 2010).

To date no targeted therapy for patients with TNBC has been any approved and chemotherapy remains the main treatment for this type of breast cancer. However recent clinical trials have shown promising results using immunotherapeutic methods to target tumour cells that evade the immune system (García-Tejido et al., 2016). For instance, in a phase I clinical trial with metastatic TNBC tumours with positive programmed cell death protein 1 ligand (PD-L1), Pembrolizumab, a monoclonal anti PD-1 antibody was used as a check-point inhibitor to inhibit lymphocyte deactivation. The initial overall responses of 18.5% have been reported in heavily pre-treated TNBC (Nanda, 2014).

### **1.3 Breast cancer hallmarks, biomarkers and subtypes**

Breast cancer has been described as the uncontrollable growth of epithelial cells of the breast tissue (Russo et al., 2000). Over the last three decades, scientists have focussed on the classification of breast cancer based on different traits and, accordingly, breast cancer is no longer considered a single disease in terms of diagnosis and treatment. Indeed, breast cancer is now recognised to be a highly heterogeneous disease. To understand this heterogeneity, scientists have applied many theories to describe breast cancer development; including the cancer stem cell and the clonal evolution hypotheses. Different breast tumour subtypes are associated with different risk factors, histopathological traits, outcome and response to systemic therapies (Dai et al., 2016).

In 2000 Hanahan and Weinberg described six hallmarks of cancer and in 2011 expanded these to include 'genome instability and mutations' and 'tumour-

promoting inflammation' (Hanahan and Weinberg, 2011). These hallmarks of cancer, specifically those related to the aims of this project, will be explained in the following sections.

### **1.3.1 Genome instability and gene mutation**

The preservation of the genome and ensuring genomic stability is vital for cellular integrity, to avoid mistakes arising from endogenous sources of DNA damage. These damages occur through DNA replication, recombination and through reactive oxygen species (ROS) produced during cellular metabolism. Exogenous genotoxic agents including ultraviolet light, ionizing radiation or DNA damaging chemicals can also generate genome instability. Cells activate pathways in response to these potentially deleterious events. For example, they undergo cell cycle arrest to repair acquired damage and stimulate DNA repair pathways, or if the damage is not repairable, mechanisms are activated to induce programmed cell death (apoptosis). Damage/failure of these mechanisms results in both the initiation and the progression of cancer (Nowell, 1976). Genome instability refers to either small structural changes including increased incidences of point mutation, microsatellite instability or substantial structural changes resulting from chromosome instability (Charames and Bapat, 2003). Various guardian genes and molecular pathways are involved in the maintenance of genomic stability including proteins involved in DNA damage check points (e.g. p53 and ataxia telangiectasia-mutated, ATM, protein), as well as several DNA repair pathways including nucleotide excision repair (NER), base excision repair (BER), mismatch repair (MMR) and DNA double strand break repair (DSBR) (Charames and Bapat, 2003). Errors that occur during cell division are also known sources of chromosome instability and a number of mechanisms, known as mitotic checkpoints, serve to monitor the correctness of each stage of the cell cycle before the instigation of nuclear division (Charames and Bapat, 2003).

Amongst all proteins involved in maintaining gene integrity, TP53 has been most studied (El-Deiry, 1998). A multitude of functions have been attributed to *p53* and these have led to the term 'gatekeeper of the genome' in response to the intracellular role of the TP53 protein during cellular stress such as hypoxia, oncogene activation and DNA damage. Dysfunction in *p53/TP53* leads to changes in gene stability and integrity and has been reported to result in uncontrolled proliferative activity of cancer cells. Mutated *p53* has been reported in approximately 25 to 30% of breast tumours and has emerged as an important independent prognostic marker (Børresen-Dale, 2003). It has also been observed that mutations in *p53* may confer drug resistance, for example, to the hormone therapy Tamoxifen. Various studies have also shown that sensitivity of ER-TP53- tumours to chemotherapy is decreased compared to ER-TP53+ tumours (Børresen-Dale, 2003, Lønning et al., 2007). Taken together, the evidence suggests that 'genome instability and mutations' in breast tumour is associated with resistance to conventional treatment strategies.

### **1.3.2 Supporting proliferative signalling**

Oncogenes and tumour suppressor genes are the main regulators of cell growth, proliferation, differentiation and cell death. Mutated oncogenes or tumour suppressor genes play a crucial role in both the initiation and the development of tumours (Ghourab, 1992). The most well-described hormonal and growth receptors that operate cell growth signalling in breast cancer include ER, PR and HER2. These receptors are used as differential markers for the routine subtyping of breast cancer tumours using established IHC staining protocols in pathology laboratories worldwide (Spitale et al., 2008). ERs are nuclear hormone receptors (NHRs) belonging to a large nuclear receptor family and primarily act as transcription factors. ER $\alpha$  is the major ER subtype in the mammary epithelium and is the isoform detected by antibodies used during diagnostic procedures. Approximately 75% of all breast cancer patients are diagnosed with ER $\alpha$  positive breast cancer (Anderson et al., 2002). In comparison with ER- tumours, ER+ tumours show greater

differentiation, are less aggressive, and are associated with better post-surgical outcomes (Dunnwald et al., 2007). Endocrine therapy using Tamoxifen, a selective ER modulator, and aromatase inhibitors, which ablate peripheral estrogen synthesis, has been shown to substantially improve disease-free survival after breast cancer. Although the role of PR in the classification of breast tumours is still questioned, assessment of PR status in such tumours has shown to be helpful for predicting patient benefit from endocrine therapy (Rakha et al., 2007). Endocrine treatment, particularly for metastatic tumours, has shown to be less effective for ER+PR- tumours than ER+PR+ tumours.

Another important family of receptors, upregulated in breast and also other cancers, is the HER family of receptor tyrosine kinases. These receptors span the cell membrane and on binding to extracellular growth factor ligands activate intracellular signal transduction pathways, enabling cells to respond to their environment correctly. This family of protein receptors comprises four members: Erb-B1/EGFR/HER1, Erb-B2/HER2/Neu, Erb-B3/HER3 and Erb-B4/HER4 (Nuciforo et al., 2015).

In addition to ER, PR and HER2, androgen receptor (AR) has also been assessed as a means of classification of different breast cancer subtypes. AR is another member of the family of nuclear steroid hormone receptors and is a transcription factor playing crucial roles in various signalling pathways. Following binding of androgens, including testosterone and dihydrotestosterone, AR translocates to the nucleus where it binds to promoter regions of target genes and activates transcription (Zhu et al., 1999). AR is expressed in 90% of ER positive and 55% of ER negative breast tumours (Ogawa et al., 2008, Hu et al., 2011) and is a potential marker for breast cancer prognostication and also a prospective therapeutic target.

In combination with hormonal receptors, proliferation markers especially Ki67 have been used to predict the outcome of breast cancer treatment. Ki67, encoded by the *MKI67* gene, is present mainly in dividing cells and functions to stabilise the mitotic spindle by recruiting Hk1p2 (kinesin-12) to mitotic chromosomes (Vanneste et al., 2009). In another classification of

ER+PR+HER-, Ki67 positivity was shown to relate to poorer outcome regardless of the choice of systemic therapy (Cheang et al., 2009). Expression levels of topoisomerase II alpha (TOP2A) which plays a crucial role in the relaxation of supercoiled DNA is also associated with Ki67 levels (Mueller et al., 2004). HER2-amplified breast tumours with aberrations in the TOP2A biomarker have been reported to be more responsive to anthracycline-based chemotherapy (Ejlertsen et al., 2009). Overexpression of other proliferation markers including cell cycle genes has been reported as an indicator of poor clinical outcome in ER+PR+ tumours (Loi et al., 2007).

### **1.3.3 Invasion and metastasis**

Metastasis occurs when primary tumour cells migrate and invade into surrounding blood or lymphatic vessels through the process termed intravasation. Through this process some of tumour cells circulate via the vasculature, evading immune recognition, and colonise distant organs through the process known as extravasation (Hunter et al., 2008). Many of the cellular and molecular traits that are key to this process have been documented. Amongst all steps of the molecular and cellular cascade involved in metastasis, depicted in Figure 1, two initial steps are the focus of this project and will be described in further detail below.

### **1.3.4 Detachment of cancer cells from the primary tumour**

Primary epithelial cancer cells are attached to each other and also to extracellular matrix (ECM) components through cell adhesion molecules (CAMs). Cadherins, integrins and carcinoembryonic antigen-related cell adhesion molecules (CEACAM) constitute the main groups of CAMs of breast tumours. Integrins are heterodimeric transmembrane receptors with a role in cell-cell and cell-matrix interactions, they also regulate signalling pathways involved in proliferation, migration and survival (Giancotti and Ruoslahti, 1999). Cell-cell interactions and integrin-mediated attachment to the ECM are

crucial factors for proliferation and growth of mammary epithelial cells without which cells would succumb to a form of apoptosis known as anoikis. Integrin receptors are heterodimers, consisting of two subunits:  $\alpha$  and  $\beta$  which assemble noncovalently. In mammals, 24 types of integrin have been reported as a result of assembly of 18  $\alpha$  subunits and 8  $\beta$  subunits (Campbell and Humphries, 2011). Integrins of the breast epithelia act as sensors linking ECM ligands with the intracellular actin cytoskeleton and triggering kinases in the cell.

At least eight integrin receptors have been described as receptors for different molecules of ECM of the mammary gland.  $\alpha1\beta1$ , and  $\alpha2\beta1$  are collagen receptors,  $\alpha3\beta1$ ,  $\alpha6\beta1$ , and  $\alpha6\beta4$  are laminin receptors and  $\alpha5\beta1$ ,  $\alpha v\beta1$ , and  $\alpha v\beta3$  recognise RGD domains of, for example, fibronectin and vitronectin. Integrin receptors can transduce mechanical signals from the ECM to intracellular cytoskeletal proteins for example actin, or in the case of  $\beta4$  integrin, intermediate filament (Lambert et al., 2012). These receptors also transmit biochemical signals through tyrosine kinases such as the focal adhesion kinase (FAK) and/or Src. Integrin receptors and growth factor receptors such as HER2 interact physically and cooperate with each other to activate tyrosine kinase and MAP kinase pathways. In breast cancer, integrins are the key modulator of tumour initiation (Lambert et al., 2012). Deletion of  $\beta1$  integrin in a transgenic mouse model of breast cancer was shown to impede tumourigenesis (White et al., 2004). In a similar study, loss of the cytoplasmic domain of  $\beta4$  integrin in an HER2 overexpressing mouse model increased latency and decreased aggressiveness of ErbB2-induced tumours (Guo et al., 2006).

At the onset of the metastatic process, cancer cells lose their adherence to neighbouring cells in focussed areas of the cells known as adherens junctions, this process is predominantly mediated by alterations in the expression levels of the cadherin family of proteins. A molecular signature of cadherins, notably: E-cadherin (-), N-cadherin (+), cadherin-11 (+), has been shown to be associated with epithelial mesenchymal transition (EMT, section 1.3.5) a phenomenon through which cancer cells gain a mesenchymal phenotype and the ability to move into surrounding tissues (Farahani et al., 2014).

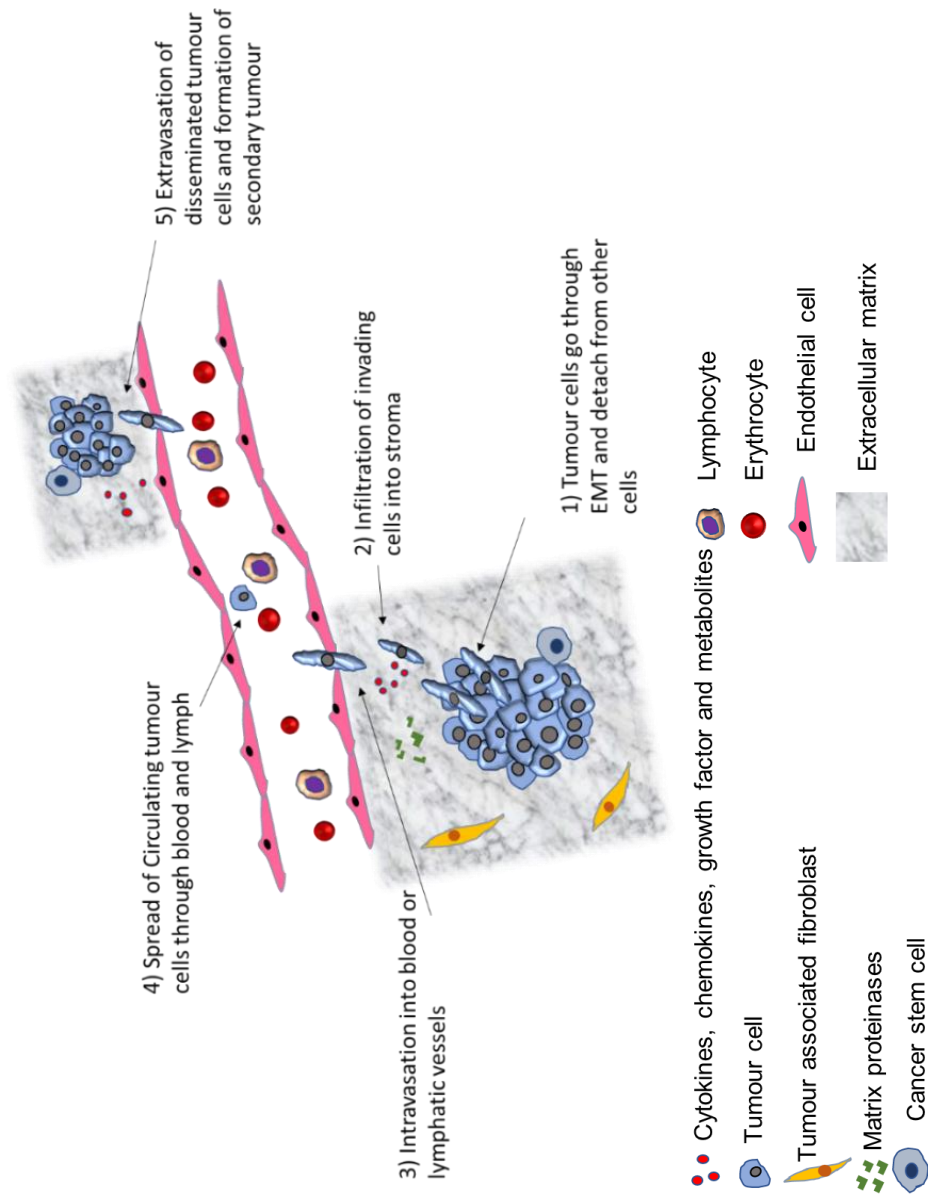


**Figure 1.** Schematic view of the main steps of the metastatic process (Reymond et al., 2013). Step 1: Tumour cells lose their adherent traits and gain mesenchymal invasive phenotype. Step 2: Tumour cells enter the blood circulatory system through intravasation reaching capillaries or vasculature. Step 3: Cells disseminate systemically throughout the body through the circulatory system blood and are arrested at the capillaries at the organ of the site of the distant metastasis. Step 4: Tumour cells cross the endothelial barrier at the organ through a process of extravasation. Step 5: Cancer cells undergo mesenchymal epithelial transition (MET) in a tissue which is appropriate for their growth.

### **1.3.5 Epithelial mesenchymal transition (EMT)**

EMT is a phenomenon through which epithelial cells lose their adherent traits and tight junctions and gain a mesenchymal phenotype, this process results in cells that are able to migrate over distances; Figure 2. Three main types of EMT have been described; type 1: biological events that occur during embryo formation, gastrulation and neural crest migration; type 2: wound healing, tissue regeneration and organ fibrosis, and, type 3: cancer metastasis (Kalluri and Weinberg, 2009). The role of EMT in breast cancer has been investigated via *in vitro* and *in vivo* studies and, taken together, the data suggest that breast cancer cells that undergo EMT exhibit a basal-like phenotype (Sarrió et al., 2008). Several molecular changes have been observed for each type of EMT, some of the changes are common to all types of EMT whilst some are specific to only one type, and these provide a variety of biomarkers enabling studies of EMT. In the following section biomarkers associated with EMT are described in particular those relevant to breast cancer.

#### **1.3.5.1 Cell-membrane markers of EMT**

The cadherin superfamily consists of a group of eight transmembrane proteins contributing to calcium-dependent homophilic and heterophilic cell-to-cell adhesion; cadherins have important roles in the maintenance of cell polarity and are involved in cell motility. Cadherins have been reported to be present in a range of tissues and are classified into three types according to their structural characteristics. Type-I includes epithelial (E-cadherin), neural (N-cadherin), placental (P-cadherin), and retinal (R-cadherin). Type-II include cadherin-11 (OB-cadherin) and vascular-endothelial cadherin (VE-cadherin); they share the same intracellular domain as type-I cadherins but differ in terms of a motif in the extracellular domain. Type-III or 'atypical cadherins' include cadherin-13 and cadherin-15; they lack the transmembrane domain identified in type-I and II cadherins. So far, evidence suggests that cadherin-13 and

cadherin-15 may be defined/considered as tumour suppressor genes. *In vivo* studies with murine tumour models have shown cadherin-13 to be downregulated in all cell types except endothelial cells (Hebbard et al., 2008). Moreover, cadherin-13 expression is repressed in breast cancer cell lines as well as primary breast cancers due to methylation of the promotor (Toyooka et al., 2001). In contrast, cadherin-13 expression is increased in the endothelial cells in breast cancer (Takeuchi et al., 1999). Loss of expression of E-cadherin occurs during all three types of EMT and is considered a hallmark of EMT. In addition to reduced gene expression levels, the loss of function at the protein level has also been associated with promotion of EMT (Okazaki et al., 1994, Huber et al., 2005). Expression levels of E-cadherin are decreased in breast, ovarian, gastric, thyroid and colorectal cancers (Sommers et al., 1989). Upregulation of N-cadherin normally occurs in cells with a mesenchymal phenotype including kidney and brain during development, and in fibroblasts and cancer cells. The upregulation of N-cadherin is accompanied by downregulation of epithelial related cadherins including E-cadherin. In recent studies 'cadherin switching' has been used as a marker to monitor EMT. In addition, a switch from E-cadherin to cadherin-11 has been observed in type 2 EMT accompanying tissue fibrosis. Cadherin-11, is mainly expressed in osteoblasts and to a very low extent in brain, lung and testicular tissue (Okazaki et al., 1994). Pohlodek *et al* have reported that cadherin-11 gene is overexpressed in the samples of invasive breast cancer. In another study led by Huang, cadherin-11 expression in prostate cancer cells was associated with increased invasion and migration as well as interaction with osteoblasts (Huang et al., 2010). Intracardial injection of cadherin-11 expressing prostate cancer cells in a murine model resulted in an increased rate of bone colonisation compared to injection of cadherin-11-knockdown prostate cancer cells (Chu et al., 2008). Similarly, when renal carcinoma cells were implanted into SCID mice, cadherin-11 levels on the surface of cells derived from bone metastases was increased compared to the cells derived from other sites of metastasis (Satcher et al., 2014). Highly metastatic prostate cancer PC3-mm2 cells showed a significant reduction in bone metastasis following the downregulation of cadherin-11 using specific short hairpin RNA (Chu et al.,

2008). These findings have led researchers to develop an antibody against the extracellular domain of cadherin 11, with the aim of reducing cancer metastasis to bone (Lee et al., 2013). In a study, Lee *et al.* produced a panel of 21 antibodies against extracellular domain of cadherin-11 among which two showed promising results for the recognition of an adhesion motif in the extracellular domain of cadherin-11. Their further investigations in which animals were treated with one of those antibodies resulted in a decrease in the metastasis of prostate cancer cells to bone (Lee et al., 2013). In another study by Pishvaian *et al.* (1999), cadherin-11 mRNA and protein levels were reported to be elevated in several invasive breast cancer cell lines including MDA-MB-231, BT549 and HS578T cells. However, there are contradictory data with regards to cadherin-11 expression levels in various cancer studies. In 2012, Li *et al.* reported cadherin-11 status showing that the cadherin-11 promoter is methylated and inactivated in cancer cell lines including nasopharyngeal, esophageal, gastric, hepatocellular, colorectal, breast and cervix. A tumour suppressor function was suggested for cadherin-11 via induction of apoptosis and inhibition of cell migration and invasion through Wnt/  $\beta$ -catenin and AKT/ Rho A signalling.

### **1.3.5.2 Cytoskeletal markers of EMT**

The cytoskeletal proteins most studied in relation to EMT are fibroblast-specific protein 1 (FSP1),  $\alpha$ -smooth muscle actin ( $\alpha$ -SMA), vimentin and  $\beta$ -catenin. FSP1 is a member of the  $\text{Ca}^{+2}$ -binding S100 protein family and is a fibroblast protein detecting both type 2 and type 3 EMT. Increased expression-levels of FSP1 have been observed as part of the type 3 EMT process of metastatic cells in different cancer models (Xue et al., 2003).  $\alpha$ -SMA is a member of the actin family of cytoskeletal proteins. Myofibroblast cells express  $\alpha$ -SMA during type 2 EMT, this contributes to tissue fibrosis. In breast cancer,  $\alpha$ -SMA has been associated with type 3 EMT and  $\alpha$ -SMA has mostly been detected in tumours of the basal phenotype (Sarrió et al., 2008).  $\beta$ -catenin is located on the intracellular side of the cytoplasmic membrane in normal epithelial cells

and in non-invasive cancer cells. Here it plays a role in cell-to-cell adhesion linking cadherin molecules to the actin cytoskeleton; it also has a central role as a transcriptional co-activator in the Wnt signalling pathway (Hatsell et al., 2003). Following activation of Wnt signalling,  $\beta$ -catenin translocates from the cytoplasm to the nucleus, where it regulates several genes promoting invasion, growth and cell transformation including *c-MYC* and *cyclin D1* (Guo et al., 2006). Vimentin, a type-III intermediate filament (IF) is a highly conserved 57-kDa protein. Vimentin IFs are markers of EMT that are constitutively expressed in mesenchymal cells, in endothelial cells lining blood vessels, renal tubular cells, macrophages, neutrophils, fibroblasts, and leukocytes (Kidd et al., 2014). A frequent alteration observed in a range of solid tissue malignancies is a switch in the levels of different types of IFs, for example cytokeratin, to the mesenchymal IF marker vimentin (Palmieri et al., 2003). Vimentin and keratins function to direct different membrane-associated proteins to the membrane (Toivola et al., 2010). Vimentin expression has been shown to be associated with the cellular formation of invadopodia during migratory and invasive processes. For example, when vimentin expression levels were reduced by interfering RNA (siRNA) a significant fall in the generation of invadopodia was observed in MDA-MB231 cells (Schoumacher et al., 2010). It is clear that a multitude of microenvironmental signalling events lead to the induction of EMT; these include TGF- $\beta$ /smad, Notch, Wnt, TNF- $\alpha$ /NF- $\kappa$ B and RTK signalling (Wu and Zhou, 2010). These signals activate several transcription factors such as the snail/sluc family, twist,  $\delta$ EF1/ZEB1, SIP1/ZEB2 and E12/E47. These transcription factors then recruit cofactors and histone deacetylases to E-Box DNA sequences located near the transcription initiation site of E-cadherin. snail was the first transcription factor identified shown to result in repression of transcription of E-cadherin and subsequently a fundamental role has been ascribed to snail in terms of EMT processes (Barrallo-Gimeno and Nieto, 2005). In addition to E-cadherin, snail may down-regulate the expression of epithelial markers including claudins, occludins, and mucin-1, and induce expression of genes activated in mesenchymal and invasive phenotypes (Wu and Zhou, 2010).

Another important class of molecules implicated in physiological and pathological EMT pathways are the matrix metalloproteases (MMP). Over the last three decades, elevated MMP levels have been shown to occur in diverse tissue pathologies, as well as in cancer (Deryugina and Quigley, 2006). Studies of tumour tissue samples from patients have shown a positive relation between tumour metastasis and expression levels of MMP1, -2, -3, -7, -9 and -13, MMPs have also emerged as valuable prognostic factors for solid tumours (Deryugina and Quigley, 2006). Hotary *et al* demonstrated that MT1-MMP, MT2-MMP and MT3-MMP but surprisingly not MMP2 and MMP9 (which are secreted type-IV collagenases) are associated with the breast cancer cell line MDA-MB231 ability to breach the basement membrane. In addition, it has been shown that MT1-MMP is able to degrade the collagen of the interstitial collagen network of the ECM whereas secreted MMPs do not (Hotary et al., 2006). MT1-MMP may utilise fibronectin, vitronectin, laminin-1, fibrin, collagen type-I, collagen type-II, collagen type-III, CD44 and tissue transglutaminase as a substrate. MT1-MMP also contributes to cellular invasion through the activation and reassembly of MMP2. Reduced invasiveness and migratory ability have been observed in genetically modified MDA-MB231 cells whose expression of MT1-MMP was eliminated. Higher expression levels of MT1-MMP has also been correlated with a poorer outcome and shorter disease-free survival of breast cancer patients (Jiang et al., 2006).

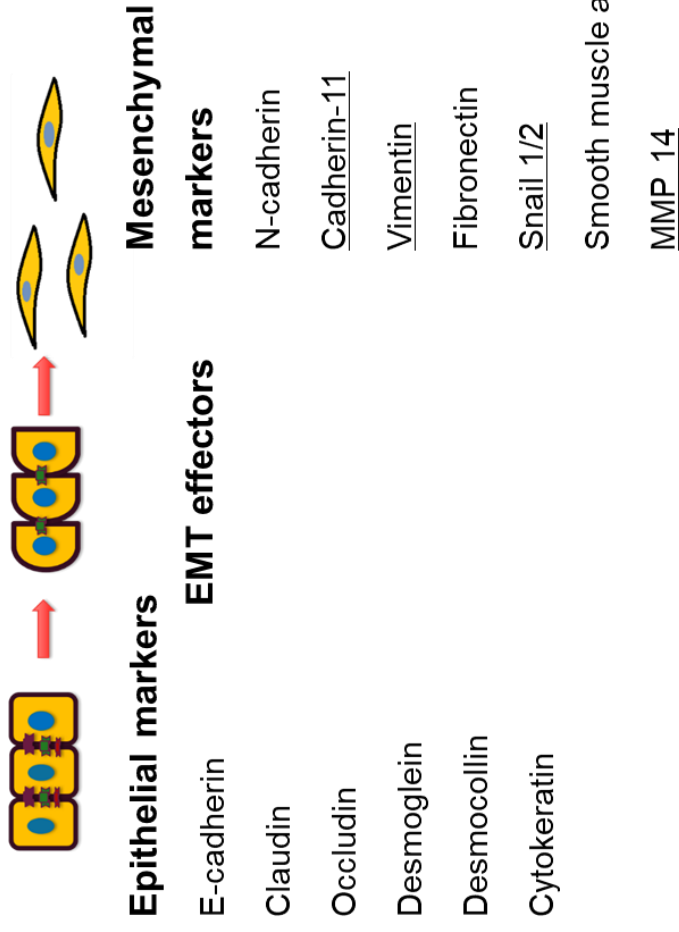


**Figure 2.** Schematic diagram showing changes in cellular structure accompanying the epithelial-mesenchymal transition (EMT). Left to right: epithelial cells lose their characteristic cuboidal shape and adopt a fibroblast-like structure. EMT is accompanied by a loss of adherent traits and a gain in markers and phenotype that facilitate cellular migration. Expression levels of the underlined markers were studied in this project.

### **1.3.6 Hypoxia and EMT**

Recent studies have shown that a hypoxic microenvironment triggers EMT by regulating expression levels of transcription factors including snail, twist, slug and ZEB, and inducing EMT-related signalling pathways including TGF- $\beta$ 1 and NF- $\kappa$ B (Matsuoka et al., 2013, Renaud et al., 2014). HIFs are heterodimeric transcription factors which consist of an  $\alpha$  subunit and a  $\beta$  subunit. Three  $\alpha$  subunits including HIF-1 $\alpha$ , HIF2 $\alpha$ , HIF3 $\alpha$  and two  $\beta$  subunits have been identified. HIF-1 $\alpha$  is a subunit with a 200-amino acid oxygen-dependent degradation domain (ODD) which allows HIF-1 $\alpha$  to be ubiquitinated and degraded by the 26S proteasome in normoxic conditions. Under hypoxic conditions, HIF-1 $\alpha$  gains stability through dimerisation with the HIF-1 $\beta$  subunit and the complex induces transcription of many genes involved in EMT. However, it has been known that HIF-1 $\alpha$  stabilisation is induced by HER2 overexpression and its downstream signalling pathways in non-hypoxic conditions (Laughner et al., 2001, Li et al., 2005). It has been shown that HER2 overexpressing breast cancer cells stabilise HIF-1 $\alpha$  protein through PI3K and AKT pathway in non-hypoxic conditions (Laughner et al., 2001).

### **1.3.7 Tumour cell invasion into the surrounding tissue**

Following the liberation of cells from adherent and tight junctions, they invade and migrate through the surrounding stroma (connective tissue). There are different modes of cellular invasion these include individual, multicellular and collective cellular movement. The migration type and dynamic depends upon characteristics of the tumour microenvironment and the molecular alterations within the tumour (Friedl and Wolf, 2009). According to the type of migration, the cancer cells may display mesenchymal or/and amoeboid-like phenotypes. However, these phenotypes are highly plastic, and transition between them have been observed and reported in previous studies.

In the case of 'single cell invasion' tumour cells with weak cell-cell interactions migrate in a random pattern independently of each other. Individual migrating cells may display an amoeboid-cell-like phenotype characterised by a higher

migratory velocity and a round cell-body phenotype, or a mesenchymal phenotype characterised by an elongated cell-body and relatively slow movement (Clark and Vignjevic, 2015). Transition between mesenchymal and amoeboid phenotypes has been reported.

'Multicellular streaming' is another type of cancer cell migration, this is characterised by two or more tumour cells with either a mesenchymal or an amoeboid phenotype, with loose or non-adhesive properties, migrating along a 'track' in an organised manner. *In vivo* cellular migration of human breast cancer cells was investigated by Patsialou *et al* using intravital multiphoton microscopy. Xenograft tumours of MDA-MB231 and TN1 cells (isolated from a patient with triple negative breast cancer) showed both individual and multicellular movements in both tumour types with a higher overall motility observed for the MDA-MB231 cells. Quantitative analysis revealed that higher movement velocity and longer protrusion distances in 'multicellular streaming' migration compared to random single cell patterns of migration in both tumour types (Patsialou et al., 2013).

In 'collective migration', a group of connected cancer cells detached from the tumour mass, migrate into the surrounding tissues and form chord, stripe and sheet-like structures. This type of invasion has been observed in the progression of several cancers including breast, prostate, colorectal, lung and skin cancers as well as squamous cell carcinoma. Two groups of cells have been distinguished in the collective movement of cancer cells: (1) 'leader' cells, constituting the frontal edge of the invasive mass, often associated with a mesenchymal phenotype and (2) 'follower' cells; located behind the 'leader' cells the 'follower' cells exhibit more intercellular contacts and retain an epithelial phenotype. Cells at the leading edge of the invasion body degrade the extracellular matrix and their intracellular actin-myosin contractile machinery facilitates the migratory process. TGF $\beta$  has been demonstrated to play a role in the switch from collective to single cell invasion modes (Giampieri et al., 2009).

### 1.3.8 Resistance to cell death

Programmed cell death (apoptosis) is an intrinsic mechanism for the maintenance of tissue homeostasis (Kerr et al., 1972). Two pathways are activated during apoptosis: (1) the extrinsic pathway, functioning through death receptors and (2) the intrinsic, mitochondrial, pathway. Initiation of apoptosis through either of the two pathways leads to the activation of cysteine aspartic acid-specific proteases (caspases), a family of conserved cysteine proteases that cleave cytoplasmic and nuclear protein substrates in a tightly regulated proteolytic cascade (McIlwain et al., 2013). Caspases have been classified based on their role in apoptosis and in inflammatory processes. Since the former is the focus of this project, the role of caspase -3, -6, -7, -8 and -9 in apoptotic processes will be explained further in this section. Procaspases are inactive monomeric forms of caspases, activated by dimerisation: caspase -8 and -9; or cleavage: caspase -3, -6 and -7. Caspase -8 and -9 are classified as 'initiator' caspases in recognition of their involvement in cleavage and activation of 'executioner' caspases i. e., caspase-3, -6 and -7. On activation, an 'executioner' caspase activates other 'executioner' enzymes, this gives rise to a feedback loop of caspase activation and rapid cell death. The extrinsic apoptotic pathway is triggered by interaction between death receptors and their ligands, these include tumour necrosis factor (TNF), CD95-ligand (CD95-L; also called Fas-L), TRAIL (also called Apo2-L), and TNF-like ligand 1A (TL1A). The intrinsic pathway is activated by non-receptor-mediated stimuli including cellular stresses, including growth factor deprivation (or lack of apoptotic inhibition), toxins, radiation, DNA damage, hypoxia. Activators of this pathway may include developmental signals that lead the cells to enter apoptosis, and, for example hormones such as corticosteroids and oestrogen (Elmore, 2007, Lewis-Wambi and Jordan, 2009). On exposure to appropriate stimuli, the inner mitochondrial membrane of the cell loses its transmembrane potential and releases pro-apoptotic proteins from the intermembrane space to the cytosol, examples of such pro-apoptotic proteins cytochrome C, Smac/DIABLO, and the serine protease HtrA2/Omi (Saelens et al., 2004). Cytochrome C, apoptotic protease activating

factor (Apaf-1), procaspase 9 and ATP combine to form the apoptosome and this activates caspase 9. Both intrinsic and extrinsic pathways merge at the execution pathway and cleavage of caspase 3 leads to the activation of endonucleases and proteases eventually resulting in cell death. Apoptotic cells are finally engulfed by phagocytic cells, identified by characteristics including DNA fragmentation, hydrolysis of peptide bonds in essential structural and nuclear proteins, cross-linked proteins, formation of apoptotic bodies and expression of ligands for phagocytic cell receptors (Elmore, 2007). A variety of pro-apoptotic and anti-apoptotic/inhibitory factors have been identified that regulate apoptosis. For example, the release of cytochrome C from mitochondria is inhibited by Bcl-2 and Bcl-XL, members of Bcl-2 family of proteins whose expression is regulated by p53. Other regulatory proteins include the inhibitor of apoptosis proteins (IAPs) a family of eight proteins sharing a common domain required for interaction with caspases (Hunter et al., 2007). A member of the IAP family, XIAP has a strong inhibitory effect on apoptosis by binding to activated caspase-3 and -7 and by inhibiting caspase-9 activation (Eckelman et al., 2006). Survivin is another IAP family member shown to have an inhibitory role in regulating apoptosis (Altieri, 2008). The extrinsic pathway triggered through death receptors leads to caspase-8 activation. This pathway is modulated by cellular FLICE-inhibitory protein (cFLIP) which functions by interfering with the recruitment of caspase -8 upon ligand binding to death receptors, thereby preventing caspase-8 activation (Micheau, 2003). A decrease in the levels - or other disfunctions of these inhibitor molecules - may result in faulty cellular apoptotic processes. Different mechanisms that modulate apoptosis and in human cancers have been revealed (Fulda, 2009) and are important as targets for development of novel treatments for cancer (Hassan et al., 2014).

## **1.4 Tumour microenvironment**

The contribution of components of the tumour microenvironment (TME) to the formation, growth, invasion and drug resistance of cancer cells have been

identified and discussed in many cancer studies and is summarised schematically in Figure 3. The focus of this section will be on TME constituents surrounding breast tumours, their possible use as prognostic and predictive markers and their contribution to the therapeutic treatment of the disease

#### **1.4.1 Biochemical phase of the tumour microenvironment**

Cancer cells interact with different components of the tumour microenvironment including cancer-associated fibroblasts (CAFs), cancer-associated adipocytes (CAAs), endothelial cells, ECM, tumour-infiltrating lymphocytes (TILs) and tumour-associated macrophages (TAMs), (Yu and Di, 2017). The ECM is the non-cellular component of the TME and is composed of a complex mixture of macromolecules with different biophysical and biochemical properties (Friedl and Wolf, 2009). These macromolecules include proteins, glycoproteins, proteoglycans and polysaccharides and constitute both parts of ECM; the basement membrane and the interstitial matrix. The former is more compact and porous than the latter and separates the epithelia and endothelia from the stroma and is composed of type-IV collagen, laminins, fibronectin and cross-linker proteins such as nidogen and entactin. In contrast, the interstitial matrix which contributes to the tensile strength of tissues, comprises fibrillar collagens such as type-I, type-II and type-III, proteoglycans and glycoproteins such as tenascin C and fibronectin (Egeblad et al., 2010b). Tissue architecture and integrity are influenced by the physical properties of the ECM including the rigidity, porosity, insolubility and topography. In addition, the ECM functions as a barrier, anchorage site and movement route, impacting cell migration and motility. The TIL population principally includes CD8+ cytotoxic T cells, CD4+ helper T cells and CD4+ regulatory T cells (Tregs). Amongst all of these, the CD8+ T cells have a major influence on the anti-tumour immune response particularly on TNBC tumours (Stanton et al., 2016). The infiltration of TILs at the invasive margin of a tumour Besides infiltrating lymphocytes, tumour-associated macrophages (TAMs) originating from monocytes are recruited by the presence of chemokines such as CCL2 secreted by tumour or stromal cells to the tumour area. The observed

polarised distribution of macrophages within tumours has led to the generation of two specific phenotypes, termed M1 and M2. TAMs exhibit greater differentiation towards the M2 phenotype. Breast cancer cells, for example MDA-MB231 cells, secrete factors that have been shown to promote M2 activation and differentiation. Unlike M1-type macrophages with pro-inflammatory impact and anti-tumour responses, TAMs may also promote an anti-inflammatory phenotype by releasing cytokines, for example IL-8, IL-6 and IL-10 and growth factors and proteases (Solinas et al., 2009). TAMs also facilitate metastasis through their role in inducing angiogenesis, contributing to matrix remodelling, augmenting tumour cell migration and invasion, and promoting an immunosuppressive phenotype (Qian and Pollard, 2010). Cancer-associated fibroblasts (CAFs) are also a significant component of the tumour microenvironment, and this is particularly relevant in breast cancer with intra- and inter-lobular CAFs described (Buchsbaum and Oh, 2016). CAFs have been found to promote cancer initiation, progression, invasion, metastasis, angiogenesis, ECM remodelling, the deposition of basement membrane components, cancer-associated inflammation and the regulation of differentiation events in associated epithelial cells (Luo et al., 2015).

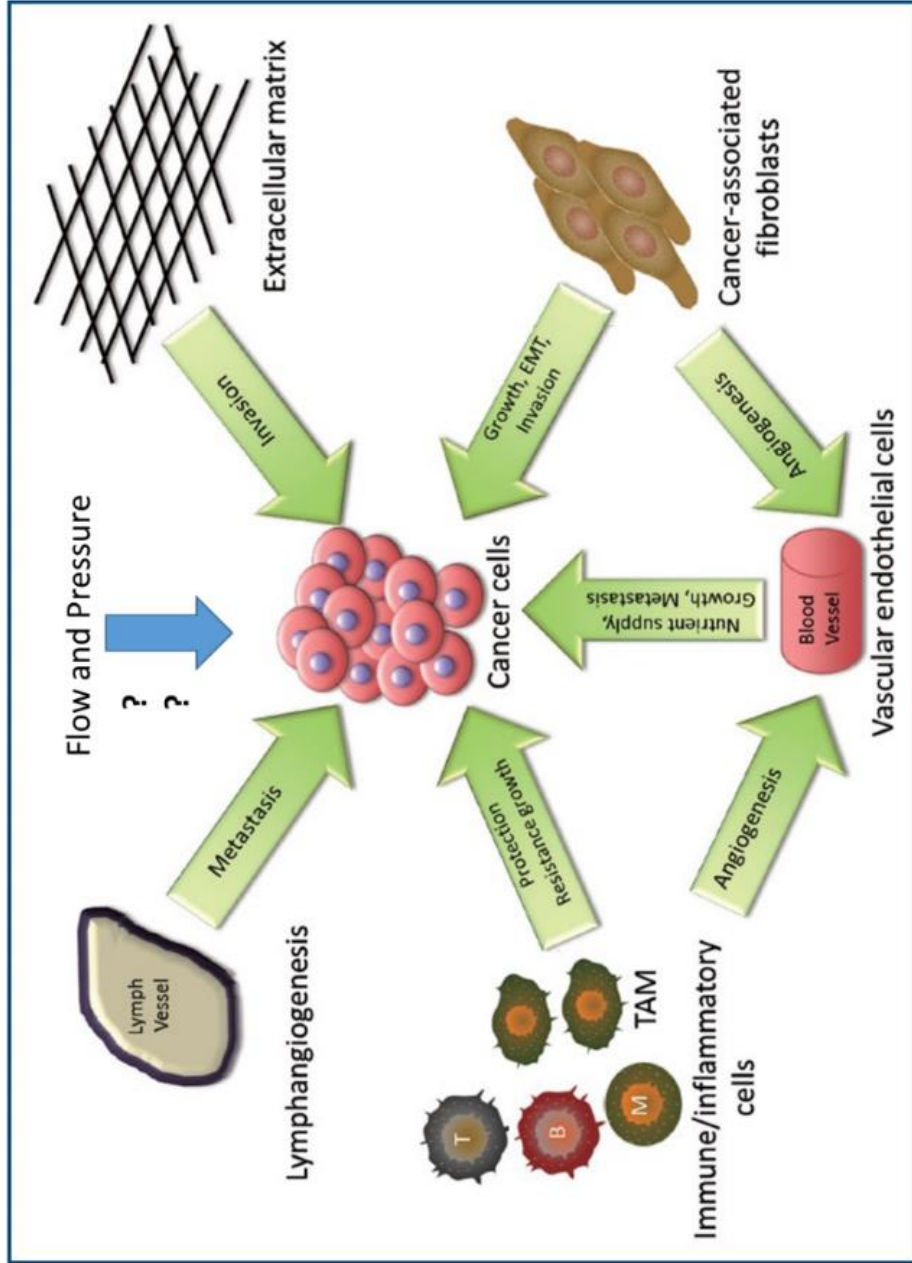


**Figure 3.** Biochemical and biomechanical components of the tumour microenvironment exert effects on the cancer cells and influence the behaviour of other infiltrating and tissue-resident cells. The role of tissue flow and interstitial fluid pressure on cellular behaviour is less well understood but indicated in the figure. Adapted from (Leyva-Illades et al., 2012) and modified by the author.

The interaction between CAFs and different breast cancer subtypes has been studied in several co-culture experiments. Takai *et al* reported that CAFs may increase TNBC progression by activating TGF- $\beta$  (Takai et al., 2016). Upregulation of podoplanin, a lymph vessel marker, was observed in stromal CAFs and was associated with higher grade and TNBC (Niemiec et al., 2014).

Increasingly the data suggests that tumour growth and development may occur through proliferation of breast epithelial cells producing fibroblast growth factor-7 (FGF-7) a potent growth factor for mammary cells (Palmieri et al., 2003). A study of a murine model reported that cancer cell growth enhanced the levels of stromal cell-derived factor 1 (SDF1), a mediator of angiogenesis secreted by CAFs (Orimo et al., 2005). Furthermore, several studies using conditioned media from CAFs as well as direct and indirect co-culture with CAFs, indicated that CAFs induce EMT in breast cancer cells (Dumont et al., 2013, Soon et al., 2013). Contrary to the normal fibroblasts which grow in a mesh-like pattern, breast CAFs deposit ECM in a parallel pattern (Dumont et al., 2013). A shift from epithelial to a mesenchymal phenotype was observed in premalignant breast cancer cells cultured in CAF-deposited ECM. Further analysis of this ECM demonstrated the existence of higher amounts of fibronectin, biglycan (a proteoglycan) and lysyl oxidase (an enzyme involved in ECM remodelling).

#### **1.4.2 Interstitial fluid flow and pressure**

As described above, cells found within the tumour microenvironment have been shown to influence tumour growth and metastasis, however, to paint a complete picture, one also needs to consider alongside the biological phases the biomechanical features of the microenvironment that has been shown to be altered in cancer. The interstitium is composed of two main compartments: interstitial fluid and ECM. Interstitial fluid transports nutrients and waste products between cells and the capillaries and also contains signalling molecules originating in distant organs or, alternatively, locally produced (paracrine and autocrine). In healthy tissue, postcapillary venules reabsorb the

major part of this fluid, and the downstream lymphatic vasculature drains the remaining fraction of the fluid which is ultimately emptied out into the venous bloodstream. However, in solid cancers, increased cell proliferation, alteration in ECM stiffness and architecture, and irregularities in the vasculature arising from the growth of new blood vessels (angiogenesis) results in a malfunction of this well organised system leading to an increased flow rate in tumour tissue. In addition to angiogenesis, lymphangiogenesis occurs in most of solid tumours (Swartz and Lund, 2012). Furthermore, the lymphatic vessels enlarge, and drainage capacity and permeability increase during progression of cancer. However, these alterations cannot effectively balance the increase in fluid exuding from the irregular blood vessels. The impaired clearance of extracellular fluid, a consequence of lack of functional intra-tumoural lymphatic vessels can result in elevated IFP within tumours with a sharp reduction in pressure at the tumour periphery (Farnsworth et al., 2006).

Elevated interstitial fluid flow (IFF) in mammary tumours was first reported by Butler *et al.* in 1975, with enhanced hydrostatic pressure and lymphatic drainage from the interstitial space noted as well as remarkable differences in afferent and efferent tumour blood haematocrit levels (Butler et al., 1975). Since then, various techniques have been used to measure increased IFF including fluorescence recovery after photo bleaching (FRAP) and magnetic resonance imaging (MRI) (Dafni et al., 2005a). Interstitial fluid velocity in normal tissues and tumours has been quantified using these techniques and is reported in the range 0.1 to 2  $\mu\text{m s}^{-1}$  (Dafni et al., 2005b). In a study conducted in 1989, the interstitial fluid velocity was measured using FRAP and found to be 0.2 to 0.8  $\mu\text{m/s}$ . However, in tumours, shielding of the cells by the ECM lowers the shear stress generated by this fluid velocity (Kamiya et al., 1988, Pedersen et al., 2010).

Other techniques have been used to measure IFP in normal and tumour tissues. These have been subdivided into 'acute' (few hours) and 'chronic' studies of IFP. The approaches used include invasive techniques - for example surgical procedures including: wick catheter (Scholander et al., 1968, Hargens, 1981), wick-in-needle technique (Fadnes et al., 1977, Wiig et al.,

1987), servo-micropipette (Wiederhielm et al., 1964) polyurethane transducer-tipped catheter (Millar) (Ozerdem and Hargens, 2005), for acute measurement, and subcutaneous capsule implantation for 4 to 6 weeks (Guyton et al., 1963) for chronic assessment of IFP. Recently, a non-invasive method introduced for estimating IFP in solid tumours using MRI technology, converting theoretical variables into measurable variables (Liu et al., 2016).

Researchers have been studying the elevation of interstitial pressure in human clinical samples and mouse models for over 30 years (Baxter and Jain, 1989, Boucher et al., 1990, Boucher et al., 1997). In 2011, Goel et al. gathered data from various published studies of IFP in normal tissues and human tumours and reported a significant increase in IFP level in tumours, figure 4 (Goel et al., 2011). In 1993, Curti *et al* reported interstitial pressure of  $\leq 110$  mmHg in subcutaneous nodules in melanoma and lymphoma patients (Curti et al., 1993). In another study using A-07 human melanoma xenografts as the primary tumour, increased IFP was shown to be associated with pulmonary and lymph node metastasis (Rofstad et al., 2002). Measurements of the IFP in 118 patients with oral squamous cell carcinoma suggested the IFP value as a significant prognostic factor for 5-year survival (Yu et al., 2014a). Elevated IFP in cervical cancer was significantly associated with poorer patient survival following radiotherapy (Milosevic et al., 2001). Elevated IFP has also been associated with lymph node metastasis in patients with cervical carcinoma (Hompland et al., 2012), mouse models of breast carcinoma (Pathak et al., 2006), and xenograft models of cervical carcinoma and melanoma (Hompland et al., 2012). These observations suggest that IFP measurement may be a potential prognostic tool for clinical examinations and treatment options of cancer patients.

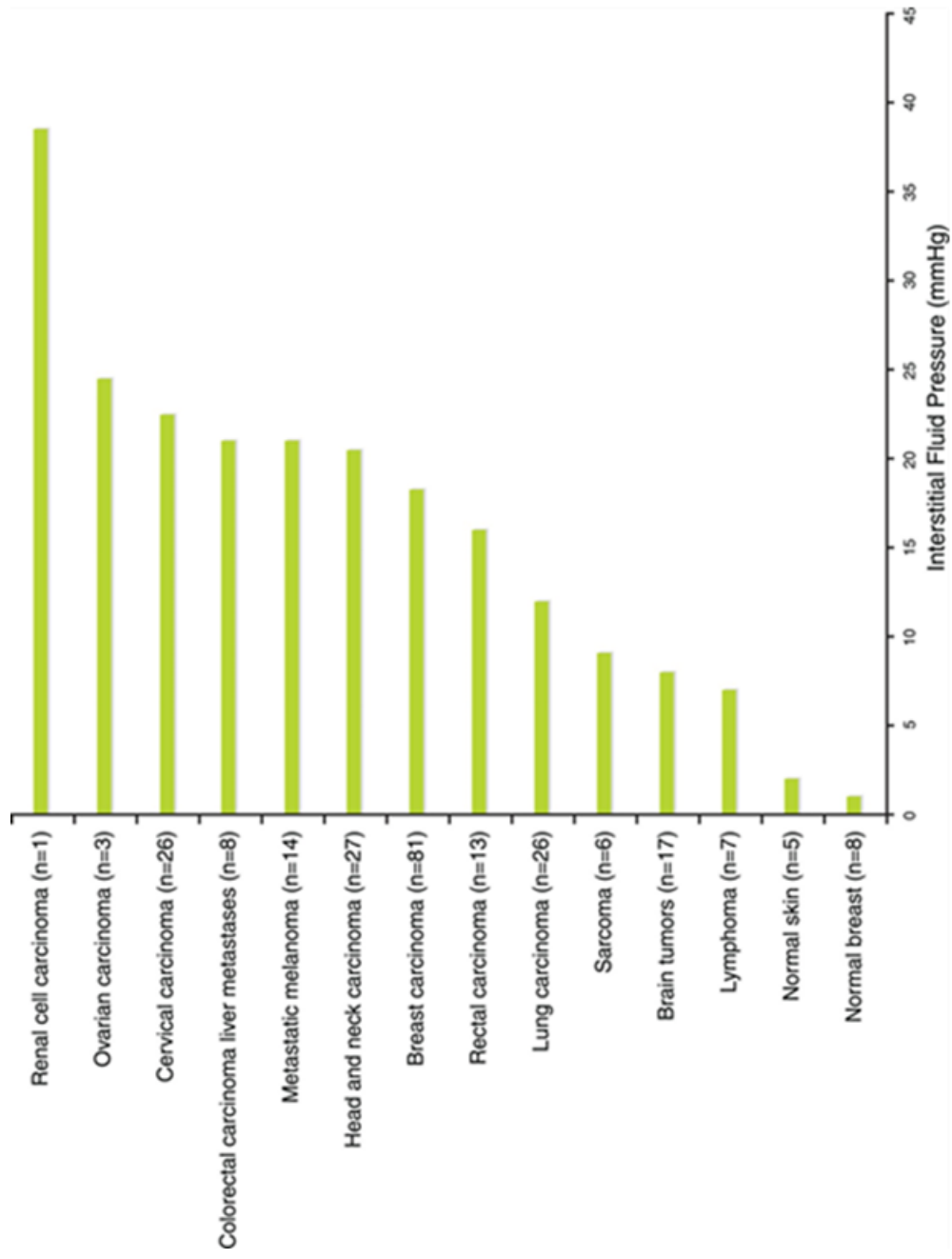


**Figure 4.** Interstitial fluid pressure (IFP) in human tumours and normal tissues. Previous studies indicated significant increase in IFP level in the solid tumours. The data were aggregated from previous studies (Goel et al., 2011).

Recently, using Boyden chambers and other engineered models, scientists have studied the effect of IFP on breast cancer cell behaviour including cellular invasion, migration and proliferation; assessing either the expression of EMT markers and MMPs or the migratory dynamics of tumour cells. Hence, elucidating molecular mechanisms through which cancer cells and stromal cells can sense and react to elevated IFP will provide knowledge that may help to guide targeted therapy.

Responding to reports of differences in the biomechanical properties of tumour and normal tissues, researchers have developed various tools designed to recapitulate interstitial flow and pressure in the tumour microenvironment. Microfluidic systems are the most commonly used devices used to generate controlled amounts of flow and pressure in 2D and 3D cell culture systems. Although these systems are being produced by different manufacturers, they are similar in their fundamental aspects (Huh et al., 2011). In general, a microfluidic system is composed of a set of micro-channels engraved or moulded into a material (glass, silicone or PDMS) constructed on a microfluidic chip which is connected to a reservoir of growth media through inlet and outlet tubes pierced into the chip. Media and gases may be injected and removed from the microfluidic chip either actively via peristaltic pump and pressure controllers or passively through hydrostatic pressure. (Boucher et al., 1990)

The recent availability of a bioreactor system (Quasi Vivo®, Kirkstall, U.K.) provided a small, inexpensive but reliable method of culturing cells under flow. The Quasi Vivo culture unit generates pulsatile-laminar-unidirectional flow which is typical for arterial blood flow. The layout of this system enables scientists to culture two or more different cell types in the connected chambers, mimicking the interactions between cells which occur in a tissue. The system has been mainly used for quick and cost-efficient cytotoxicity testing and studies on cellular metabolism. It also has a potential application in the biotechnology, pharmaceutical, chemical, cosmetics and research industries. For the novel application of this bioreactor in this study, the supplier was asked to redesign the system to be able to generate a higher pressure in the chambers. According to optimisation experiments they performed, by using 4

flow restrictors and applying the flow of 550  $\mu\text{L}/\text{min}$  in a two chambers system, we can increase the pressure inside the chamber to  $\sim 19$  mm Hg, while the pressure without using the flow restrictors is  $\sim 1$  mm Hg. Since 550  $\mu\text{L}/\text{min}$  is a high flow rate, to evaluate the effect of lower flow rate (alone), a flow rate of 150  $\mu\text{L}/\text{min}$  was also applied.

### **1.4.3 Interstitial flow and progression of cancer**

The movement of fluid passing through intercellular spaces in the ECM has been shown to be a factor leading to alterations in the tumour microenvironment. The effect of IF on cancer cells may be categorised into direct; the effects on the cancer cells themselves, or indirect; the impact on other components of the tumour such as the stromal cells and extracellular matrix. The direct effects of IF on cancer cells have been studied in multiple 2-dimensional (2D) and 3-dimensional (3D) cancer models (Shieh et al., 2011). Exposing breast cancer cells to IF in a 3D collagen model led to increased migration both in 3D culture inserts and in 3D flow chambers (Shields et al., 2007, Haessler et al., 2012). Applying IFP was shown to alter expression of genes associated with EMT and promote collective invasion in breast cancer cells (Piotrowski-Daspit et al., 2016). These findings suggest fluid flow within the tumour might be a prognostic indicator of invasion and metastasis.

During progression of cancer, fibroblasts are recruited and transformed to become cancer-associated fibroblasts (CAFs). Alterations in fluid flow and pressure have been reported to affect this transformation. Myofibroblasts are also transformed from fibroblasts and their phenotype resemble CAFs. Myofibroblasts are identified by elevated alpha smooth muscle actin ( $\alpha$ -SMA) expression, increased contractility, and elevated secretion of MMPs, cytokines and growth factors involved in tumour migration and angiogenesis. TGF- $\beta$ 1 secreted by cancer cells and fibroblasts, is an inducer of fibroblast to myofibroblast or CAF differentiation (De Wever et al., 2004, Orimo et al., 2005). Exposure of fibroblasts to increased IFF has been shown to result in

the induction of TGF- $\beta$ 1 and consequently myofibroblast differentiation even in the absence of a tumour (Ng et al., 2005). Implementing IF (0.5  $\mu$ m/s) in a coculture of dermal fibroblasts and MDA-MB-435S melanoma cells using a collagen matrix and modified 3D Boyden chambers, resulted in increased tumour cell invasion and fibroblast activation mediated by TGF- $\beta$ 1 (Shieh et al., 2011).

## 1.5 *In vivo* models of breast cancer

It would be of great value to be able to test drug efficacy and the resistance of cancers to certain drugs by assessing the drug responsiveness of primary tumour cells (from patients), this could be evaluated either *in vivo* or *in vitro* ultimately at the outset, when clinical treatment commences. Several *in vitro* and *in vivo* strategies are being developed in an attempt to tackle this issue. Amongst all kinds of *in vivo* strategies, 'Mouse Avatar' and 'Co-clinical Trials' are the most advanced projects so far. The main focus of the co-clinical trial project is to use either genetically engineered mouse models (GEMMs) or patient-derived tumour xenografts (PDX) to guide patient therapy in on-going human clinical trials. In this paradigm, mouse trials and human trials are developed in parallel to provide fast and real-time transfer of outcomes from mouse treatment to human clinical trials, Figure 5 (Nardella et al., 2011). On the other hand, 'Mouse Avatars' use patient-derived tumour xenografts (PDX) with the aim of helping clinicians choose optimal chemotherapeutic agents (Marangoni and Poupon, 2014). Although the concept of tailoring therapy with this approach is appealing, studies have indicated technical drawbacks both in terms of scientific and non-scientific limitations (Mueller and Reisfeld, 1991). For example, the maintenance of these *in vivo* models is very expensive, leading to claims that the systems are ultimately unaffordable, moreover, because the xenograft models encompass several steps including implantation, propagation and drug-screening, the time required before determining the optimum treatment protocol remains a problem and patient mortality has been reported before the start of therapy (Malaney et al., 2014).

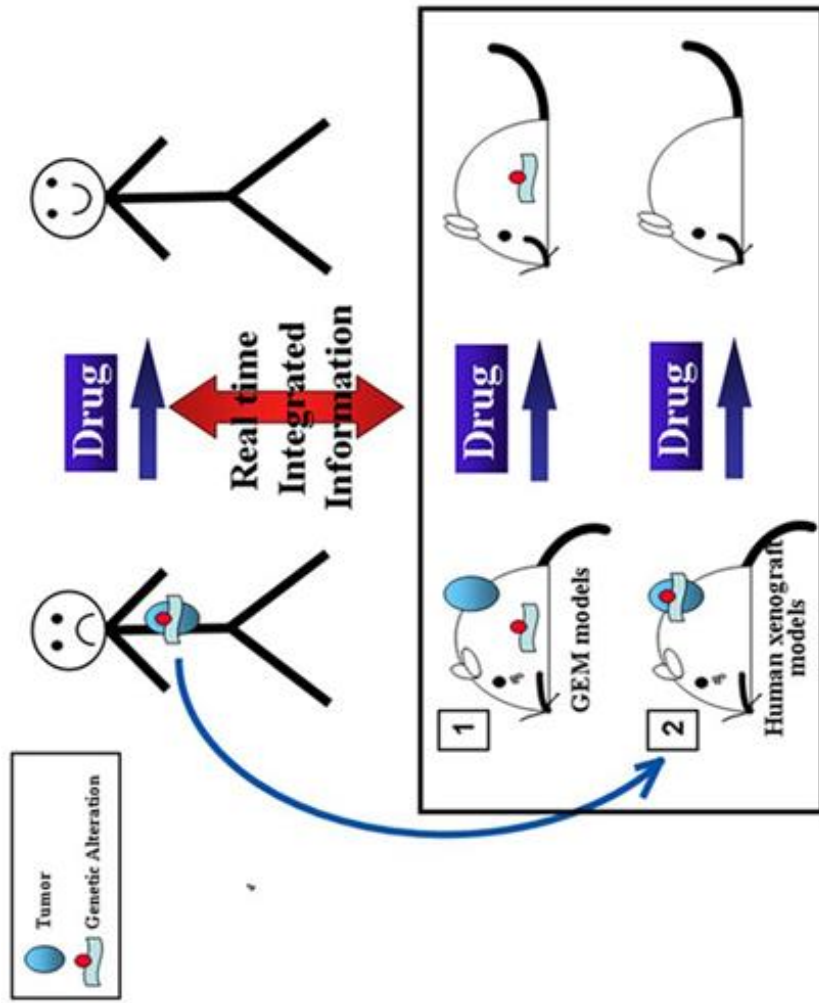


**Figure 5.** Co-clinical trial paradigm (Nardella et al., 2011).

## 1.6 *In vitro* tissue culture models of breast cancer

In addition to *in vivo* models, several *in vitro* systems have been developed with the aim of stratifying breast cancer patients to different treatment regimens. Although conventional monolayer (2D) cell culture models are convenient to set up and have been used in different areas of biological research for decades, they have limitations in terms of the physiological relevance of these methods for detailed tumour studies. Despite the increased complexity that may be developed in a 2D cell culture environment, for example using stromal cell co-culture, the limitation of 2D cell culture for capturing tumour heterogeneity is well accepted (Debnath and Brugge, 2005). The microenvironment that surrounds cancer cells within a solid tumour consists of cellular components including stromal cells, infiltrating immune cells, lymphatics, vasculature and acellular components including the ECM, growth factors and cytokines. Several methods have been developed that aim to provide a complex cell culture system that includes the interplay between these components and cancer cells, a phenomenon that occurs in the *in vivo* condition.

Recently, a range of 3D models have been developed to better reflect the complexity of tumours. As a general concept, 3D cancer models can be divided into two main categories: ECM inclusive and ECM exclusive (spheroids). Tumour cells have been maintained in cell culture as spheroids since the 1970s and have been used in a range of studies including those aimed at the formation of the breast acinar structure and breast tumour models (Debnath and Brugge, 2005). The techniques and devices that have been mainly used to make spheroids are summarised in table 1.

<b>Technique</b>	<b>Device</b>	<b>Reference(s)</b>
Hanging drop method	Hanging drop plate(s)	(Fennema et al., 2013)
Spontaneous spheroid formation	Ultra-Low attachment plates	(Vinci et al., 2012)
Suspension culture	Spinner flasks, bioreactors	(Hoarau-Véchet et al., 2018, Kwok et al., 2018)
Magnetic levitation	magnetic nanoparticles	(Souza et al., 2010)

**Table 1.** The key methods developed for the preparation of cancer cell spheroids.

A feature of each of these techniques is that the cancer cells are prevented from adhering to the surface of the wells/vessels and forced to aggregate and form spheroids (Hoarau-Véchet et al., 2018). Adding stromal cells such as fibroblasts and endothelial cells and applying magnetic levitation has improved the physiology and reproducibility of the spheroid-based experiments (Gottfried et al., 2006, Kunz-Schughart et al., 2006). Several morphological characteristics for example epithelial-myoeepithelial interactions and drug response have been studied using spheroids. The preparation of cancer cell spheroids has allowed investigations aimed at understanding the resistance of cancer cells to cytotoxic agents such as doxorubicin and cisplatin (Kerr et al., 1986, Kobayashi et al., 1993, Frankel et al., 1997).

A drawback of this approach, however, is that the ECM, a key component of the tumour microenvironment, is generally omitted when spheroids are prepared suspended in culture medium. To address this shortcoming, scientists have created 3D scaffolds with the aim of recapitulating the ECM as an essential natural environment. This approach recognises the role of the ECM in both intra- and extra-cellular signalling, cell proliferation,

differentiation, migration, invasion and drug uptake. Biodegradable and biocompatible scaffold materials used in cancer biology applications are usually classified into two main groups: (1) naturally derived matrix materials including collagen, fibronectin, laminin and hyaluronic acid; and (2) synthetic polymer-based materials such as poly (lactic-co-glycolic) acid (PLGA) and poly- $\epsilon$ -caprolactone (PCL)(Rijal and Li, 2016) Engelbreth-Holm-Swarm ECM extract (Matrigel) material, collagen and decellularised ECM are the most commonly used biomaterials for modelling breast tumours as they offer support for cell growth, differentiation and migration compared to synthetic materials. The trend toward the use of different synthetic and natural extracellular matrix has been reviewed by Rijal *et al* (Rijal and Li, 2016).

## **1.7 Naturally derived matrix materials**

The main constituents of the ECM in mammalian tissues are collagen, elastin, laminin and proteoglycans (Frantz *et al.*, 2010). The design of a 3D tissue culture to mimic the natural structure of the ECM in human tissues as closely as possible would, therefore, include collagen, Matrigel™ and fibronectin. To this end gelatin, alginate, chitosan and silk fibroin have been tested but these are from non-human sources. Collagen type-I has been the most commonly used scaffolding material used for modelling of breast tumours either alone or in combination with other components of the ECM tissue such as fibronectin, laminin, hyaluronic acid and Matrigel™ (Rijal and Li, 2016). Collagen is the most abundant protein of human connective tissue and is categorised to 28 types of either fibrillar or non-fibrillar forms.

Fibrillar type-I collagen accounts for 90% of collagen found in the human body and has been the most frequently used natural material for 3D culture and tissue engineering studies. In humans, collagen type-I fibrils are mainly present in skin, tendon, vascular ligature, organs and bone whilst in the normal mammary gland, interstitial ECM contains fibrillar collagens (I, III and V) and basement membrane contains the non-fibrillar type-IV collagen. In breast cancer a reduction in the levels of collagen IV and an increase in levels of

collagen I, III and V has been reported (Egeblad et al., 2010a, Oskarsson, 2013). Earlier studies of malignant tumours showed that the expression levels of mRNA for type-I and type-III procollagen increased in the fibroblastic cells resident in the stroma. Furthermore, an *in vivo* study of a ductal infiltrating breast carcinoma reported increased deposition of bundles of collagen type-I and III at the invasive front of the tumour (Kauppila et al., 1998).

Cancer invasion requires remodelling of the ECM - this is primarily facilitated by the degradation of collagen, re-deposition, cross-linking and stiffening and is accompanied by infiltration of immune system cells and re-differentiation of monocytes at the invasive front. During tumorigenesis, the smooth and twisted structure of collagen characteristic of normal breast tissue alters to become a stiff, thick and linear collagen, this is associated with a change in epithelial cell polarity and alterations in cell-cell adhesion, this in turn enhances growth factor signalling, EMT and invasion, features associated with a metastatic phenotype (Egeblad et al., 2010a). Increases in ECM cross-linking alongside deposition of fibronectin, proteoglycans and collagens I, III and IV have been reported in other types of invasive cancers (Zhu et al., 1995, Huijbers et al., 2010). The mentioned modifications may lead to generation of invasion 'highways' for cancer cells whereby cells migrate along the collagen fibres. Drug delivery and drug efficacy has been shown to be affected by collagen density and other physical and molecular features of the ECM network (Egeblad et al., 2010a).

In addition to material derived from mammalian tissues, other biomaterials extracted from natural sources, have been used as biodegradable scaffolds. For example, MCF-7 breast cancer cells grown on the polymeric polysaccharide chitosan (produced from the chitin of the exoskeleton of crustaceans), showed growth kinetics comparable with those cultured in tissue culture flasks (Dhiman et al., 2004). MDA-MB231 cells cultured on silk fibrin scaffolds displayed enhanced MMP-9 activity, suggesting a higher invasion potential of the cells when grown in 3D culture. Concurrently it was reported that the cells produced the same yield of lactate from glucose consumption as *in vivo* conditions, indicating that the scaffolds were able to maintain the

metabolic activity of the MD-MB231 cells (Jastrzebska et al., 2015). In various studies mixtures of different natural biomaterials have created unique scaffold structure with improved biophysical and biochemical properties. For instance, a mixture of silk fibroin and chitosan results in a unique scaffold with more fibro-porous structure which is non-toxic and highly permeable for water and oxygen, supporting cell growth and adhesion (Li et al., 2017). The multitude of studies with different matrices and cell types have shown the importance of cell culture methods on cell growth, invasion and drug responsiveness. Elucidating the molecular mechanisms that might be affected in response to different microenvironments, will provide the more reliable cell culture methods for use in the drug discovery process. It may also aid the development of novel methods for personalised therapy strategies.

## **1.8 Doxorubicin and resistance to therapy**

Doxorubicin, a chemotherapeutic drug with a molecular weight of 543 g/mol, was first extracted from *Streptomyces peucetius* var. *caesius* in the 1970's (Arcamone et al., 1969). Doxorubicin belongs to the anthracycline category of chemotherapeutics which act through the intercalation of DNA, inhibition of topoisomerase II and the formation of free radicals (Tacar et al., 2013). Since it was discovered doxorubicin has been in routine use for the treatment of a range of cancers including breast, lung, gastric, ovarian, thyroid, non-Hodgkin's and Hodgkin's lymphoma, multiple myeloma, sarcoma, and paediatric cancers (Lao et al., 2013, Rathos et al., 2013, PDQPTE, 2002, Saini et al., 2018). In clinical practice, doxorubicin is administered independently/alone or in combination with other chemotherapeutic or targeted biological agents or encapsulated in liposomes or other nanoparticle materials for treatment of various types of cancers. Since breast cancer cells were used in this project, the primary focus was the toxicity of doxorubicin on breast cancer cells.

Current approaches for the adjuvant therapy of breast cancer is a combination of anthracyclines, such as doxorubicin and epirubicin; taxanes, including paclitaxel and docetaxel, along with fluorouracil and cyclophosphamide

(Hernandez-Aya and Gonzalez-Angulo, 2013). However, resistance to chemotherapy has been reported for many breast cancer patients. Such resistance mechanisms may be acquired after exposure to the therapeutic agent or may be inherent characteristics which exist in the tumour prior to treatment, figure 6.

Cancer cells may acquire resistance to therapy as a result of the accumulation of mutations and sequential genetic changes occurring during the development of cancer over time. Acquired resistance may occur in cancer cells which have survived exposure to an initial therapeutic regimen, whilst inherent (*de novo*) resistance is associated with intrinsic factors within the cancer cells themselves. Resistance may also be mediated by environmental factors such as the attachment of the cancer cells to the ECM (Dittmer and Leyh, 2015). As an example, culturing MCF-7 and MDA-MB231 breast cancer cells in 3D ECM-based model has been shown to result in a reduction in doxorubicin efficacy. However, the application of a  $\beta$ 1-integrin blocking antibody prior to addition of doxorubicin to MDA-MB231 cells cultured in ECM (Matrigel), resulted in a significant increase in sensitivity of MDA-MB231 cells to doxorubicin in a dose dependent manner (Lovitt et al., 2018). This approach has indicated the importance of understanding molecular mechanisms underlying interaction of tumour cells with the microenvironment and a potential route through which cancer cells may acquire resistance to therapy. This should be noted with regards to chemotherapeutic drugs when a non-responsive patient receives serious life-threatening side effects without gaining any benefit from the therapy.

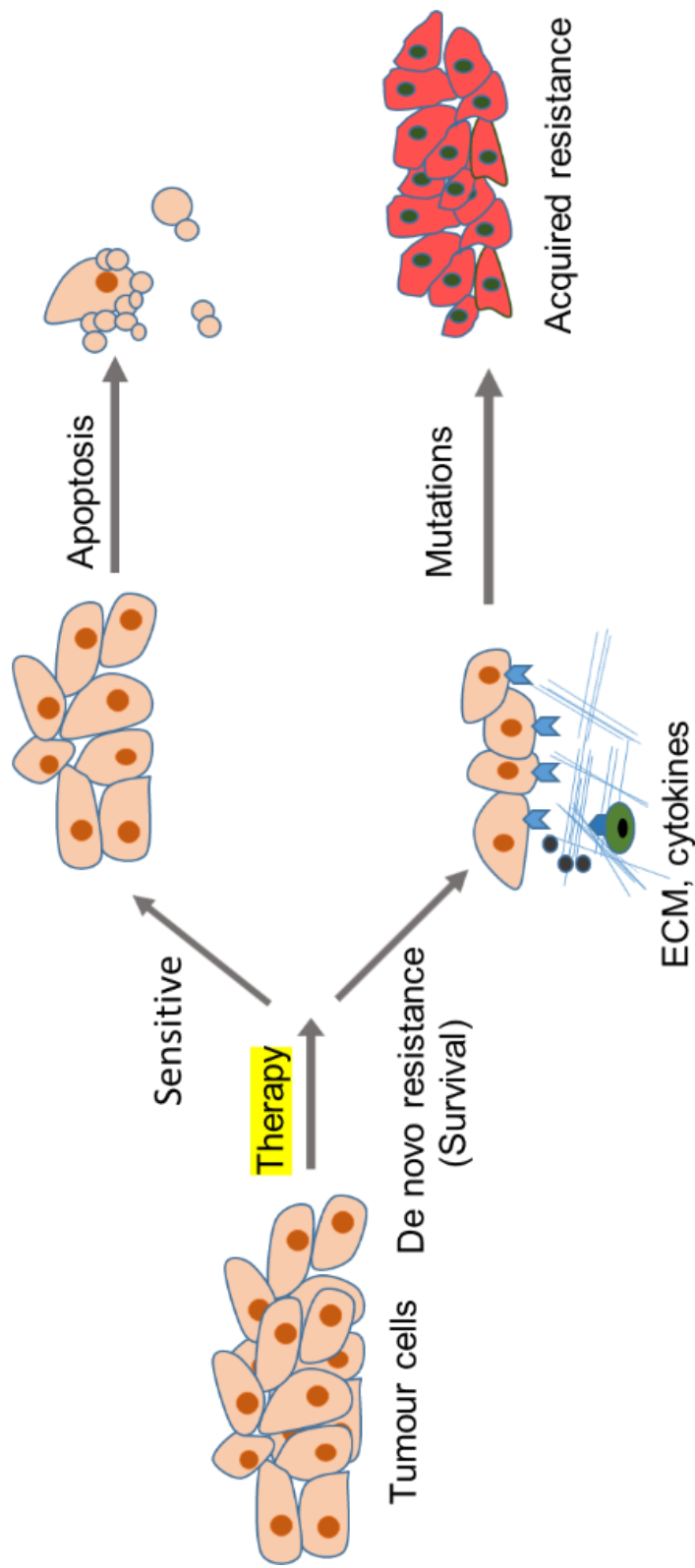


**Figure 6.** The components of the tumour microenvironment contribute to environment-mediated drug resistance. A fraction of tumour cells which interact with microenvironmental factors, survive treatment. These cells remain as minimal residual disease (not shown). Over time, more mutations occur, resulting in more complicated and a diverse resistance-acquired phenotype which ultimately results in disease recurrence with lower chance of response to therapy. Therefore, developing therapeutic agents that disrupt the interaction between cancer cells and microenvironmental factors can reduce the chance of cancer recurrence.

## 1.9 Aims and objectives

The aim of this project was to study the effect of the tumour microenvironment, in particular, fluid flow and pressure, on breast cancer cell behaviour and responsiveness to the chemotherapeutic agent doxorubicin.

The long-term aspiration for this research was to create an *in vitro* tumour model which would provide a more physiologically relevant environment for studying molecular mechanisms underlying breast tumour growth and invasion and for evaluating drug efficacy in drug discovery processes.

The objective in the first part of the project was to compare the behaviour and sensitivity of breast cancer cells to doxorubicin when cells were grown (1) in 2D culture; (2) in 3D spheroids and (3) in 3D after embedding in collagen type-I using the RAFT system to form 'artificial cancer masses' (ACM). The second focus of the project was an assessment of the biochemical effect of interstitial fluid flow and pressure on tumour cell invasion, levels of markers of EMT, proliferation, hypoxia, apoptosis-related markers and drug responsiveness.

# **CHAPTER 2**

## **MATERIAL AND METHODS**

## **2.1 Materials and equipment**

### **2.1.1 General reagents, buffers and other chemicals**

The details of general chemicals and reagents used in this study are listed in Appendix 1.

### **2.1.2 Media, buffers, reagents and consumables used in cell culture, cell harvest and cell lysate processes**

High glucose (4.5 g/L) Dulbecco's modified Eagle's medium (DMEM) (Hyclone, Life Technologies, U.K.); foetal bovine serum (FBS) (Gibco, Life Technologies, U.K.); Trypsin-EDTA Solution 10X (Sigma-Aldrich, U.K.); Rat Tail Collagen Type-I >2 mg/mL Chloroform Treated (First Link Ltd, U.K.); Phosphate-Buffered Saline (PBS) (Gibco, U.K.); Minimum Essential Medium (MEM) (Lonza, U.K.); Antibiotic Antimycotic Solution 100X (Sigma-Aldrich, U.K.); Neutralising buffer (1.6 M NaOH in 840 mM HEPES buffer) (home-made); RAFT™ absorbers for 96-well and 24-well plates (Lonza, U.K.); Collagenase type-I (Gibco, U.K.); Hanks' Balanced Salt solution (HBSS) (Sigma, U.K.); RIPA Buffer (Sigma, U.K.); 4-(2-hydroxyethyl)-1-piperazineethanesulfonic acid (HEPES) buffer (Thermofisher Scientific, USA).

### **2.1.3 Kits**

#### **2.1.3.1 RNA extraction, cDNA library construction and quantitative polymerase reaction (qPCR)**

The RNeasy Micro Kit was used to extract RNA from the cancer cells the QuantiTect Reverse Transcription Kit was used to produce cDNA from mRNA (Qiagen Ltd, U.K.). Gene expression levels were measured using the QuantiNova SYBR Green RT-PCR Kit (Qiagen Ltd, U.K.).

### **2.1.3.2 Protein measurement kit**

The Pierce™ BCA Protein Assay Kit was utilised to measure total protein concentration in the cell lysates (Thermofisher Scientific, USA).

### **2.1.3.3 Alamar blue reagent**

The metabolic activity of cells cultured in 2D and 3D was measured using the Alamar blue reagent kit (Invitrogen, U.K.)

## **2.1.4 Electrophoresis buffers and reagents**

### **2.1.4.1 Agarose gel electrophoresis**

The integrity of extracted RNA and the size of qPCR products were assessed using agarose gel electrophoresis. The materials used were: agarose (Sigma, U.K.), Gel Red (Biotium, USA), tris-borate-EDTA buffer 1X (homemade TBE: 108 g Tris, 55 g boric acid, 40 mL 0.5 M Na<sub>2</sub>EDTA, pH 8.0 in 900 mL distilled water), loading buffer (home-made). DNA Gel Loading Dye (6X) (Thermofisher Scientific, USA), DNA ladder (New England Biolabs, USA).

### **2.1.4.2 Sodium dodecyl sulphate-polyacrylamide gel electrophoresis (SDS-PAGE)**

Separation of proteins was carried out using SDS-PAGE. The following materials were used: acrylamide/bis-acrylamide 30% v/v (Sigma, U.K.); sodium dodecyl sulphate (SDS) (Sigma, U.K.); running buffer: 14.4 g Tris base, 3.03 g glycine and 1 g SDS, loading buffer 2x (Sigma-Aldrich, U.K.), Tris-HCl pH, 6.8, Tris HCl pH, 8.8, catalysts: N,N,N',N'-

Tetramethylethylenediamine (TEMED) (Severn Biotech Ltd, U.K.) and ammonium persulfate (APS) (Sigma-Aldrich, U.K.); Precision Plus Protein Dual Colour Standards (Bio-Rad, U.K.).

### **2.1.5 Western blotting reagents**

Transfer buffer (25 mM Tris, 0.2 mM Glycine, 20% v/v methanol, pH 8.3); Ponceau S solution (Sigma, U.K.); filter paper (ThermoFisher Scientific, USA); Nitrocellulose Membrane (ThermoFisher Scientific, USA); enhanced chemiluminescent (ECL) substrate (ThermoFisher Scientific, USA), bovine serum albumin (BSA) (Sigma, U.K.). phosphate-buffered saline with 0.05% Tween-20 (PBST).

### **2.1.6 Antibodies**

Antibodies used for immunostaining of the cells and Western blot analysis.

#### **2.1.6.1 Primary antibodies**

Rabbit monoclonal anti-ErbB 2 antibody (ab134182, Abcam, U.K.); rabbit monoclonal anti-vimentin (Cell Signalling Technology, USA); rabbit polyclonal anti- $\beta$ -actin antibody (Abcam, U.K.); rabbit polyclonal anti GAPDH antibody (Abcam, U.K.).

#### **2.1.6.2 Secondary antibodies**

Goat polyclonal anti-rabbit IgG H&L (HRP) pre-adsorbed (Abcam, U.K.); goat polyclonal anti-rabbit IgG H&L (Alexa Fluor 488) (Abcam, U.K.).

### **2.1.7 Doxorubicin**

Doxorubicin was used in its hydrophilic form (doxorubicin hydrochloride) from Thermofisher Scientific.

## **2.2 Methods**

### **2.2.1 Cell culture**

Human breast cancer cell lines, MDA-MB231 and SKBR3 (available at the University of Westminster, purchased from ATCC). Normal fibroblast cells isolated from breast tissue outside the cancer margin and distal to the cancer growth were kindly provided by Dr Hazel Welch, Division of Surgical and Interventional Sciences, Royal Free and University College London Medical School, University College London. The cells were cultured in monolayer (2D) and multilayer/matrix (3D) formats.

#### **2.2.1.1 2D monolayer cell culture**

MDA-MB231, SKBR3 and normal fibroblast cells were cultured in high glucose Dulbecco's modified Eagle's medium (DMEM) (Hyclone, Life Technologies) supplemented with 10% v/v foetal bovine serum (FBS) (Gibco, Life Technologies) and maintained in a humidified atmosphere at 37°C in 5% v/v CO<sub>2</sub>. For routine passage, the cells were allowed to reach 80% confluency, the media was removed, cells were washed by PBS twice, 10X trypsin-EDTA was added to detach the cells from the surface of the cell culture flask and from each other. Due to the different cell attachment properties across the cell lines, the incubation time in this step ranged from 30 to 60 seconds for MDA-MB231 cells and 3 minutes for SKBR3 cells. Cells grown as 2D monolayers were transferred to a collagen scaffold for the preparation of the 'artificial cancer mass' (ACM) system as described below.

### 2.2.1.2 Three-dimensional tumour models

An artificial cancer mass (ACM) was prepared using the RAFT 3D cell culture system in 96-well plates, following the manufacturer's instructions (Lonza, U.K.). An overview of the preparation of the ACM is shown in Figure 7. The proportions of reagents used for constructing ACMs are shown in table 2. In brief, 2.8 mL of minimal essential medium (10X MEM) was added to a mixing vessel, then, slowly 22.4 mL of rat-tail collagen type- I (2 mg/mL) was added, care was taken to avoid introducing air bubbles, swirling the solution carefully around the mixing vessel. The solution was neutralised by addition of 1.624 mL of neutralising solution (1.6 M NaOH in 840 mM HEPES buffer). A solution containing the cells (cell stock solution) prepared previously and added to the collagen type- I scaffold mixture slowly.

The number of cells in the cell stock solution for seeding 50,000 cells per well required  $1.92 \times 10^6$  cells per plate in the cell stock solution. The final mixture of collagen-MEM-cell solution was mixed gently and aliquoted into the 96-well plate (240  $\mu$ L per well) and placed in the incubator set at 37 °C for 15 minutes

Plate	No. of well	10X MEM (mL)	2 mg/mL collagen (mL)	Neutralising solution (mL)	Cell stock (mL)	Cell seeded collagen (mL)
96-well plate	96	2.8	22.4	1.624	1.200	0.240
24-well plate	24	3.5	28.2	2.042	1.500	1.300

**Table 2.** Proportion of reagents used for preparation and construction of ACMs.

to form a cell populated collagen hydrogel. In the next step biocompatible hydrophilic RAFT absorbers were placed on top of each well for 15 minutes (at room temperature). Absorption of liquid resulted in a 40-fold increase in the concentration of cell-collagen mixture and a final concentration of 80 mg/mL

collagen (manufacturer's instructions). After removal of the absorbers, in order to prevent the gel dehydrating, 100  $\mu$ L of culture medium (DMEM with 10% v/v FBS) was added to each 100  $\mu$ M thick RAFT gel. For preparation of the ACM the RAFT gel was initially embedded in a looser collagen matrix of 1.6 mg/mL in 24-well plate RAFT system. The gel was placed in the incubator set at 37 °C for 15 minutes to allow it to set and then absorbers were applied for 15 minutes to remove the liquid from the collagen (at room temperature). After removing the absorbers, 1 mL of culture medium, DMEM with 10% v/v FBS, was added to each ACM.

Prior to the co-culture of cancer cells with normal fibroblasts cells, the fibroblasts were cultured only in the 24-well plate RAFT system and not in the 96-well plate to enable the diffusion into the media of growth factors and other stimuli released from fibroblasts. The fibroblast cells were embedded in the collagen matrix, and  $3 \times 10^4$  cells were placed within each well.

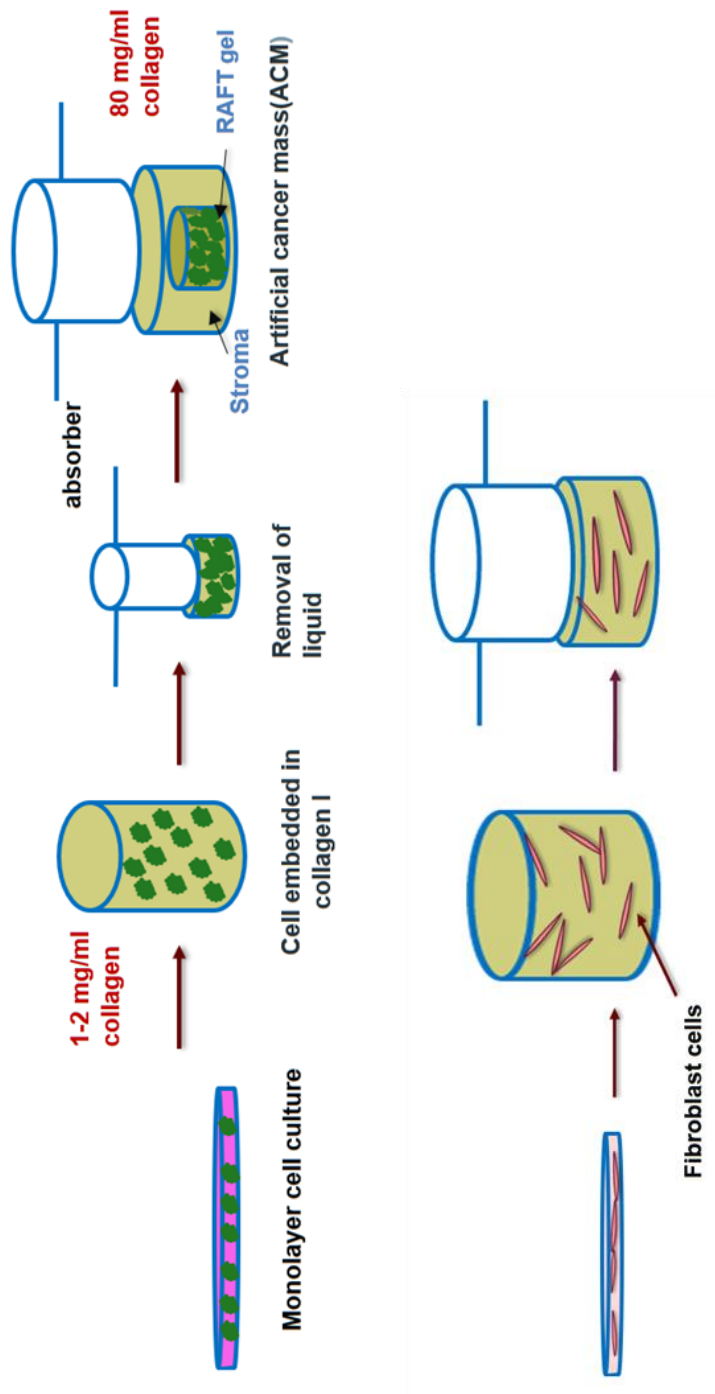


**Figure 7.** The preparation of the 3D 'artificial cancer mass' (ACM) used in this study. Panel A: Breast cancer cells were mixed with rat tail type-I collagen. To provide a dense 'cancer mass' the RAFT system (Lonza, U.K.) was used to absorb significant, reproducible, quantities of liquid away from the cell culture/collagen mixture. This enabled the formation of a dense cancer mass (RAFT gel). The RAFT gel was then embedded in a cell-free looser rat tail type-I collagen matrix and absorbers were applied to remove further liquid resulting in a final thickness ACM of 100  $\mu\text{m}$ . Panel B: Fibroblasts were embedded in rat tail type-I collagen in a 24-well plate format. After the gel had solidified, an absorber was applied to remove the liquid. The system is based on Nyga et al., 2013.

### **2.2.1.3 Applying interstitial fluid flow and pressure using the Quasi Vivo system**

A dynamic growth environment incorporating flow and pressure was created by using the Quasi Vivo QV500 system (Kirkstall, U.K.). This system consists of cell culture chambers made from polydimethylsiloxane (PDMS); a biocompatible, transparent and flexible silicone, reservoir bottle, inlet and outlet tubing and filter. All the compartments of the Quasi Vivo system are autoclavable and can be reused except the filter which has to be replaced for each experiment.

To construct the circuit in the Quasi Vivo system a 'series' configuration was used. The two chambers containing the cells were plugged in sequence by connecting the outlet tubing of the first chamber, in the direction of flow, to the inlet tubing of the second chamber. In turn, the outlet tubing of the second chamber was connected to the 'return tubing' enabling the media to return to the reservoir bottle through a length of outlet tubing (2.4 mm) and a Luer lock. A length of smaller diameter tubing (1.6 mm) was used to connect the inlet of the first chamber to the reservoir bottle using a Luer lock. The tubing was mounted on a peristaltic pump roller enabling the transfer of the media from the reservoir bottle to the chambers in a circulatory flow system (Figure 8A). Dimensions and materials of different compartments of the Quasi Vivo QV500 system are shown in Table 3.

Cells cultured in 3D as ACMs were allowed to settle for 48 hours before being transferred to the Quasi Vivo QV500 chamber. The flow of media was generated using a Masterflex peristaltic pump housed in the 37°C, 5% v/v CO<sub>2</sub>, humidified incubator (Figure 8C). The pump produced a pulsatile-laminar-unidirectional flow of the media in the Quasi Vivo circuit at various flow rates. However, other variables including number of chambers, the diameter and length of the tubing, the position of chambers and reservoir in relation to the pump and the type of pump, may affect the actual flow rates in the system. Hence, the system was calibrated for every new design and flow rate to ensure the flow rate is correct. The calibration process is described in section 2.2.1.4

Chamber width	15 mm internal
Chamber depth	10 mm from culture surface to top of chamber base
Materials	Chamber: PDMS; Tubing: Tygon; Luers & reservoir bottle: polypropylene
Overall dimensions	23 mm height x 37 mm diameter
Diameter of tubing	Inlet: 1.6 mm; Outlet: 2.4 mm
Volume of chamber	2 mL

**Table 3.** Specification of Quasi Vivo® system

The suppliers of the Quasi Vivo system (Kirkstall U.K.) estimated that a flow rate of 550  $\mu\text{L}/\text{min}$  corresponds to an interstitial fluid pressure, IFP, of 1.1 mm Hg (personal communication to T. Azimi. This IFP is consistent with the pressure in normal breast tissue. Four one-way Luer check-valves, female-male styrene acrylonitrile (SAN) with silicone diaphragm (Cole-Parmer, U.K.) were used to restrict the flow and consequently increase the pressure inside the chambers to 19 mmHg (Figure 8B). These valves that are referred to 'flow restrictors', they were biocompatible and meet the USP Class VI/ISO 10993 specifications.

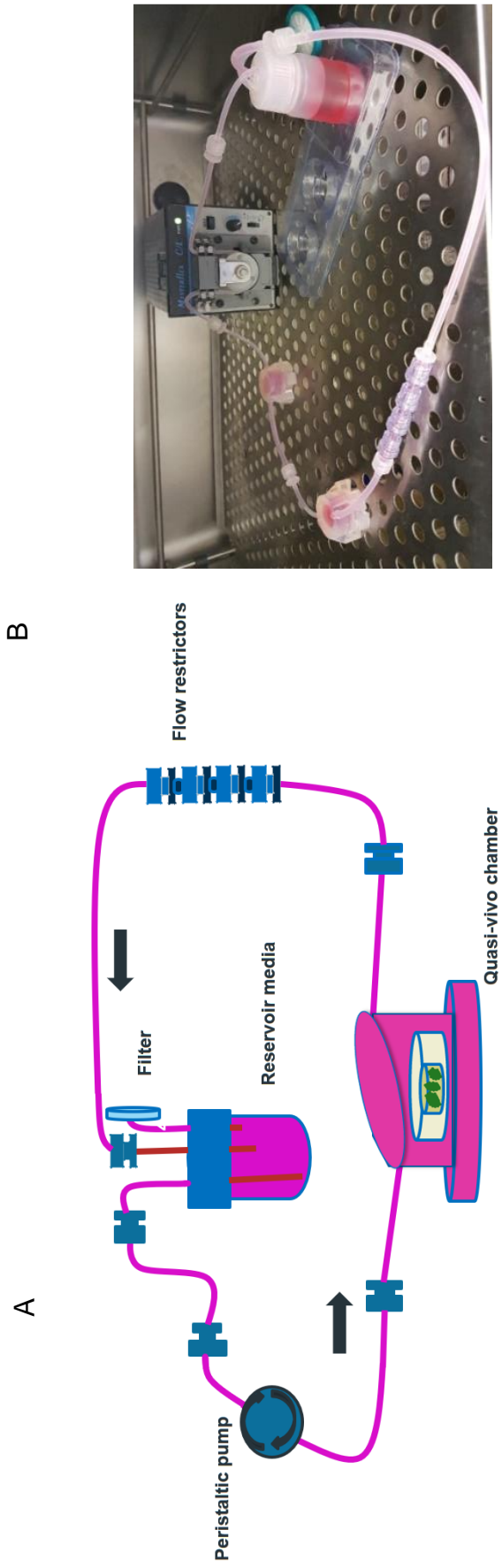


**Figure 8.** The flow system developed and utilised in this project. Panel A: schematic view of the Quasi Vivo QV500 with implementation of the flow restrictors enabling an increase in the fluid pressure. Panel B: the bioreactor with artificial cancer masses, ACM, in each of the chambers, a pressure of 1.6 mm Hg was generated by use of the Masterflex peristaltic pump housed at 37°C, in a humidified 5% v/v CO<sub>2</sub>, atmosphere.

#### **2.2.1.4 Calibration of the Quasi Vivo system**

The Masterflex peristaltic pump used in this study was used initially. First, in a series configuration, the two chambers were filled with sterile PBS buffer and the pump was allowed to flow. After the air bubbles were expelled from the system the liquid output was collected from the final chamber over a minute and weighed. This procedure was repeated three times and the mean average value indicated the flow rate ( $\mu\text{l min}^{-1}$ ) of the liquid in the system. Using this method, the flow rate was measured and adjusted according to the experiment undertaken, varying the pump speed, with and without flow restrictor(s).

#### **2.2.2 Immunostaining**

Cells seeded in 2D and 3D (ACMs) were immunostained to determine cell invasion pattern and expression of specific proteins including HER2 and vimentin at cellular level. The protocol used for immune staining cells in 2D had been optimised previously in Dr. Dwek's lab. ACMs were stained using the optimised protocol kindly provided by Judith Pape from UCL.

##### **2.2.2.1 Immunostaining of cells in 2D (monolayer)**

Cells were grown in 6-well plates (2D) for a week in order to keep the growth conditions as close as possible to cells grown in 3D. After the cells reached 70-80% confluency, they were washed with PBS and fixed for 30 minutes in 10% V/V formalin in PBS (pH 7.4). Formalin was washed away, and PBS was added to each well. The cells were left in the fridge (4 °C) until they were used for immunostaining. Before starting immunostaining, process PBS was removed and 5% BSA in PBS (blocking solution) was added. The plate gently was incubated rocking at room temperature for 30 minutes. The wells were washed with PBS for 5 minutes (twice and gently rocking). Then primary

antibody was diluted in PBS by following the manufacturer instruction. Primary antibodies and their optimum concentration used are listed in table 4. The diluted primary antibody was added to the wells and incubated gently rocking at room temperature for 1 hour or in cold room overnight. Then wells were washed three times for 5 minutes in PBS buffer gently rocking.

Cells were incubated with secondary fluorescent labelled antibody: goat anti-rabbit IgG (Alexa Fluor 488) at the final concentration of 10 µg/mL in PBS at room temperature and for an hour while gently rocking. From this step onward, the ACM was housed under aluminium foil to prevent the Alexa Fluor quenching. Cells were washed with PBS three times for 5 minutes. In order to counterstain the nuclei, To-Pro-3 dye or DAPI was used. Before using To-Pro-3, in order to remove RNA in the cytosol, cells were incubated with ribonuclease A (Sigma, U.K.) at the concentration of 100 µg/mL at room temperature for 20 minutes. Then wells were washed with PBS twice for 5 minutes and incubated with To-Pro-3 (Life Technology, USA) at 1 µM in PBS at room temperature, gently rocking for 20 minutes. Then wells were washed three times for 5 minutes in PBS. For the negative control, the addition of primary antibody was omitted and all other steps in the protocol was applied.

<b>Antibody</b>	<b>Concentration</b>	<b>Supplier</b>
Goat anti-rabbit IgG (Alexa Fluor 488)	10 µg/mL	Abcam
Anti-ErbB2	1.228 µg/mL	Abcam
Anti-vimentin	Dilution: 1/100	Cell Signalling Technology

**Table 4.** Antibodies used in immunostaining processes.

### **2.2.2.2 Immunostaining of cells in 3D (ACM)**

Cells grown in 3D in 24-well plates were washed three times with PBS and fixed in 4% w/v formaldehyde for 30 minutes. ACMs were permeabilised with 1% w/v BSA, 0.2% v/v Triton in PBS at room temperature for 1 hour and washed with PBS three times for 5 minutes. The primary antibody was diluted to the same concentration used in 2D staining in 1% w/v BSA, 0.2% v/v Triton in PBS and was applied to the ACM and incubated at 4 °C overnight. The following day the ACMs were equilibrated to room temperature for 1 hour and washed three times with PBS, each wash for 5 minutes. The secondary antibody: goat anti-rabbit IgG, Alexa Fluor 488 was prepared in 1% w/v BSA, 0.2% v/v Triton in PBS at the same concentration used for the 2D immunostaining and allowed to incubate for 2.5 hour at room temperature. The rest of the experiment was undertaken under aluminium foil to avoid Alexa Fluor quenching. The ACMs were washed three times with PBS for 5 minutes each and the nuclei of the cells stained with DAPI.

### **2.2.3 Harvesting cancer cells for gene and protein analysis**

MDA-MB231 and SKBR3 cells cultured in 2D monolayers were washed with PBS and detached from the culture surface using trypsin-EDTA 10X (Sigma, U.K.) for 30 - 60 seconds. Since the spheroids were not attached to the surface and were floating in the well, trypsin-EDTA treatment was not needed and spheroids of 5 wells were pooled together in a Falcon tube. 10 mL media (high glucose DMEM) was added to the cells and was centrifuged in a Falcon tube at 1500 RPM for 5 minutes. To remove all the phenol-red dye from the DMEM the cell pellet was re-suspended in 3 mL PBS and re-centrifuged at 1500 RPM for 5 minutes, the PBS was removed, and the cell pellet was either stored at -80 °C or used for RNA extraction and/or protein extraction straight away.

To harvest cells cultured in ACMs, firstly, the ACMs were treated with 200 units/mL collagenase I (Gibco, U.K.) in HBSS buffer (450  $\mu$ L) for each ACM) for 60 minutes in a plate shaker incubator (Stuart, U.K.). When the collagen had solubilised, the mixture was centrifuged at 1700 rcf for 5 minutes and the cell pellet used for the RNA extraction or for the Western blot analysis purposes.

#### **2.2.4 Cell lysate preparation for SDS-PAGE**

The cells harvested from 2D cell cultures and ACMs (as described in section 2.2.3) were lysed using the mixture of RIPA buffer (Sigma, U.K.) and 10% v/v protease inhibitor cocktail (Sigma, U.K.). The number of cells cultured in 3D was 50,000 cells per ACM and for each experiment only two ACMs were used (since only two quasi vivo chambers were used in each run). Therefore, in order to increase the protein concentration only 100  $\mu$ L of RIPA buffer and proteinase A mixture was added to the two pooled ACM. The cells cultured in 2D ( $\sim 10^6$  cells) were lysed using 500  $\mu$ L RIPA buffer mixture. Cells were mixed with RIPA buffer and protease Inhibitor by pipetting and maintained on iced water for 15 minutes. The resulting cell lysate was centrifuged at 13,000 RPM at 4 °C for 15 minutes. The supernatant was carefully collected in a new sterile tube and stored at -80 °C until use.

#### **2.2.5 Bicinchoninic acid (BCA) Protein assay**

The protein concentration of cell lysates obtained from the cells cultured under different growth conditions was estimated using the BCA kit (ThermoFisher Scientific, USA). The assay was performed by following the instructions provided by manufacturer. In brief, a working solution was prepared by mixing 50 parts of reagent A (containing sodium carbonate, sodium bicarbonate, bicinchoninic acid and sodium tartrate in 0.1M sodium hydroxide) and 1 part reagent B (containing 4% cupric sulphate). A set of protein standards (range

= 125- 2000 µg/mL) was prepared by serial dilution of bovine serum albumin (BSA) standard solution at a stock solution concentration of 2 mg/mL provided by the manufacturer. For microplate-based procedures, 200 µL working solution and 10 µL of sample (standard/cell lysate/RIPA buffer) were added to each well and mixed thoroughly on a plate shaker for 30 seconds. Since RIPA buffer had been used for lysing the cells, it was added into the blank well. The plate was covered and incubated at 37 °C for 30 minutes after which the plate was allowed to cool to room temperature and the absorbance read at 562 nm (Spectrostar, BMG LabTech, Germany). A standard curve was prepared, and the equation of the line used to calculate protein concentration, using the absorbance values of the lysate samples (Appendix 2).

### **2.2.6 SDS polyacrylamide gel electrophoresis (PAGE)**

SDS-PAGE was firstly introduced by Ulrich K. Laemmli in 1970. The technique was used to separate proteins in the cell lysates. A Mini-protein electrophoresis system (Bio-Rad Laboratories, U.K.) was used for these experiments. The reagents used for two gels with gel dimensions 7.0 x 8.3 cm (H x W); 1 mm thickness are shown in Table 5.

The ingredients of resolving and stacking gels were mixed according to the proportions shown in Table 5. A set of clean glass plates and spacers (1 mm thickness) was assembled in a gel holder on a casting stand. After checking the system for leaking and being assured that system is properly sealed, the 10% w/v ammonium persulphate and TEMED were quickly added to the resolving gel mixture. 2.5 mL of the gel mixture was poured in the space between the glass plates, overlaid with water and left to polymerise for 15 minutes. The water was poured off and 4% stacking gel was prepared with the same procedure and poured on top of the polymerised resolving gel. A 1 mm comb was inserted between the glass plates in order to form the wells for loading the samples. After the gel was polymerised, the comb was removed, and wells were washed with water. Then gel was assembled into the running

module, placed in the tank, and top and bottom of gel was covered with running buffer (Tris base 14.4 g, glycine 3.03 g and SDS 1 g).

The cell lysate samples were mixed with Laemmli sample buffer (2X) (Bio-Rad) in 1:1 ratio, heated for 5 minutes at 100 °C, centrifuged briefly and loaded on the gel. 10 µL of protein standard (Bio-Rad, U.K.) was also loaded on the gel to estimate the size of bands after detection step. The gel was electro-phoresed for 120 minutes at 110 V. Two gels were run for each analysis, one to evaluate SDS-PAGE protein separation and the other used for Western blotting.

<b>Stock solution</b>	<b>10% Resolving gel</b>	<b>4% Stacking gel</b>
30% Acrylamide/Bis Acrylamide	4 mL	0.5 mL
1.M Tris-HCl (pH 8.8)	2.5 mL	-
MilliQ water	3.3 mL	2.1 mL
10% SDS	100 µL	30 µL
0.5M Tris HCl (pH 6.8)	-	0.380
<b>Before pouring the gel</b>		
10% Ammonium per- sulphate	100 µL	30 µL
TEMED	4 µL	3 µL

**Table 5.** Quantity of reagents used for SDS-PAGE

### **2.2.7 Coomassie Brilliant Blue staining of protein gels**

After SDS-PAGE, protein bands were visualised by staining the gel with 0.025% w/v Coomassie Blue R-250 in 10% v/v acetic acid overnight, and de-

stained in a mixture of H<sub>2</sub>O, methanol, and acetic acid in a ratio of 50/40/10 (v/v/v).

### **2.2.8 Western Blotting (wet blot)**

Western blotting was performed using the method initially developed by Towbin *et al.* (1979). However, some modifications were made in the procedures. A Mini Trans-Blot Cell (Bio-Rad, U.K.) was used for this experiment. For each gel, one piece of nitrocellulose membrane (Thermo Scientific, USA), two pre-cut Western blotting filter papers (Thermo Scientific), and two fibre pads were soaked in the transfer buffer and assembled into a cassette in a correct orientation and order (providing the movement of proteins from gel to the nitrocellulose blot). The cassette was inserted inside an electrode module and was placed in the buffer tank along with an ice cooling unit (stored in -20 °C). The buffer tank was filled with transfer buffer (25 mM Tris, 0.2 mM Glycine, 20% v/v methanol, pH 8.3). The protein transfer was performed at 100 V for 2 hours at 4 °C (cold room).

After the Western blotting step, in order to ensure the proteins had been transferred successfully, the nitrocellulose membrane (blot) was removed from the cassette and stained in 0.1% w/v Ponceau S 5% v/v acetic acid (Sigma, U.K.) for 2 minutes. Then the membrane was washed quickly with water for 4-5 minutes. In the case of primary antibodies (HER2,  $\beta$ -actin and GAPDH) from Abcam company, the blot was blocked using 5% w/v BSA in PBST buffer (0.1% Tween 20 in PBS) for 1 hour at room temperature, while for the primary antibodies supplied by Cell Signalling Technology (CST), 5% w/v milk protein PBST was recommended by the manufacturer. After blocking, the blot was washed with PBST buffer three times for 5 minutes and incubated in the dilution of primary antibody recommended by the manufacturer in a 5% w/v BSA in PBST at 4 °C, gently rocking overnight. The blot was washed three times for 5 minutes each with 15 mL with PBST and incubated with the loading control (in this study anti-GAPDH and anti-beta Actin antibodies (Abcam, U.K.) for 1.5 hour at room temperature. The blot was washed three times for 5

minutes each with 15 mL with PBST. The blot was incubated with secondary antibody (Goat anti-rabbit IgG conjugated with HRP) diluted (1/5000) in 5% w/v skimmed milk powder in PBST (if the primary ab was from CST) or 5% w/v BSA in PBST (if the primary ab was from Abcam) for 1 hour, gently rocking at room temperature. The blot was washed three times for 5 minutes each with 15 mL with PBST. Before starting the detection procedure, the blots were stored in PBS to avoid dehydration. The enhanced chemiluminescent (ECL) detection system (Thermofisher, USA) was used to detect the antibody-protein binding. Super Signal West Femto Trial Kit (Thermo scientific, USA) was used for this purpose. A working solution was prepared by mixing 1:1 ratio of the two reagents included in the kit (Luminol/Enhancer and Stable Peroxide Buffer). The mixture was added on the blot and incubated for 5 minutes. The remaining solution was absorbed by blue tissue and the blot was visualised using the Biospectrum Imaging System called UVP camera.

## **2.2.9 Gene expression analysis**

For studying gene expression levels in the samples using qPCR method, initially cells were collected as a pellet, RNA was extracted, and mRNA was reverse transcribed into complementary DNA (cDNA).

### **2.2.9.1 RNA extraction**

The cells cultured under different conditions were harvested with the procedures described previously in section 2.2.3. Total RNA was extracted using RNeasy Micro kit (Qiagen, Germany) according to the manufacturer's instructions. In brief, 350  $\mu$ L buffer RLT was added to the cell pellet and homogenized by pipetting. One volume of 70% v/v ethanol was added to the lysate and mixed well by pipetting. The mixture was transferred to a RNeasy

MinElute spin column (included in the kit and stored at 4 °C) and centrifuging for 15 secs at 13,000 RPM. The flow-through was discarded and 350 µL buffer RW1 was added to the column, centrifuging for 15 secs at 13,000 RPM. The flow-through was discarded and a mixture containing 10 µL of DNase I stock solution and 70 µL of buffer RDD (both included in the kit) was added directly to the RNeasy MinElute spin column membrane. The column was placed on the bench top at room temperature for 15 minutes. 350 µL buffer RW1 was added to the column and centrifuged for 15 sec at 13,000 RPM. The collection tube was discarded, and the column was housed in a new 2 mL collection tube. 500 µL Buffer RPE was added to the column and centrifuged for 15 sec at 13,000 RPM. The flow-through was discarded and 500 µL of previously prepared 80% v/v ethanol was added to the column. The column was centrifuged for 2 minutes at 13,000 RPM. The collection tube was discarded, and column was placed in a new 2 mL collection tube. The column was centrifuged for 5 min to dry the membrane. The flow-through and collection tube were discarded, and column was placed in a new sterile 1.5 mL collection tube. 20 µL RNase-free water was added directly to the centre of the spin column membrane. The spin column was centrifuged for 1 min at 13,000 RPM. All steps were performed using a Pico 17 centrifuge (Thermo scientific, USA) and at room temperature.

### **2.2.9.2 Evaluation of RNA integrity and purity**

The concentration of total RNA was measured using a Nanodrop spectrophotometer (Thermofisher Scientific, USA) at 260/280 nm. The RNA integrity was evaluated by separation of the RNA using a 1% w/v agarose gel prepared in-house; 0.5 g agarose in 50 mL TBE buffer (10.8 g Tris, 5.5 g boric acid and 4 mL 0.5 M NaEDTA, pH 8.0 in 1 litre water). RNA samples were mixed with 6 X loading buffer (BioLabs, U.K.) and 6 µL of the mixture was loaded on the gel. 7 µL of 1Kb DNA ladder (BioLabs, U.K.) was used to estimate the base pair size of separated bands. The gel was placed in an electrophoresis tank

(Bio-Rad, U.K.) filled with TBE buffer and electrophoresed at 120 V for 1 hour with the Gel Red dye system and visualised using UV light (Appendix 3).

### **2.2.9.3 Reverse transcription of mRNA to complementary DNA (cDNA)**

The mRNA was reverse transcribed into complementary DNA (cDNA) using the QuantiTect Reverse Transcription Kit (Qiagen, Germany) according to the manufacturer's instructions. Briefly, 1 µg RNA was used for the preparation of each of the cDNA libraries. In the case of samples with lower amounts of RNA, 500 ng RNA was used. In an Eppendorf tube, the RNA was mixed with 2 µL of gDNA (genomic DNA) wipe-out reagent and the volume were adjusted to 14 µL with RNase free water. The mixture was incubated on a dry bath (Bio-Rad, U.K.) at 42 °C for 2 minutes. A mixture of 1 µL reverse transcriptase (RT) enzyme, 4 µL of buffer and 1 µL of primer mix was prepared and added to the tube containing RNA, mixed by pipetting and incubated at 42 °C for 15 minutes. To stop the reaction (deactivating the RT enzyme), the tube was incubated at 95°C for 3 minutes. cDNA was stored at -80 °C freezer for future use.

### **2.2.9.4 Quantitative polymerase reaction chain qPCR**

The cDNA library was used for the relative quantification of expression of EMT-related genes including *vimentin*, *snail1*, *cadherin-11*, *MMP14*, apoptotic markers including Caspase 3, Caspase 9 and BCL2 and hypoxia marker including HIF1α and proliferation marker Ki67. The primer efficiency was assessed for each primer pair using the known concentrations of cDNA. The standard curve and R<sup>2</sup> values obtained from primer efficiency tests. The reaction tubes were prepared using Quanti-Nova SYBR Green kit (Qiagen) and the manufacturer's instructions were followed. In brief, for each reaction

tube with final volume of 20  $\mu$ L, 4  $\mu$ L of cDNA, containing 40 ng, 4  $\mu$ L molecular biology grade water (Fisher Scientific, USA), 1  $\mu$ L of 10 pmol/ $\mu$ L concentrated forward and reverse primer, and 4  $\mu$ L of water was added into the sterile PCR tube. When the number of sample were more than 36, strip tubes (Qiagen,U.K.) were used. Negative controls were used in every run of qPCR: non-template control (NTC) and –RT controls (prepared by omitting the reverse transcriptase step during the preparation of the cDNA library). The tubes were placed in Rotor Gene real-time cycler (Qiagen, Germany) and cycling program was set as shown in Table 6. The sequences of the forward and reverse primers for the genes studied in this project are listed in table 7.

The expression levels of GAPDH and  $\beta$ -actin, as an endogenous control gene, was measured in all samples in order to normalise input amounts. qPCR product sizes were estimated using the NCBI data base (Primer BLAST) and were assessed by separation of the PCR products using a 1.5% w/v agarose gel electrophoresis.

<b>Step</b>	<b>Time</b>	<b>Temperature</b>
PCR initial heat activation	2 min	95°C
2 step cycling		
Denaturation	5 sec	95°C
Combined annealing/extension	10 sec	60°C
Number of cycles	40	

**Table 6.** Cycling conditions for the qPCR analysis

Gene	Forward primer	Reverse primer
Vimentin	AGATGGCCCTTGACATTGAG	CCAGAGGGAGTGAATCCAGA
Snail1	TTTCTGGTTCTGTGTCCTCTGCC T	TGAGTCTGTCAGCCTTTGTCCTGT
MMP14	ATAAACCCAAAAACCCACC	AAACACCCAATGCTTGTCTC
Cadherin-1	CCCAGTACACGTTGATGCCT	GACGTTCCACATTGGACCT
GAPDH	GACAGTCAGCCGCATCTTCT	TTAAAAGCAGCCCTGGTGAC
Caspase-3	CAGCAAACCTCAGGGAAAC	TCACCCAACCACCCTGGTCTT
Caspase-9	GCTCTTCCTTTGTTTCATCTCC	GCTGCTTGCCTGTTAGTTC
BCL2	TCGCCCTGTGGATGACTGA	CAGAGACAGCCAGGAGAAATCA
Ki67	CCACACTGTGTCGTCGTTTG	CCGTGCGCTTATCCATTCA
HIF-1 $\alpha$	CGTTCCTTCGATCAGTTGTC	TCAGTGGTGGCAGTGGTAGT
$\beta$ -Actin	CTGTGGCATCCACGAAACTA	CGCTCAGGAGGAGCAATG

**Table 7.** List of primer sequences used for qRT-PCR.

### 2.2.10 Alamar blue cell viability assay

When cells are alive, they maintain a reducing environment in the cytosol. Resazurin (MW= 229 g/mol), the main compound in Alamar blue reagent is a non-toxic, cell permeable dye, blue in colour and non-fluorescent. Following entry into the cells Alamar blue reagent is reduced to Resorufin, a red highly fluorescent component. MDA-MB231 and SKBR3 cells were cultured at a density of  $5 \times 10^4$  cells per ACM/well for 3D culture and  $3 \times 10^4$  for 2D monolayer. Metabolic activity was assessed over 14 days using the Alamar

blue assay according to the manufacturer's protocol (Invitrogen). In brief, a 10% v/v solution of Alamar blue in phenol and FBS free media was added to each well. For the negative control, the solution was also added to the wells without cells. Then plate was placed in the incubator at 37 °C, 5% CO<sub>2</sub> for 4 hours. The optimum incubation time and cell number had been determined beforehand. The absorbance values were measure using microplate reader (BMG, Labtech, U.K.) at a wavelength of 570 nm and 600 nm to calculate the percentage reduction of Alamar blue reagent using following formula:

$$\% \text{ Reduction of Alamar blue reagent} = \frac{(\text{Eoxi}_{600} \times \text{A}_{570}) - (\text{Eoxi}_{570} \times \text{A}_{600})}{(\text{Ered}_{570} \times \text{C}_{600}) - (\text{Ered}_{600} \times \text{C}_{570})} \times 100$$

$\text{Eoxi}_{570}$  = molar extinction coefficient (E) of oxidized Alamar blue Reagent at 570nm =80586

$\text{Eoxi}_{600}$  = E of oxidized Alamar blue Reagent at 600nm = 117216

$\text{A}_{570}$  = absorbance of test wells at 570nm

$\text{A}_{600}$  = absorbance of test wells at 600nm

$\text{Ered}_{570}$  = E of reduced Alamar blue at 570nm = 155677

$\text{Ered}_{600}$  = E of reduced Alamar blue at 600nm = 14652

$\text{C}_{570}$  = absorbance of negative control well (media, Alamar blue reagent, no cells) at 570nm

$\text{C}_{600}$  = absorbance of negative control well (media, Alamar blue reagent, no cells) at 600nm

### **2.2.11 Drug treatment in 2D and 3D**

SKBR3 and MDA-MB231 cells cultured in 2D and 3D conditions were treated with doxorubicin (a DNA-damaging chemotherapeutic drug, MW= 543 g/mol). For 2D monolayer experiments, first, cells were seeded at the density of  $3 \times 10^4$  and grown overnight. Cells were serum starved with 2% v/v FBS DMEM for 24 hours before treatment. For 3D culture,  $5 \times 10^4$  cells were seeded in each gel for the two cell lines. Cells were allowed to acclimatize to the new environment and to form cell clusters for 5 days prior to serum-starvation. To find the best concentration of the drug for treatment, cells were treated with different concentrations of doxorubicin (20  $\mu$ M, 10  $\mu$ M, 5  $\mu$ M, 1  $\mu$ M and 0.5  $\mu$ M) diluted in serum-free DMEM for 48 hours. Controls were treated with serum free DMEM only. The Alamar blue assay was used to assess cell viability after doxorubicin treatment. In order to compare drug response in static and dynamic conditions the concentration of 5  $\mu$ M doxorubicin was selected for the treatment of cells in ACM. For each experiment, eight ACMs were constructed and maintained in static conditions for five days to allow cells to acclimatise to the 3D environment. Then, four ACMs were transferred to the Quasi Vivo chambers, and a flow of 550  $\mu$ L/min of media was applied. Two separate systems of two-chamber Quasi Vivo with separate reservoir bottles were used in order to keep untreated and treated ACMs separate and under the same flow condition. For static condition, 2 ACMs were treated and 2 were kept as untreated controls.

### **2.3 Statistical Tests**

Statistical analysis was performed using paired t-test when comparing mRNA expression of the genes and the cell viability in different culture conditions. a P-value of less than 0.05 was considered statistically significant. At least three dynamic experiments and three static controls were performed per flow rate for viability tests. Origin Lab software was used for analysing all the data and calculation of P values.

# CHAPTER 3

## RESULT

### **3.1 Viability of cancer cells cultured in 2D and 3D**

MDA-MB231 and SKBR3 cells were cultured as 2D monolayers and in collagen type-I as ACMs, as shown in Figure 9, below. Since the space for cells cultured in 2D was limited to the well surface, fewer cells were initially seeded in the 2D cultures (20,000 cells/well) compared to 3D cultures (50,000 cells/ACM).

The viability of MDA-MB231 and SKBR3 cells cultured in the ACM with collagen type-I was compared, over a 7-day time course, with cells from the same passage number of cells cultured in 2D monolayer. The percentage reduction of the Alamar blue reagent was calculated and considered as a surrogate measure of the percentage of cell viability, Figure 10.

The metabolic activity of SKBR3 cells cultured in both 2D and 3D increased after 3 days. However, the rate of increase in metabolic activity was lower in 3D cell culture compared with 2D (not statistically significant). After 7 days the metabolic activity of cells decreased from 95% to 70% when the cells were cultured in 3D but in contrast, the metabolic activity increased slightly from 72% to 80% in cells grown in 2D culture. The results illustrated that SKBR3 cells were less metabolically active when grown in 3D cell culture compared to 2D monolayers. In contrast, when MDA-MB231 cells were grown in 2D compared with 3D they exhibited a 75% and 30% increase respectively ( $P < 0.05$ ). The metabolic activity of MDA-MB231 cells continued to increase by 21% in 2D and 7% in 3D conditions until day 7 ( $P < 0.05$ ). Overall, the results demonstrated that MDA-MB231 and SKBR3 cells were less metabolically active when grown in 3D compared with 2D cell culture.

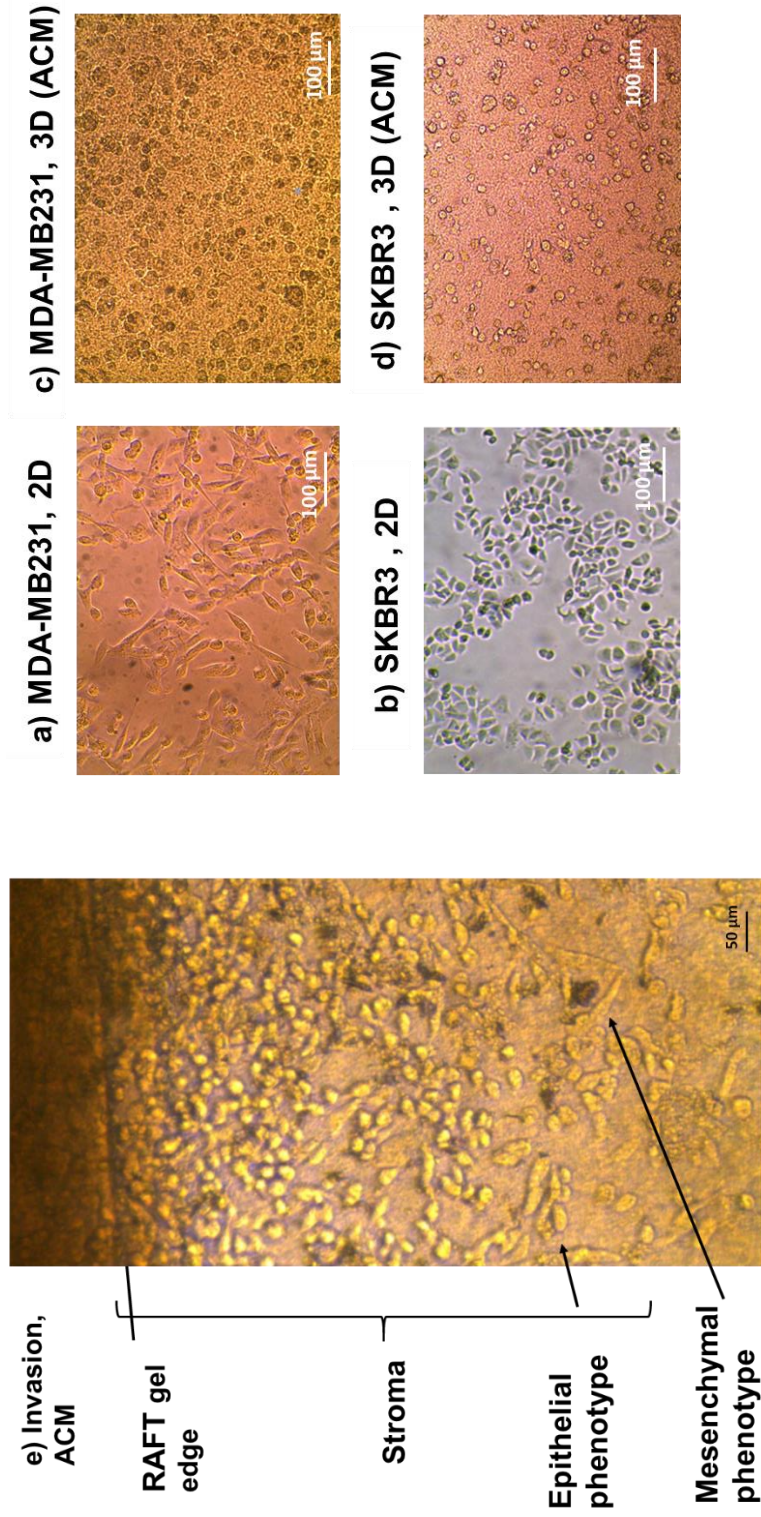


**Figure 9.** Phenotype of MDA-MB231 and SKBR3 breast cancer cells grown in 2D monolayer and 3D. The artificial cancer mass (ACM) was prepared using collagen type-I with the RAFT system. The images show that imaged on the first day, after seeding with cells, using the inverted light microscope. The images show that although MDA-MB231 and SKBR3 have different phenotypes in 2D culture: MDA-MB231 cells, panel a) are more spindle and SKBR3 cells, panel b) are more rounded; they adopt a similar phenotype, panel c) and panel d) both rounded when grown in a 10% dense collagen type-I as ACM. However, as can be observed in panel e) MDA-MB231 cells of ACM regain a spindle-like phenotype when they invade towards acellular collagen (surrounding stroma), image was taken on day 14.

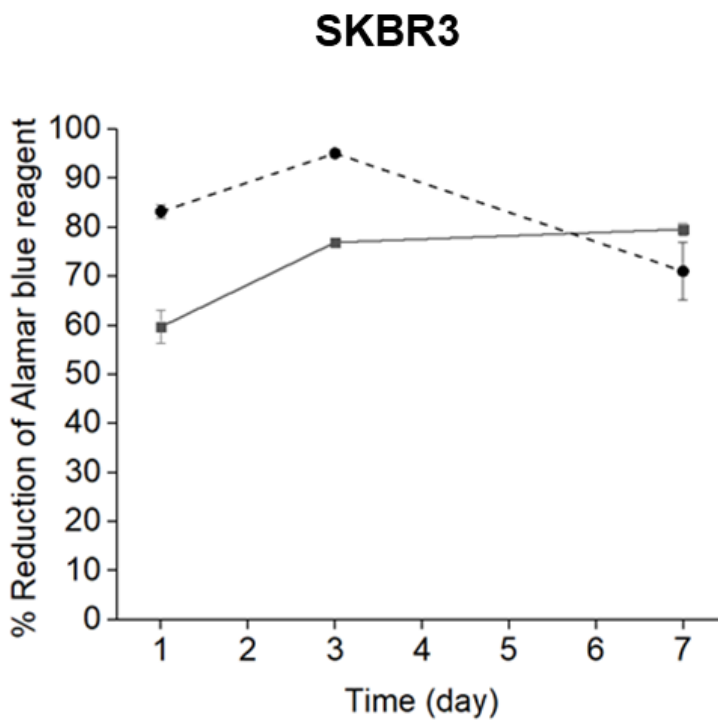
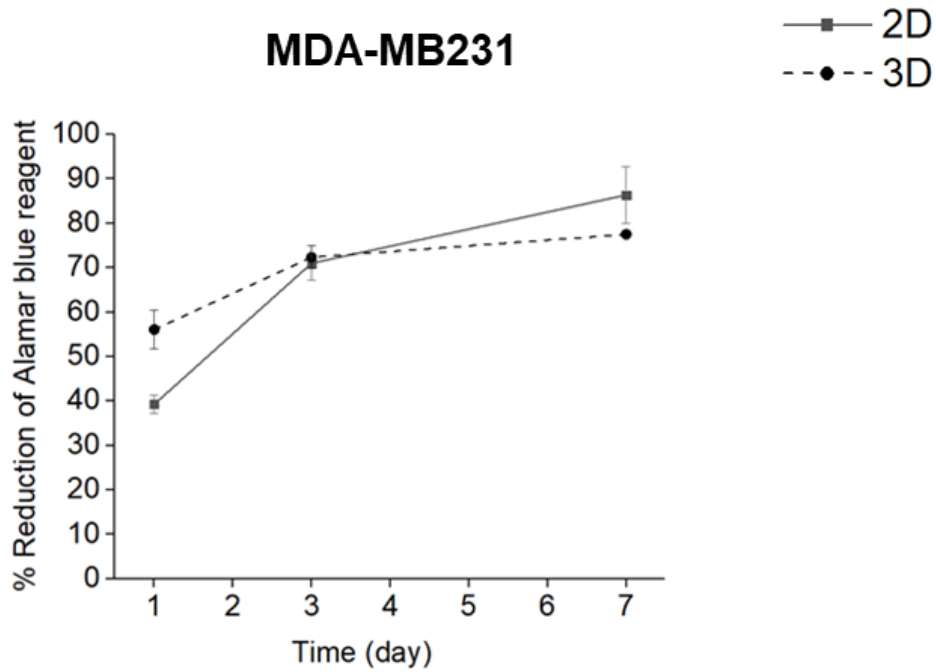


**Figure 10.** reduction of alamar blue reagent indicating the metabolic activity of MDA-MB231 and SKBR3 cells grown over a 7-day period in 2D or in 3D (ACM). Overall, the rate of increase in metabolic activity reduced in both cells grown in 3D compared to 2D. Mean average values  $\pm$  SD (n=3).

### **3.2 Ki67 mRNA expression in 2D and 3D cell culture**

To check if the results obtained in the cell viability assays (described above) were associated with changes in cell proliferation or metabolic activity the expression levels of a cell proliferation marker, Ki67, was assessed. Relative quantification of Ki67 mRNA levels for cells grown in 2D monolayers, 3D cultures embedded in collagen type-I (ACM) and without collagen (spheroids) for a week, was assessed using qRT-PCR. Gene expression levels were calculated for all samples and the levels were compared to cells cultured in 2D (control). GAPDH was used as the internal reference gene to normalize the cycle threshold (Ct) values of the mRNA. Three biological repeats were conducted, Figure 11.

A significant decrease in Ki67 mRNA expression-levels were observed in both cell lines when they were cultured in collagen type-I in 3D (ACM) compared to 2D conditions, figure 11. MDA-MB231 cells exhibited a 0.33 fold and SKBR3 cells exhibited a 0.35 fold reduction in Ki67 mRNAs level when grown as ACM compared with 2D cell culture. In contrast, when cells were grown as spheroids there was a significant increase in relative gene expression for Ki67: MDA-MB231 exhibited a 1.5 fold increase and SKBR3 exhibited a 2 fold increase in Ki67 mRNA compared to the control 2D culture. These results demonstrate that cancer cells proliferation is affected by the microenvironment and cells grown as spheroids express more Ki67 compared with cells grown in contact with collagen type-I.

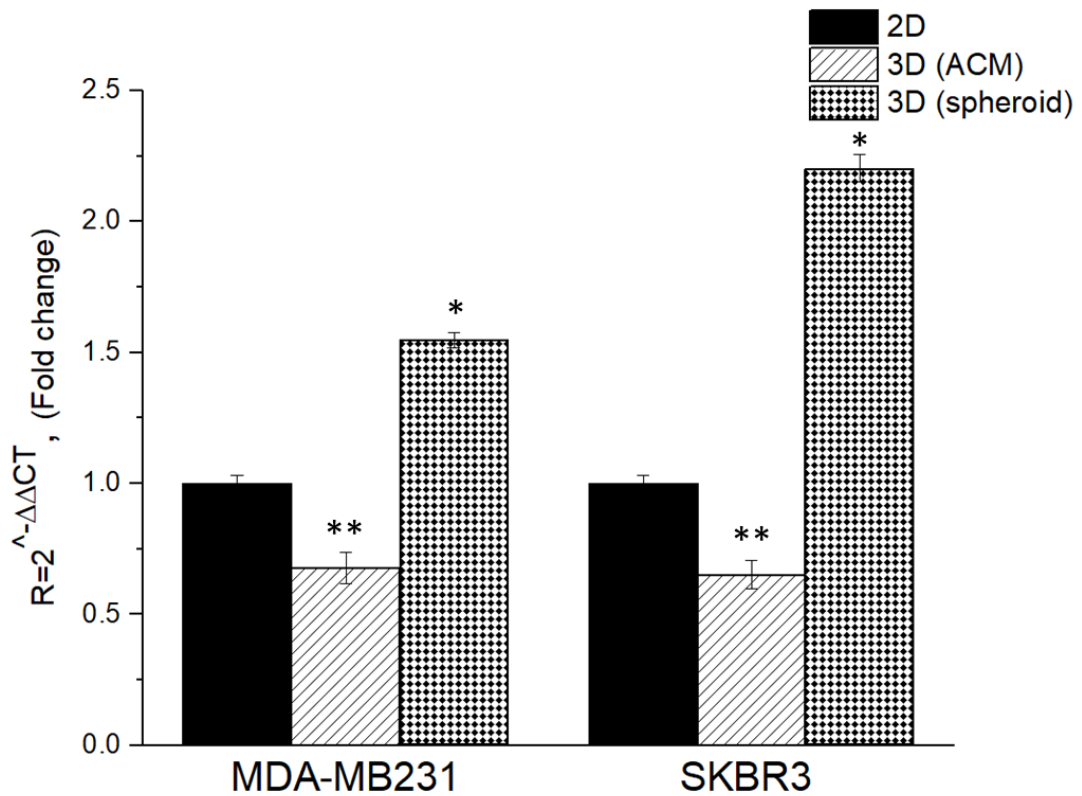


**Figure 11.** Quantification of Ki67 mRNA expression level in MDA-MB231 and SKBR3 cells cultured in 3D (ACM) and 3D (spheroid) relative to 2D culture. Ki67 mRNA level increased significantly when cells were cultured as spheroids compared to 2D culture. However, its expression decreased significantly when cells were grown in collagen matrix (ACM). The experiment was performed using quantitative real time PCR technique and mRNA expression levels were normalised with GAPDH as reference  $\Delta\Delta CT$  was calculated by subtracting  $\Delta CT$  2D culture (control) from  $\Delta CT$  of each culture condition.  $R = 2^{-\Delta\Delta CT}$ , corresponds to the fold change. Data presented is mean average  $\pm$  SD (n = 3). Asterisks denote significant differences in gene expression, paired Student's t-test; \*P < 0.05; \*\*P < 0.01; \*\*\*P < 0.001

### 3.3 Investigating hypoxia status by measuring HIF-1 $\alpha$ mRNA expression

To investigate if the growth of MDA-MB231 and SKBR3 cells in 3D culture format (with and without ECM) can generate a hypoxic environment, the mRNA expression level of HIF-1 $\alpha$  was measured using qPCR.

HIF-1 $\alpha$  is an oxygen sensitive subunit of HIF-1 protein and its expression is induced under hypoxic conditions. The relative gene expression was calculated for all samples in relation to control samples (cells cultured in 2D)

with gene expression normalised to GAPDH as an internal reference gene. The data have been obtained from three experiments performed in triplicate, Figure 12, There was no significant difference between HIF-1 $\alpha$  mRNA level of MDA-MB231 cells cultured in ACMs compared to that for cells cultured in 2D. HIF-1 $\alpha$  levels in SKBR3 cells was significantly increased, in ACM conditions. However, growing both cell lines as spheroid resulted in significant increase in HIF-1 $\alpha$  mRNA level with 7 fold and 37 fold increase in MDA-MB231 and SKBR3 cells respectively.

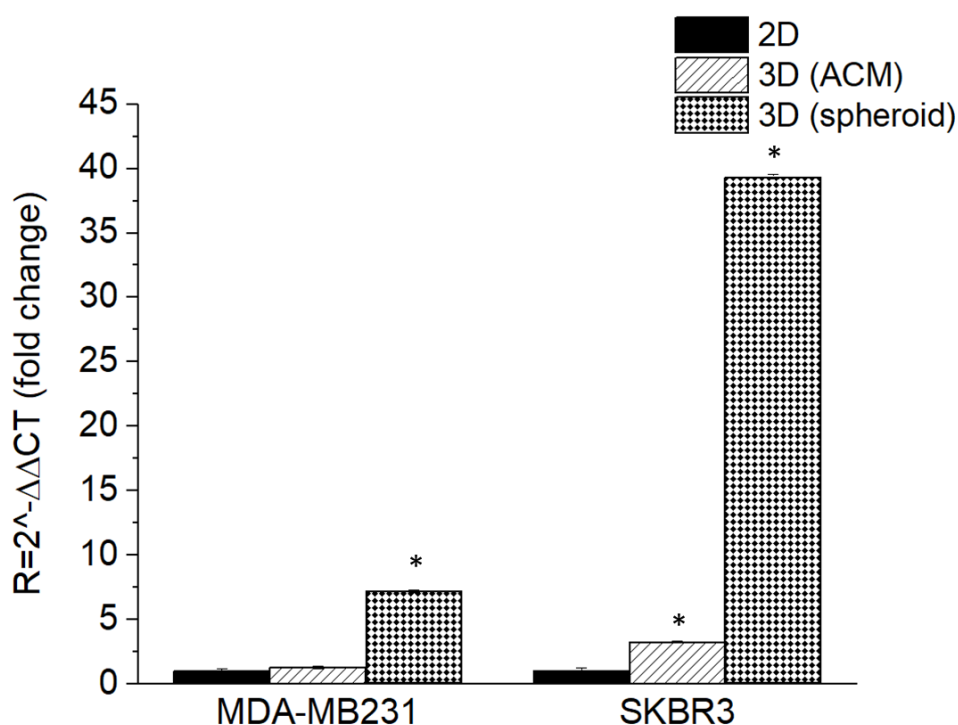


**Figure 12.** Quantification of HIF-1 $\alpha$  mRNA expression levels in MDA-MB231 and SKBR3 cells cultured in ACM and spheroid relative to its level in 2D culture after a week. HIF-1 $\alpha$  mRNA expression level increased significantly when both cells grown in spheroid format compared to 2D culture. Its expression also increased significantly when SKBR3 cells cultured in collagen matrix. The experiment was performed using quantitative real time PCR technique and mRNA expression levels were normalised with reference to GAPDH.  $\Delta\Delta CT$  was calculated by subtracting  $\Delta CT$  2D culture (control) from  $\Delta CT$  of each culture condition.  $R = 2^{-\Delta\Delta CT}$ , corresponds to the fold change. Data presented are mean average values  $\pm$  SD (n=3). Asterisks denote significant differences in gene expression, paired Student's t-test; \*P < 0.05.

### 3.3 EMT mRNA expression levels in MDA-MB231

In this part of study, the aim was to investigate if maintaining cells in 3D culture, ACM and spheroid, affects the EMT status of MDA-MB231 cells. Since expression levels of the selected EMT marker genes were too low in SKBR3 cells, they were excluded from this part of study. Accordingly, qRT-PCR was used to assess the levels of mesenchymal cell markers: snail, Cadherin-11, Vimentin and MMP14 (MT1-MMP) for cells grown in 2D, and in 3D as ACM and spheroids for 7 days. Relative gene expression was determined for samples grown in 3D compared with those grown in 2D in relation to control samples (MDA-MB cells cultured in 2D) and corrected to Ct values of the housekeeping gene (GAPDH). The data has been obtained from three experiments performed in triplicate, Figure 13.

Although the vimentin mRNA level was shown to be slightly higher in both 3D cultures compared to 2D condition, no significant difference between the 3 samples (3 culture conditions) was evident.

Different trends were observed in results obtained from analysing MMP14 and snail1 mRNA expression level in MDA-MB231 cells. Compared to 2D culture, MMP14 mRNA level increased significantly by 2 folds in ACM and 3 folds in spheroid. A significant elevation in snail1 expression was also observed, with 2.7 (ACM) and 3 (spheroid) folds increase compared to 2D condition.

In contrast, a significant reduction (75%) in Cadherin-11 mRNA level was observed in MDA-MB231 cells cultured in (ACM) compared to the cells in 2D. However, when cells were grown as spheroids, Cadherin-11 mRNA level increased significantly by 5-fold. These results suggest that 3D microenvironment may induce the expression of MMP14 and snail 1 genes regardless of ECM presence and that vimentin expression was less affected by altering the microenvironment. In contrast, different microenvironments and culture conditions may have an influence on cadherin11 expression.

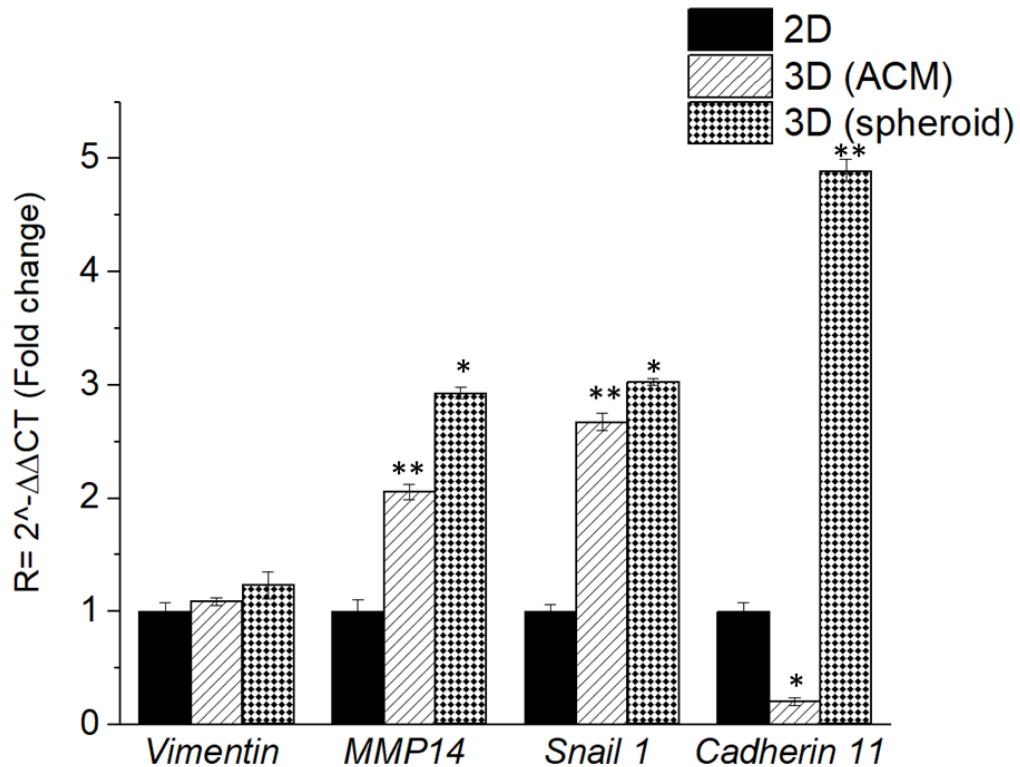


**Figure 13.** Quantification of expression level of the genes involved in EMT in MDA-MB231 cells cultured in 3D (ACM) and 3D (spheroid) relative to 2D culture. The expression levels of MMP14, snail and cadherin 11 increased significantly when cells were grown as spheroid. The mRNA expression of MMP14 and snail 1 also increased in cells grown in collagen matrix while cadherin 11 expression showed a significant reduction compared to 2D condition. Vimentin mRNA expression increased slightly in 3D spheroid and ACM culture compared to 2D condition (non-significant). The experiment was performed using quantitative real time PCR technique and mRNA expression levels were normalised against GAPDH.  $\Delta\Delta CT$  was calculated by subtracting  $\Delta CT$  2D culture (control) from  $\Delta CT$  of each culture condition.  $R = 2^{-\Delta\Delta CT}$ , corresponds to the fold change. Data presented are mean average values  $\pm$  SD (n=3).

### 3.4 Western blot analysis and immunostaining for vimentin protein in MDA-MB231 cells

To confirm the results obtained from qRT-PCR analysis of vimentin in MDA-MB231, the protein level was assessed using Western blot analysis. Since ACMs were selected as 3D model to be used in the next step of the project (applying flow), only ACM (using collagen type-I) were selected to be assessed in this regard. The MDA-MB231 cells cultured in 3D (ACM) conditions were harvested following collagenase treatment of the ACM as described in 2.2.3

The total protein concentration was measured using BCA assay and 10 µg of total protein from each sample (2D and 3D) was separated using SDS-PAGE and probed against vimentin antibodies after being transferred to nitrocellulose membrane. An anti-GAPDH antibody was used as a reference protein (loading control). Secondary antibody conjugated with HRP was used to detect primary antibodies bonded to the proteins on nitrocellulose paper and an enhanced chemiluminescence reaction system was used to detect the bands. Additionally, immunostaining experiments were performed to confirm the presence and distribution of target proteins in cells. Since the cells were embedded in collagen, the staining protocol followed for cells in ACM was slightly different from that used for cells in 2D culture.

The western blot result is shown in Figure 14(a). The vimentin protein was present in increased levels in MDA-MB231 cells grown in 3D (ACM) compared to those grown in 2D for 2 weeks. Since the anti-vimentin antibody used in western blot was against phosphorylated and non-phosphorylated types of vimentin, we assumed that the observed two bands correspond to phosphorylated and non-phosphorylated forms of vimentin. As can be seen in the Western blot result, the relative amounts of phosphorylated vimentin are increased in cells cultured in collagen (ACM) compared with cells cultured in 2D. This result suggested that although vimentin mRNA levels in 2D and 3D culture were not predominantly different, more vimentin filaments become phosphorylated through post translational modifications when the cancer cells are grown as 3D (ACM). Vimentin phosphorylation can lead to disassembly of vimentin filaments which increases cancer cell motility and invasion (Yasui et al., 2001). Vimentin protein levels were confirmed by images obtained from immunostaining of MDA-MB231 cells cultured in 2D and 3D for 2 weeks. Although different fluorescent microscopes were used due to limitations in the confocal microscopy apparatus, the images of the cell aggregates show that MDA-MB231 cells express almost the same amount of vimentin protein in their cytosol as they present in 2D, Figure 14 (b).

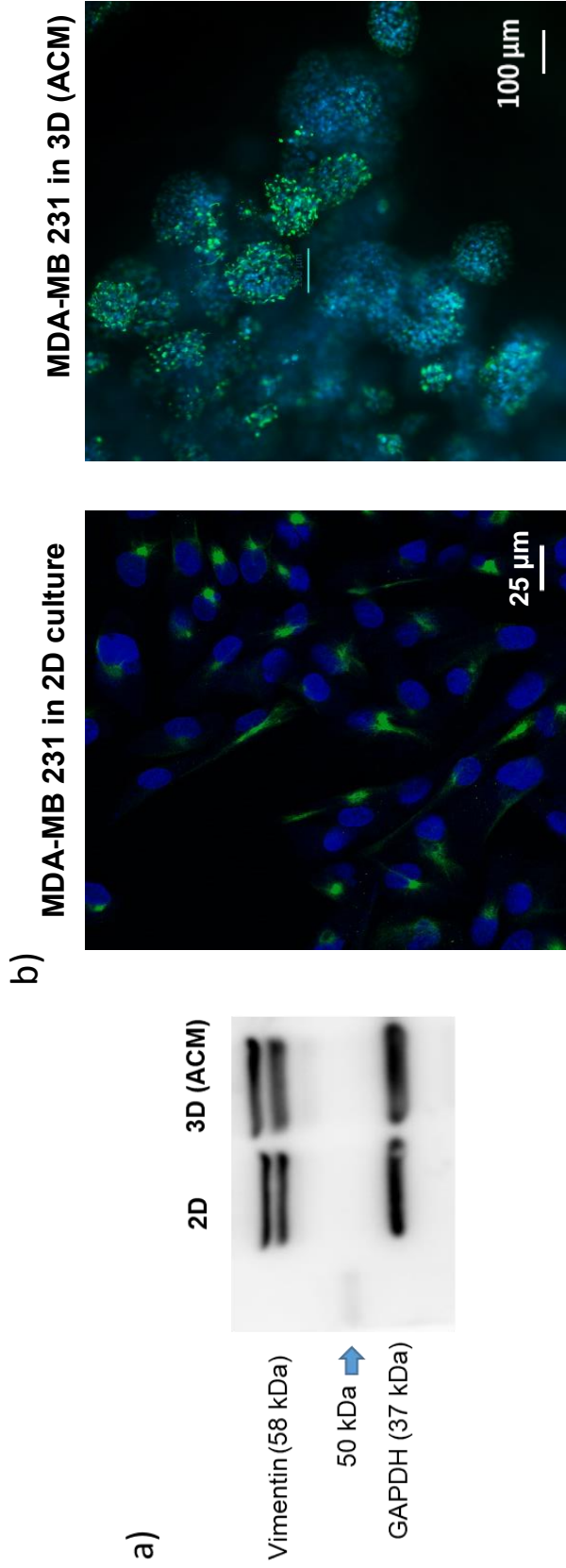


**Figure 14.** Analysis of level of vimentin protein in MDA-MB231 cells grown in 2D and 3D (ACM) culture. Panel a) Western blot analysis of vimentin protein in MDA-MB231 cells grown in 2D and 3D (ACM) cultures. 10  $\mu$ g protein was loaded in each well. GAPDH antibody was used as loading control. Vimentin protein level increased in the presence of collagen compared to 2D. Panel b) Immunofluorescent staining of MDA-MB231 using vimentin antibody. Left panel, taken using confocal microscopy, shows MDA-MB231 cells grown in 2D and stained with To-pro-3 (blue) and vimentin antibody (green). Right panel, taken using fluorescent microscope, shows MDA-MB231 cells grown in ACM and stained with DAPI (blue) and vimentin antibody (green). The cell aggregates formed in collagen expressed almost the same amount of vimentin protein as they do in 2D culture. Representative images taken from n=3 experiments.

### 3.5 Expression of HER2 in SKBR3 cells cultured in 2D and 3D

As described earlier, SKBR3 cells are highly positive for HER2 expression. To investigate the impact of different culture conditions on the level of HER2 mRNA expression, RNA was extracted from SKBR3 cells grown in 2D, ACM and spheroid for a week. Then, cDNA was prepared using reverse transcriptase kit and qPCR reactions performed. Relative to the 2D culture method, the HER2 mRNA level was higher by 1.3- and 1.7-fold when cells were grown as ACM and spheroid respectively, Figure 15. However, only spheroid culture conditions resulted in a statistically significant difference in gene expression, ( $p < 0.05$ ).

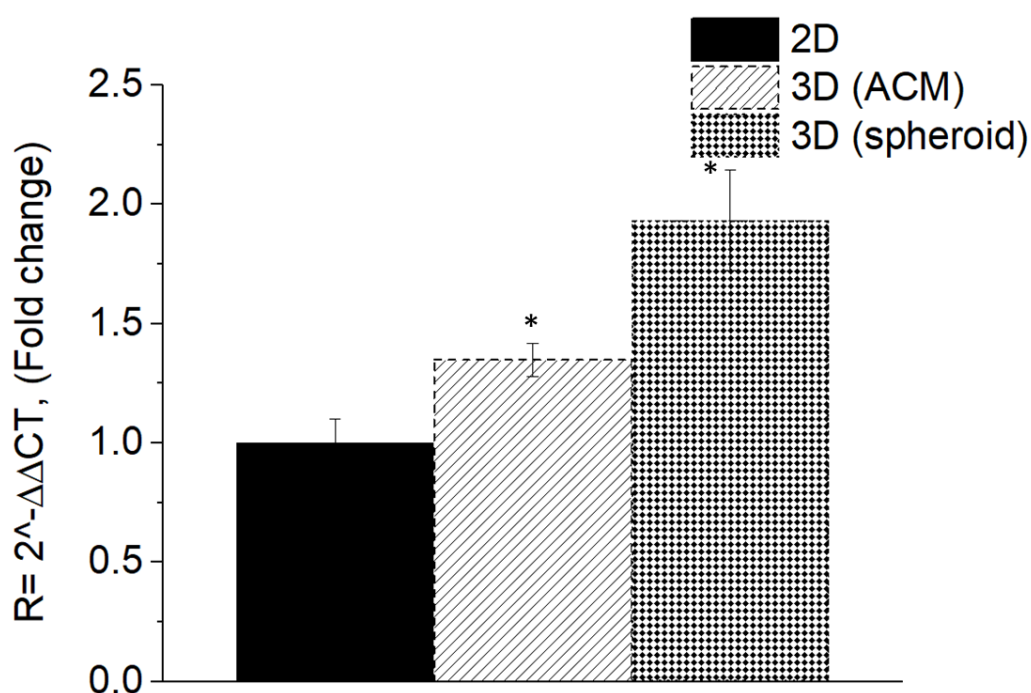


**Figure 15.** Quantification of HER2 mRNA expression in SKBR3 cells cultured as ACM and spheroid relative to its expression in cells grown in 2D condition. HER2 expression increased significantly in cells grown as spheroid and ACM compared to 2D culture. The experiment was performed using quantitative real time PCR and mRNA expression levels normalised against GAPDH.  $\Delta\Delta CT$  was calculated by subtracting  $\Delta CT$  2D culture (control) from  $\Delta CT$  of each culture condition.  $R = 2^{-\Delta\Delta CT}$ , corresponds to the fold change. Data presented: mean average  $\pm$ SD ( $n=3$ ).

### **3.6 Western blot analysis and immunostaining of HER2 protein in SKBR3 cells**

To confirm the results of the HER2 expression analysis obtained using the qPCR technique, the HER2 protein levels of SKBR3 cells cultured in 2D and 3D (ACM) was measured using Western blot and immunostaining assays. For HER2 Western blot analysis, SKBR3 cells were not treated with collagenase to avoid loss of HER2 from cell membrane. The ACMs were disrupted using lysis buffer (RIPA buffer) added to two pooled ACMs and a homogeniser (T25 digital Ultra-Turrax, U.K.). The anti-GAPDH antibody was used as loading control. The HER2 protein levels were slightly higher when the cells were cultured in collagen type-I as ACMs compared with 2D, Figure 16. However, the bands showing higher molecular weight indicate higher levels of phosphorylated HER2 compared to non-phosphorylated HER2 in both 2D and 3D cultured cells.

In addition to the results of the Western blot analysis, microscopy images taken following immunostaining of SKBR3 cells using the anti-HER2 antibody indicated the presence of HER2 protein in the cell membrane of the cells grown in 2D and cell aggregates that formed in 3D culture (Figure 16b).

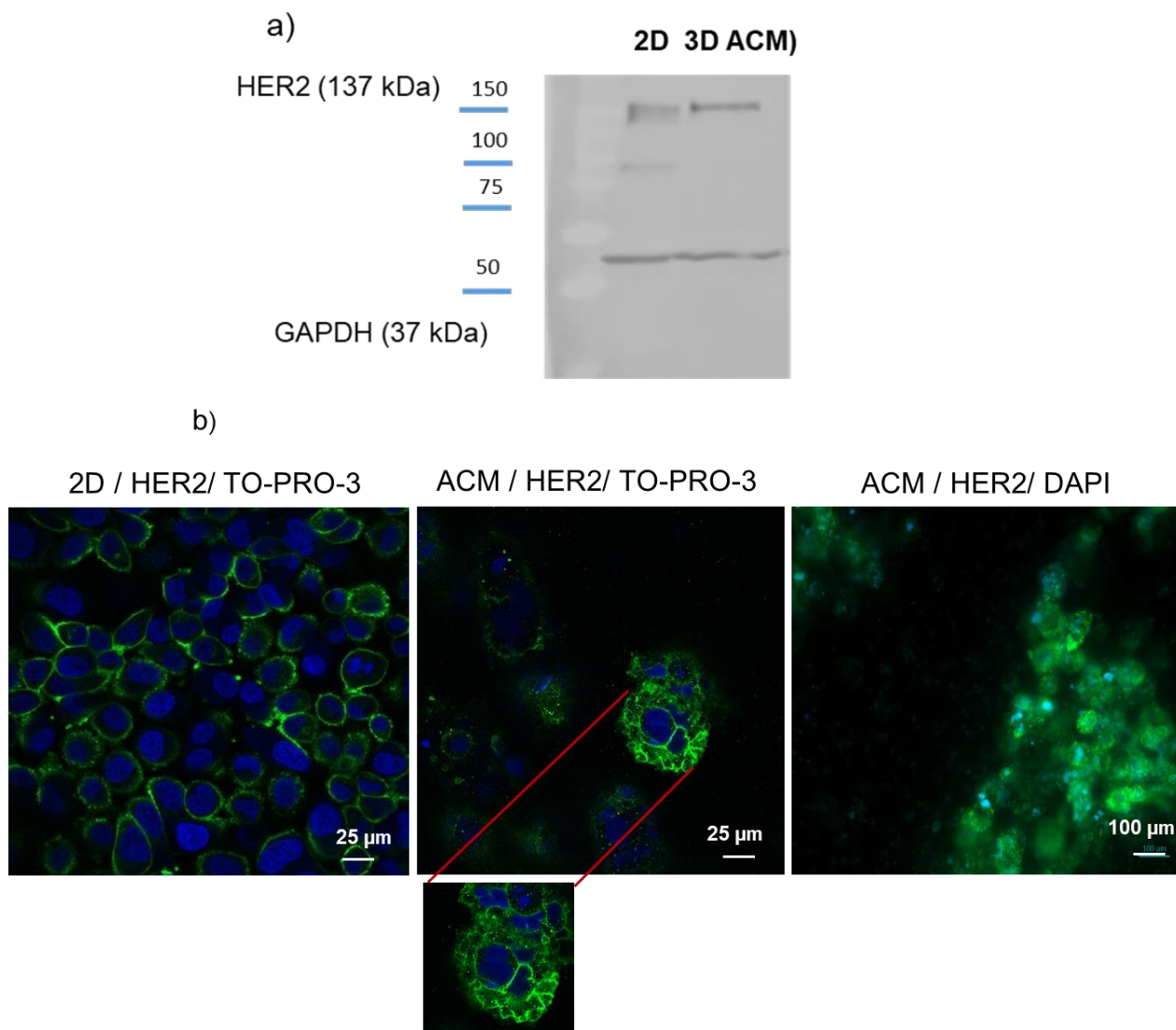


**Figure 16.** HER2 protein level in SKBR3 cells grown in 2D and 3D (ACM) condition. Panel a) Western blot analysis of HER2 protein in SKBR3 cells grown as 2D or 3D (ACM) cultures. 10  $\mu$ g protein was loaded in each well. GAPDH antibody was used as loading control. Panel b) Immunofluorescent staining of SKBR3 using HER2 antibody. Left picture, taken using confocal microscopy, shows SKBR3 cells grown in 2D and stained with To-Pro-3 (blue) and HER2 antibody (green). The middle image shows SKBR3 cell aggregates in ACM imaged using confocal microscope. The right image, taken using Zeiss Apo Tom 0.2 fluorescent microscope, shows SKBR3 cells grown in ACM and stained with DAPI (blue) and anti-HER2 antibody (green). The images indicated the presence of HER2 protein in SKBR3 cells cultured in 2D and 3D collagen matrix. Representative images taken from n=2 experiments imaged in triplicate.

### **3.7 mRNA expression of apoptosis-related genes**

To investigate if apoptotic changes occurred in MDA-MB231 and SKBR3 cells cultured in 3D (ACM), qPCR analysis was performed focusing on a panel of three apoptosis related genes including caspase 3, caspase 9 and BCL2. The transcriptional expression levels of BCL2, an anti-apoptosis factor, was significantly upregulated in MDA-MB231 cells grown in ACM, with a 5-fold increase compared to 2D conditions, Figure 17. However, no significant difference was observed in the mRNA expression levels of the proapoptotic markers caspase -3 and caspase -9 when MDA-MB231 cells were cultured in 3D. There was a reduction in the mRNA level of these proapoptotic genes in SKBR3 cells cultured in 3D (ACM) while a significant 1.4-fold increase was observed in BCL2 mRNA levels was observed in these cells. These results suggest that 3D collagen microenvironment do not induce the expression of pro-apoptotic markers in SKBR3 and MDA-MB231 cells. However, this environment may be associated with upregulation of the anti-apoptotic marker, BCL2.

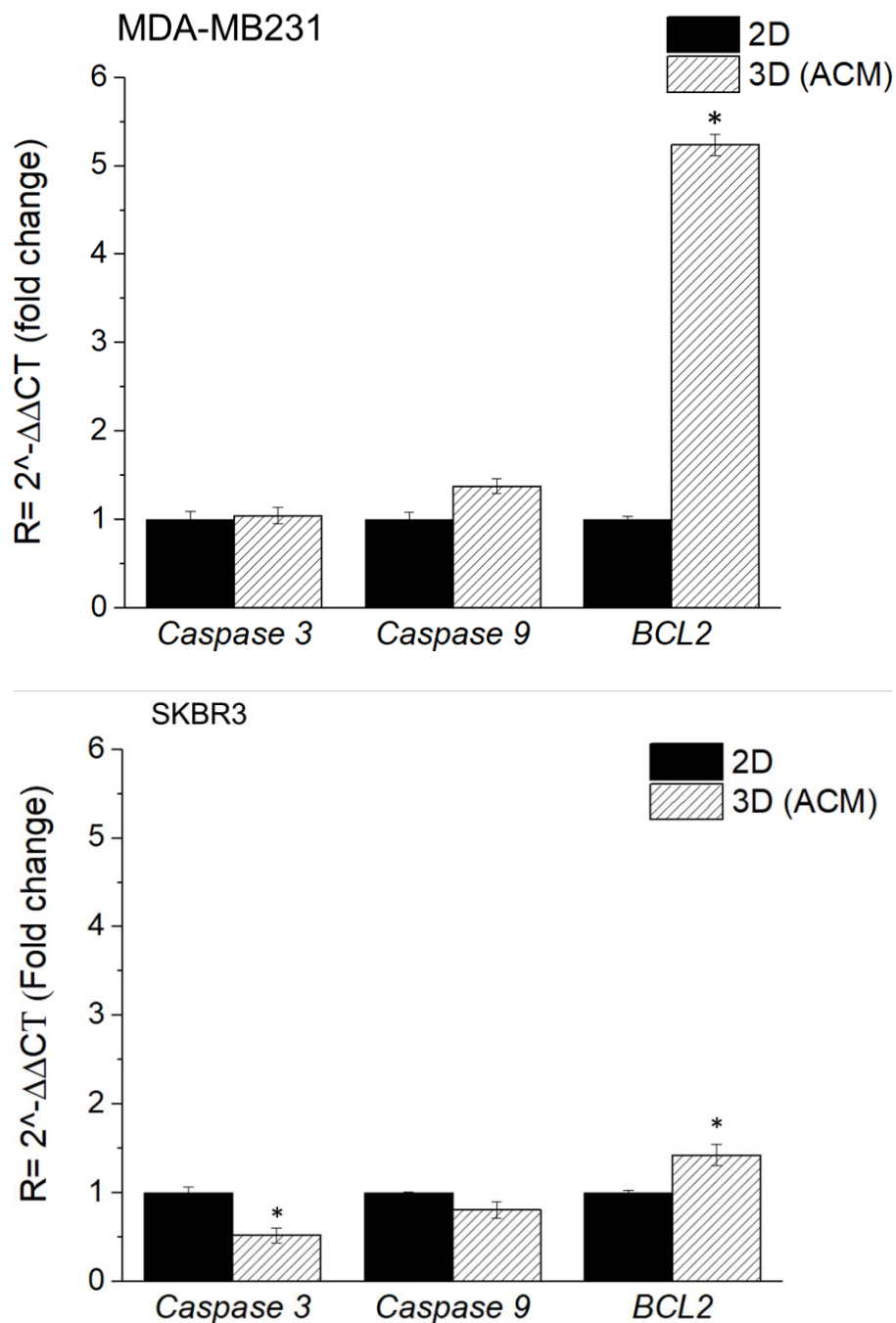


**Figure 17.** Relative quantification of apoptosis related genes in MDA-MB231 and SKBR3 cells cultured in 2D and 3D. The results indicated that BCL2 anti-apoptotic gene was upregulated in both cells when they were grown in 3D (ACM) condition compared to 2D condition. Transcriptional expression of indicated genes was measured by real-time qPCR. mRNA expression levels were normalised against GAPDH.  $\Delta\Delta CT$  was calculated by subtracting  $\Delta CT$  2D culture (control) from  $\Delta CT$  of each culture condition.  $R = 2^{-\Delta\Delta CT}$ , corresponds to the fold change. Data were presented are mean average  $\pm$  SD (n=3)

### 3.8 Efficacy of doxorubicin in 2D and 3D culture

To investigate if 3D culture and the microenvironment surrounding the cancer cells affected the cytotoxicity of doxorubicin, viability of the cells cultured in 2D and 3D (ACM) was measured after doxorubicin treatment using Alamar blue assay. To find out the appropriate concentration of doxorubicin for treating breast cancer cells in the next phase of study (comparing static and dynamic culture conditions), cells grown in 2D and 3D culture were treated with different concentrations of doxorubicin.

MDA-MB231 cells were insensitive to lower concentrations of doxorubicin (0.1  $\mu\text{M}$  and 0.5  $\mu\text{M}$ ) in both culture conditions while they responded to 1  $\mu\text{M}$  doxorubicin only in 2D culture. However, when MDA-MB231 cells were grown in 3D conditions they were significantly less sensitive to doxorubicin at concentrations of 5  $\mu\text{M}$  and 10  $\mu\text{M}$  compared to those grown in 2D, with increase in cell viability from 30% to 70% in concentration of 5  $\mu\text{M}$  and from 28% to 65% in concentration of 10  $\mu\text{M}$ , Figure 18. SKBR3 cells grown in 2D, showed a dose dependant decrease in cell viability in response to doxorubicin treatment, Figure 18. As observed with the MDA-MB231 cells, SKBR3 cells showed least sensitivity to lower concentrations (0.1  $\mu\text{M}$  and 0.5  $\mu\text{M}$ ) of doxorubicin. However, SKBR3 cells grown in both 2D and 3D, appeared to respond to doxorubicin at concentrations of 5 $\mu\text{M}$  and 10 $\mu\text{M}$ . The viability of the cells treated with 5  $\mu\text{M}$  doxorubicin appeared to be significantly (2.3 fold,  $p < 0.01$ ) greater in the cells grown in 3D compared to those in 2D. Also, at concentration of 10  $\mu\text{M}$ , the percent viability in SKBR3 cells grown in 3D culture appeared to be significantly (~1.6-fold,  $P < 0.01$ ) higher than those grown in 2D monolayer format.

Collectively, the results obtained from this part of project showed that both cell lines appeared to be more resistant to doxorubicin when cells cultured in ECM in 3D culture compared to 2D culture.

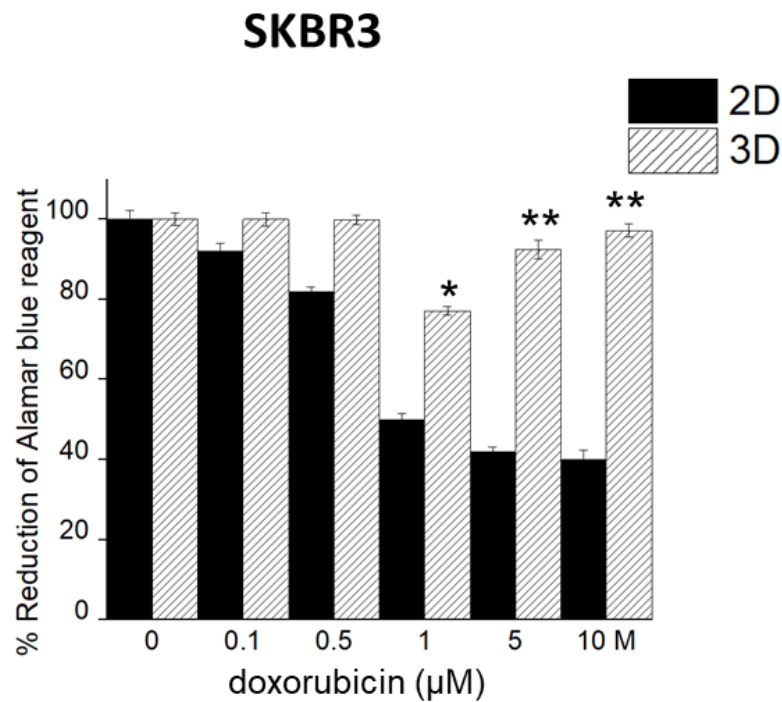
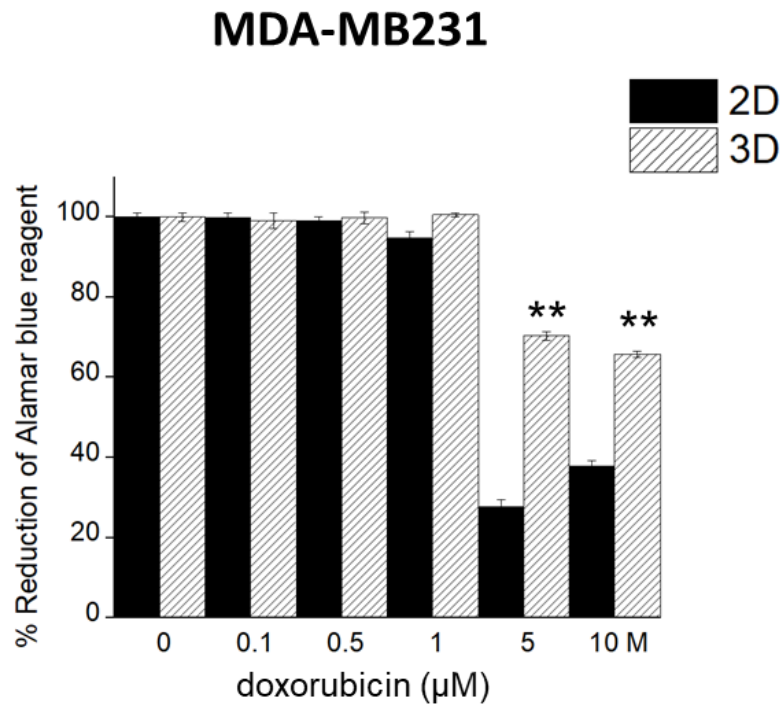


**Figure 18.** The cytotoxic effect of doxorubicin on MDA-MB231 and SKBR3 cells cultured in 2D and 3D. Both cell types showed less sensitivity to specific concentrations of doxorubicin when they were grown in 3D collagen matrix (ACM) compared to 2D condition. Three wells were assessed for each concentration. Data were presented as mean  $\pm$  SD (n = 3)

### **3.9 Cell aggregates and invasion bodies formed in static and flow/pressure conditions**

The cancer cells were grown in collagen type-I using RAFT system (ACM) and were maintained in static and flow/pressure conditions for two weeks (MDA-MB231) and one week (SKBR3). The formation of cell aggregates and invasion bodies were monitored using light microscopy and fluorescent microscopy (by staining only nuclei). To observe the number of cells in each aggregate, the nuclei of the cells in ACMs were stained with DAPI and imaged by the Apo Tom 0.2 microscope. Figure 19 shows a monochrome image of DAPI staining of the ACMs of both cell lines in static and flow/pressure conditions. As can be seen in Figure 19, left panel, from observing the nuclei of the MDA-MB231 ACMs, they formed more structured mass-shaped clusters whilst a grape-like morphology was adopted by the cells cultured under flow and pressure. Also, flow/pressure was associated with lower number of cells in MDA-MB231 cell aggregates compared to static condition.

When comparing the overall distribution of cancer cells in ACMs maintained in static and dynamic condition for a month, MDA-MB231 cells were dispersed more evenly over the ACM area while the shape of the invasion bodies - protrusion of cancer cells from the centre of ACM to the surrounding collagen - were more organised in static conditions, whereas in the presence of flow and pressure, cell protrusion was disorganised, and the edges were more jagged. In the case of SKBR3, no difference between the ACMs was noticed.

The size of SKBR3 cell aggregates and the number of cells in each cluster were not different in ACMs maintained in static and flow/pressure Figure 19, right panel. Also, comparing the two cell lines, SKBR3 cells formed smaller aggregates compared to MDA-MB231 cells. Also, the same distribution of SKBR3 cells in ACMs maintained in static and flow/pressure conditions was observed after a week. Overall, these results suggest that different breast cancer cells may react to changes in the fluid dynamics within their microenvironment in a different manner.

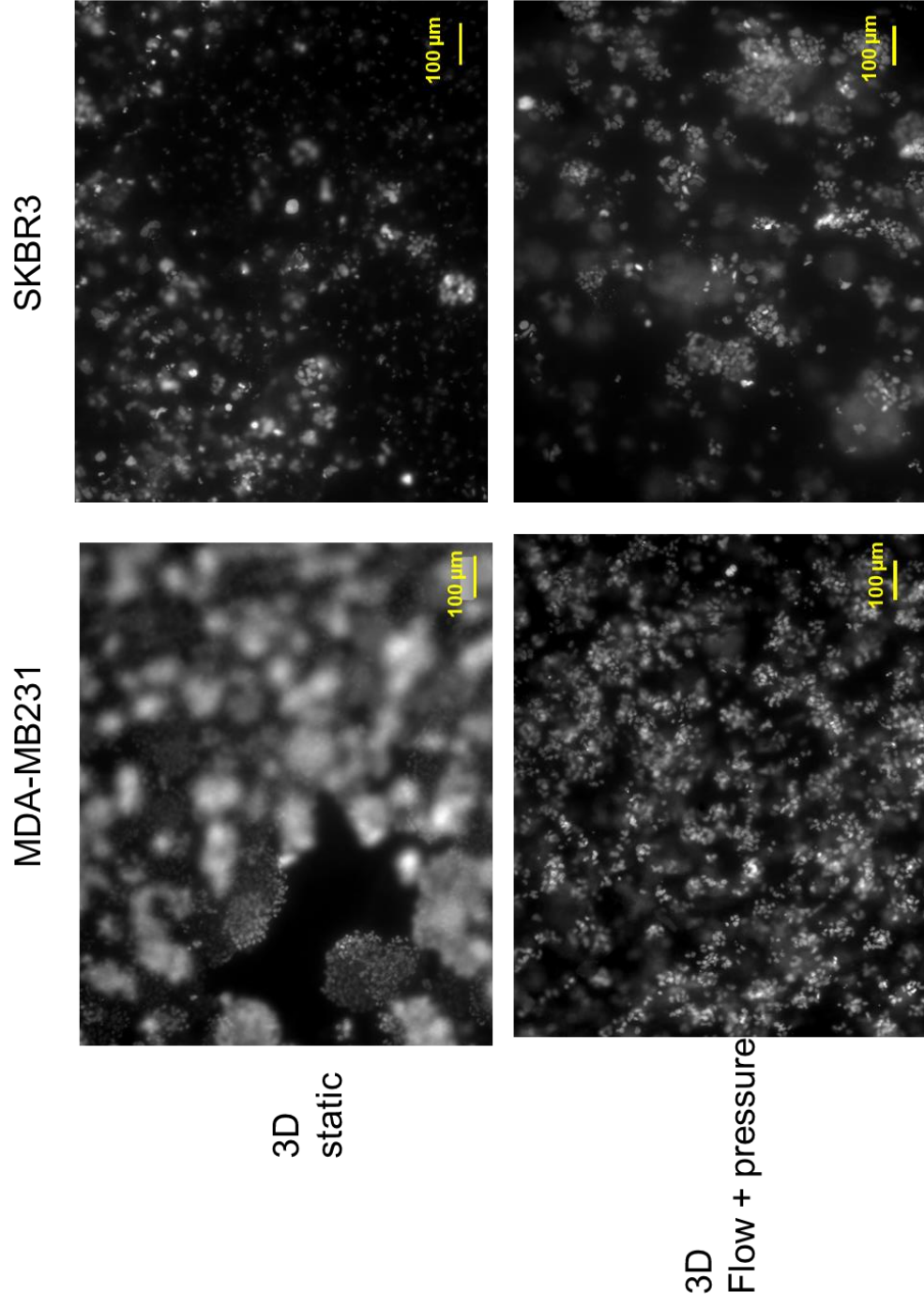


**Figure 19.** Microscopic images of the aggregates of MDA-MB231 (left panel) and SKBR3 (right panel) cells cultured in 3D (ACM) and maintained in static (top panel) and flow/pressure (bottom panel) for 2 weeks (MDA-MB231) and 1 week (SKBR3) using Apo Tom 0.2 microscope.

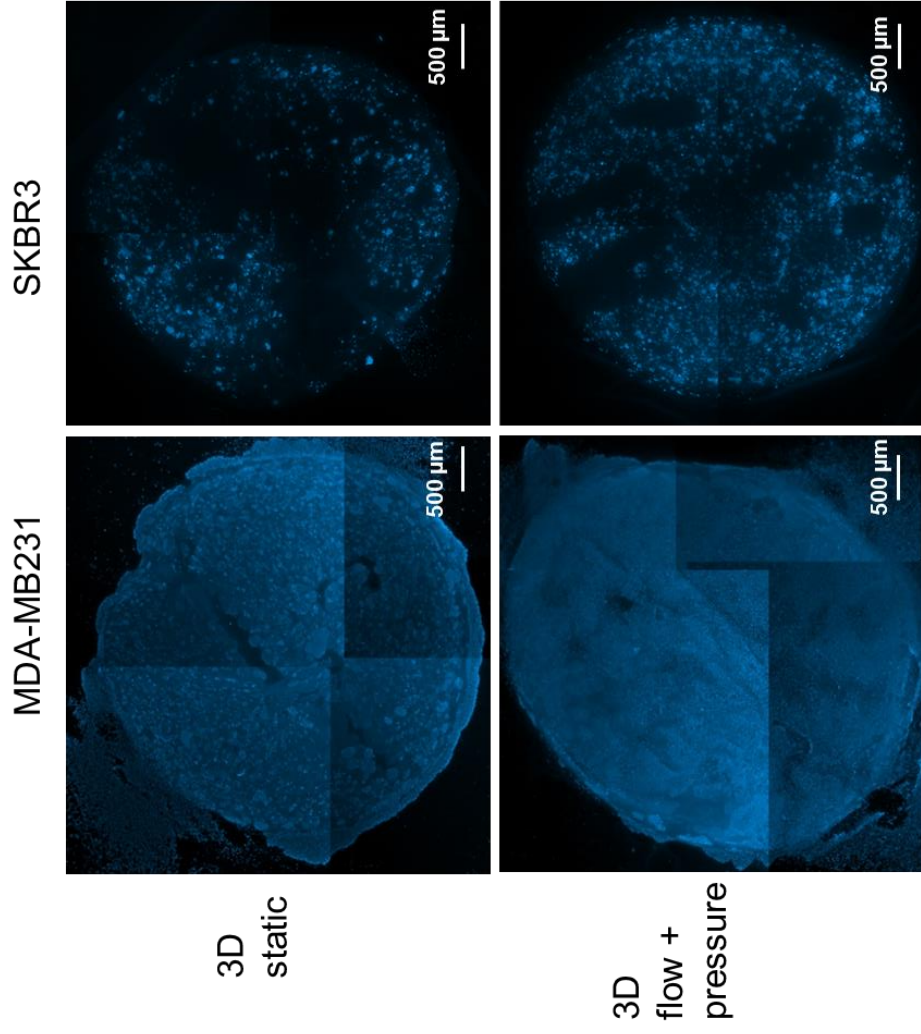


**Figure 20.** Nuclei of MDA-MB231 cells in ACM stained with DAPI. ACMs were maintained for a month under static and flow/conditions. Four images were taken of each quarter using the 2.5x objective of the Apo Tom 0.2 microscope. These images were then used to create the collages above. MDA-MB231 cells were dispersed more evenly over the ACM area while the shape of the invasion bodies was more organised in static conditions. There was no significant difference between distribution of SKBR3 cells in both conditions.

### **3.10 Comparing cell viability of cancer cells in static and flow/ pressure**

To investigate the effect of flow and pressure on cell viability of cancer cells, MDA-MB231 and SKBR3 cells cultured in 3D RAFT system (ACMs) were maintained under static and flow/ pressure (flow of 550  $\mu\text{L}/\text{min}$  and pressure of  $\sim 19$  mmHg) conditions for 14 (MDA-MB231) and 7 (SKBR3) days. Two ACMs were used for each condition. For the cells grown under static conditions, half of the media was replaced with fresh media every other day and for those grown in flow, this was done every 4 days due to the higher volume of the media (20 mL) that needed to run the Quasi Vivo system. Cell viability was measured using Alamar blue assay at three-time points: a day after constructing the ACMs (day 1), day 7 and 14 (for MDA-MB231 cells only).

As shown in Figure 21, the viability of MDA-MB231 cells maintained under flow/ pressure appeared to be less than those maintained in the static condition over a 14-days period. On the first day, all ACMs showed the same level of cell viability indicating that the cell density was the same in all ACMs before putting them under different conditions (static and flow + pressure). After 7 days, the viability of the cells in static condition increased by 50% while those grown in the flow /pressure condition, increased by only 15%, indicating a significant decrease in cell viability in flow/pressure system ( $P < 0.05$ ). However, the same increase gradient was observed in both conditions between 7<sup>th</sup> and 14<sup>th</sup> days, with only a 3.2% increase for both conditions. Overall, MDA-MB231 cells exhibited a 30% decrease in cell viability when cultured in flow/ pressure compared to static condition.

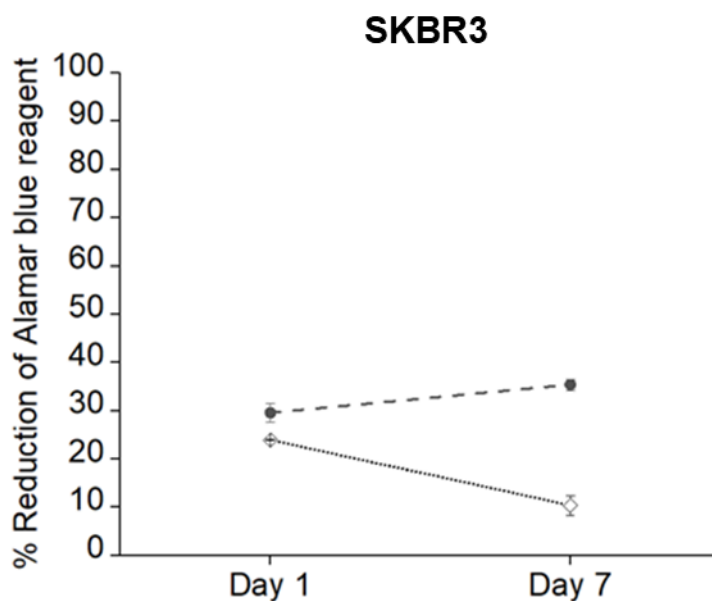
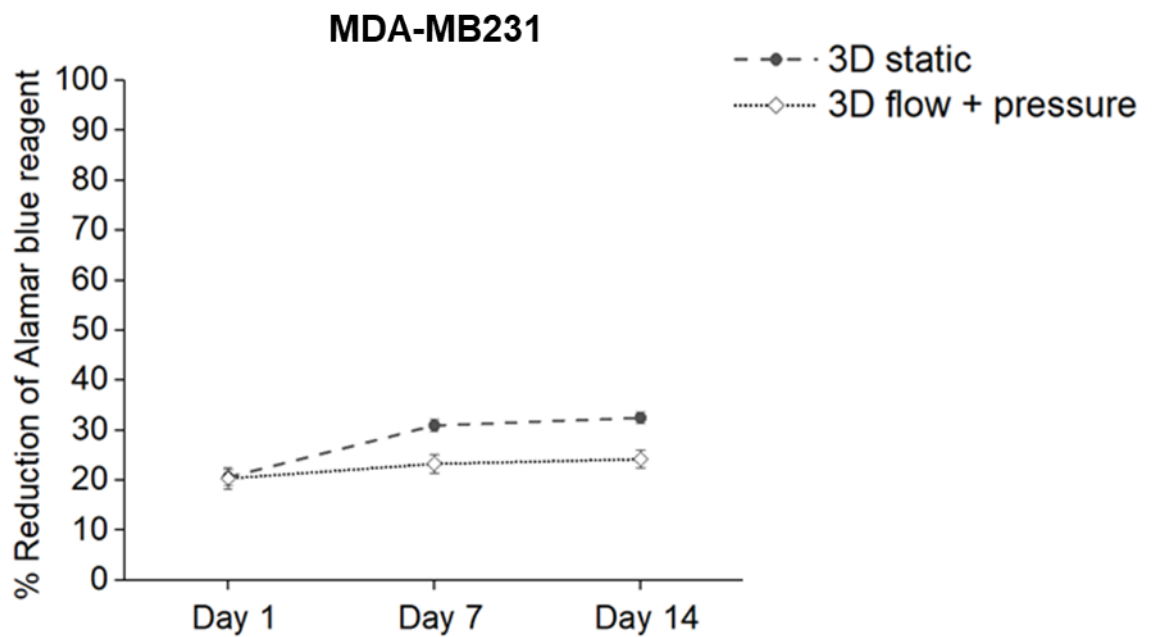


**Figure 21.** The effect of fluid flow and pressure on cell viability when cells are grown in 3D under static and flow conditions, measured by Alamar blue assay. Upper graph, MDA-MB231 cells grown over a 14-day, bottom graph, SKBR3 grown over a 7-day period. Both cell types were less metabolically active in the presence of flow and pressure compared to static condition. Data presented are mean average  $\pm$  SD (n=3).

Since the cellular viability of SKBR3 cells grown in 3D and flow + pressure conditions decreased considerably after a week, the Alamar blue assay was performed only on days 1 and 7. Four ACMs were formed using RAFT system and 2 ACMs were allocated to each condition. Cell viability was measured at day 1 after seeding was slightly different in each condition.

Cells grown under the static conditions demonstrated a 20% increase in cell viability while those cultured under flow/ pressure exhibited no increase in cell viability, but surprisingly their viability fell by 58% compared to first day. In general, these results indicate that SKBR3 cells cultured in 3D (ACMs) and flow condition are significantly ( $P < 0.05$ ) less viable compared to those grown in 3D/static condition.

### **3.11 Ki67 mRNA expression level in the cancer cells cultured in static and dynamic conditions**

Metabolic (oxidation-reduction) reactions maintain a reduced environment in the cell's cytosol which can reduce Alamar blue reagent and change its colour from blue to pink. Given this fact, any change in percentage of reduction of Alamar blue reagent can be either due to alteration in cell proliferation and growth or changes in the metabolic activity of the cells themselves. To identify if cells cultured under static and flow/pressure conditions differ in terms of cell proliferation, Ki67 expression levels were measured using qPCR. In both conditions, 3D static and flow/pressure, cells exhibited lower expression levels of Ki67 compared to when they were cultured on 2D surfaces (Appendix 4). However, comparing static and flow/pressure conditions, there was a significant ( $P < 0.01$ ) increase in Ki67 mRNA expression levels in the cells (both cell lines) maintained in flow/pressure compared to those grown in static condition. Figure 22 The Ki67 expression level increased by 1.31 and 1.33 fold in MDA-MB231 and SKBR3 cells respectively, when they were grown under the flow/pressure condition compared to the static condition. These

results indicated that the dynamic environment (flow/pressure) increased expression of proliferation markers in MDA-MB231 and SKBR3 breast cancer cell lines. Also, these results indicate that the decrease in metabolic activity, which was found in previous Alamar blue assay is not due to lower proliferation rate in cells cultured in flow but likely due to lower rate in metabolic reactions themselves.

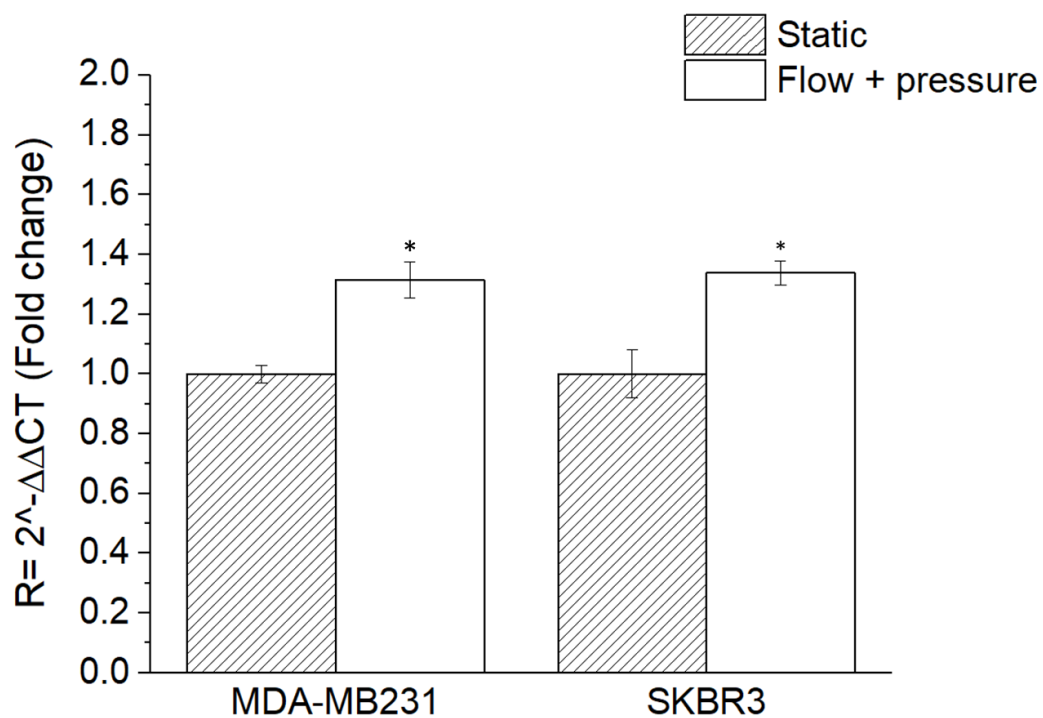


**Figure 22.** Relative quantification of Ki67 gene expression levels in MDA-MB231 and SKBR3 cells cultured in static and flow/pressure conditions. Ki67 mRNA level of both cell types increased significantly in the presence of flow and pressure compared to static condition.  $\Delta\Delta CT$  was calculated by subtracting  $\Delta CT$  2D culture (control) from  $\Delta CT$  of each culture condition.  $R = 2^{-\Delta\Delta CT}$ , corresponds to the fold change. Data is mean average  $\pm$  SD (n=3).

### **3.12 Hypoxia status of the cells grown in 3D/static and 3D/dynamic conditions**

To investigate if flow and pressure might generate hypoxic conditions in cancer cells grown in 3D scaffolds (ACM), HIF-1 $\alpha$  mRNA expression levels were measured in MDA-MB231 and SKBR3 cells grown in 3D and maintained under three different conditions: static, flow (150  $\mu$ l/min) and flow/pressure (550  $\mu$ l/min, ~19mmHg), Figure 23. The R (fold change) (Schmittgen and Livak, 2008), was calculated by considering cells cultured in static condition as the control group. A significant increase in expression of HIF1- $\alpha$  mRNA was observed in cells cultured in flow condition (2.2 fold) compared to those cultured in static condition. However, when ACMs were maintained under flow/pressure conditions, there was no significant difference in HIF1- $\alpha$  expression. A similar pattern was observed in SKBR3 cells cultured in the different conditions. Flow was associated with a significant increase (1.8 fold,  $P < 0.05$ ) in HIF-1 $\alpha$  gene expression whereas flow and pressure resulted in no significant difference in expression of this gene compared to the static condition. These results suggest that cells cultured under flow rate (of 150  $\mu$ L/min) may be under more hypoxic conditions compared to those cultured in the higher flow rate of 550  $\mu$ l/min + pressure (~19 mmHg).

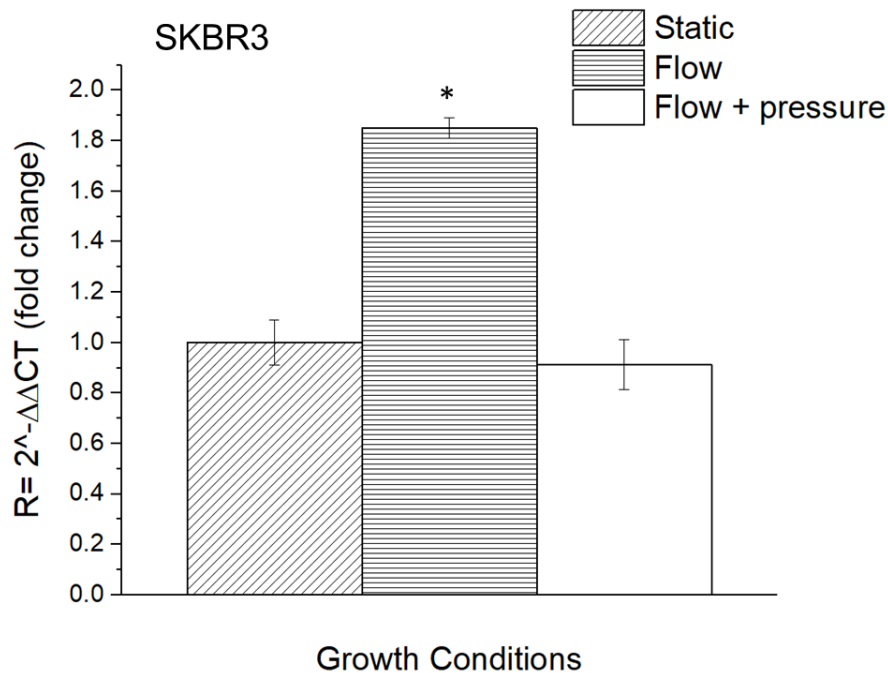
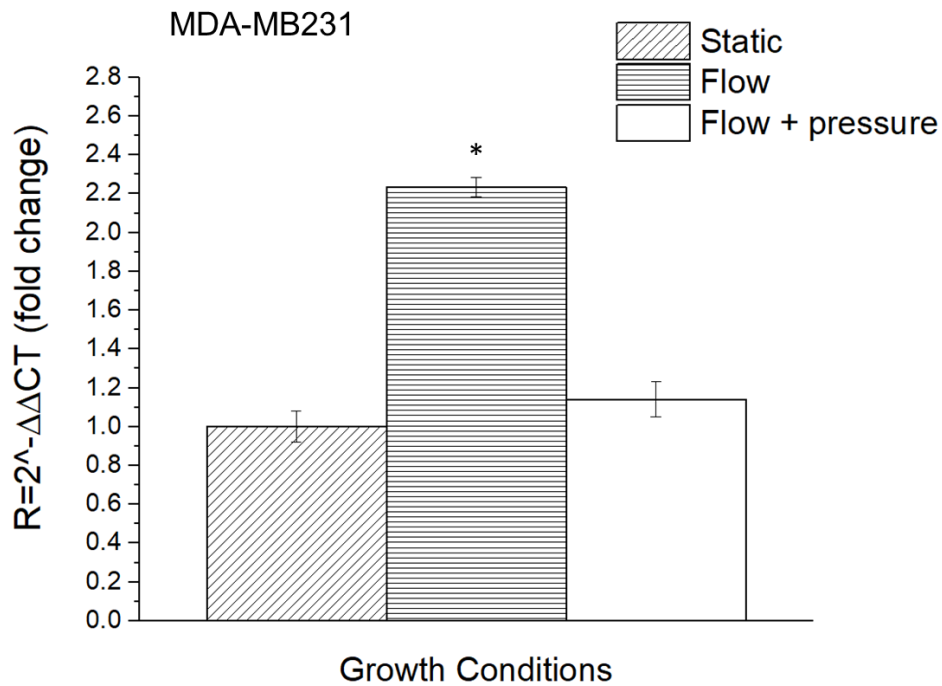


**Figure 23.** Relative quantification of HIF-1 $\alpha$  mRNA expression levels in MDA-MB231 cells cultured in 3D static, 3D flow and 3D flow + pressure after 2 weeks. HIF-1 $\alpha$  expression increased significantly in flow condition compared to static condition however it remained unchanged in flow + pressure. The experiment was performed using quantitative real time PCR and mRNA expression levels were normalised against GAPDH.  $\Delta\Delta CT$  was calculated by subtracting  $\Delta CT$  static culture (control) from  $\Delta CT$  of the other culture conditions.  $R = 2^{-\Delta\Delta CT}$ , corresponds to the fold change. Data presented are mean average  $\pm$  SD (n = 3).

### **3.13 EMT marker expression in MDA-MB231 cultured in static and dynamic conditions**

Having defined the effect of 3D culture and cell-ECM contacts on expression of mesenchymal markers in MDA-MB231 cells (section 3.5), the effect of flow and pressure on expression of these markers in MDA-MB231 cells cultured in 3D (ACM) was evaluated. Six ACMs were constructed in 24-well plates and maintained at 37°C with 5% CO<sub>2</sub> in static condition for one day. On day 2, two ACMs were kept in the static condition, two ACMs were transferred to flow (150 µL/min) and two ACMs were transferred to flow/pressure (550 µL/min & ~19 mmHg) culture conditions. After two weeks, the cells in all ACMs were collected and cDNA was prepared from extracted RNA. Cells grown in static were considered as control samples. Equal amounts of cDNA was used for qPCR analysis of the genes in all conditions.

The 2D culture was considered as control and relative gene expression was calculated. There was generally an increase in gene expression for Vimentin, MMP14 and snail1 in MDA-MB231 cells cultured in 3D and maintained in all three conditions (static, flow and flow/pressure) relative to cells grown in conventional 2D monolayer culture. The only exception observed was the reduction of vimentin (40%) mRNA level in the cells cultured in flow/pressure. However, there was a 1.6 fold increase in its expression level when the ACMs maintained under flow of 150 µl/min (Appendix 5) As it was also shown in previous section (3.4) there was no significant increase in vimentin mRNA level when they grew in 3D/static compared to 2D condition. Figure 24 shows the mRNA expression of the three genes for MDA-MB231 cells grown in the dynamic condition relative to static condition. Vimentin expression increased by 1.7-fold ( $P < 0.05$ ) in the presence of flow and decreased by 0.7 ( $P < 0.05$ ) fold when flow/pressure was applied. Analysis of MMP14 mRNA level in MDA-MB231 cells cultured in flow and flow/pressure indicated a 1.5-fold increase in both conditions compared to static. These results show that presence of fluid flow and pressure in the microenvironment of MDA-MB231 cell growth, result in elevated expression of MMP14. Like vimentin and MMP14, snail 1 mRNA

expression level increased when MDA-MB231 cells were grown in flow compared to when grown in static conditions, with 2.5- fold increase ( $P < 0.01$ ). However, flow/pressure conditions appeared to have no effect on snail1 mRNA expression level compared to static conditions.

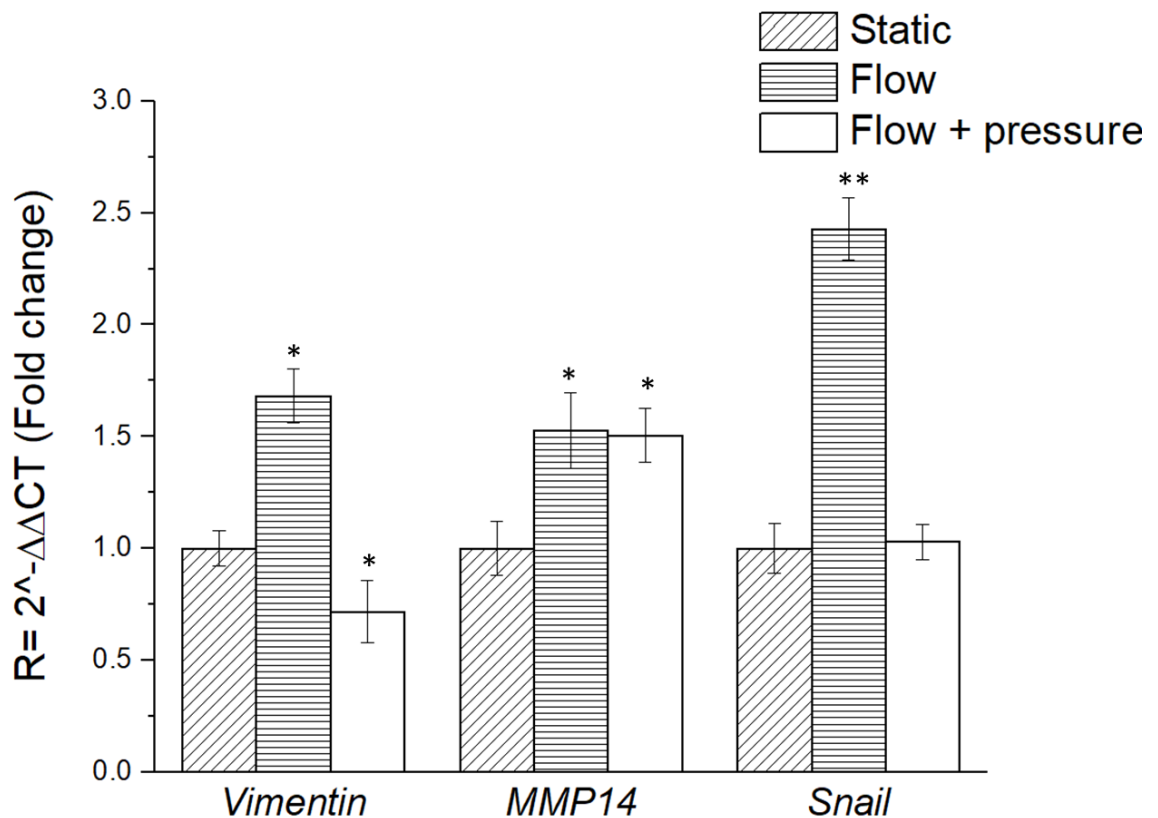


**Figure 24.** Relative quantification of vimentin, MMP14 and snail1 mRNA expression levels in MDA-MB231 cells cultured in 3D/static, 3D/flow and 3D/flow/pressure after 2 weeks. The experiment was performed using quantitative real time PCR technique and mRNA expression levels were normalised against GAPDH.  $\Delta\Delta CT$  was calculated by subtracting  $\Delta CT$  of static culture (control) from  $\Delta CT$  of each culture condition.  $R = 2^{-\Delta\Delta CT}$ , corresponds to the fold change. Data is mean average  $\pm$  SD ( $n=3$ ).

### 3.14 Western blot and immunostaining of vimentin protein in MDA-MB231 cells cultured in static and flow/pressure condition

To confirm the results obtained from qRT-PCR analysis for vimentin in MDA-MB231, the protein level of vimentin was assessed using Western blot. Additionally, immunostaining was performed to confirm the presence and the location of the proteins in the cells. The same staining protocol was followed for ACMs maintained in static and flow/pressure condition. The Western blot results of 2D and 3D conditions has been previously discussed in section 3.5. Figure 25 shows that the vimentin protein level significantly decreased in MDA-MB231 cells grown in flow/pressure compared to those grown in static for 2 weeks. Two bands correspond to phosphorylated and non-phosphorylated forms of vimentin.

Vimentin protein level was confirmed by images obtained from immunostaining of MDA-MB231 cells cultured in static and flow/pressure for 2 weeks. The images of cell aggregates showed that MDA-MB231 cells express lower amount of vimentin protein in their cytosol in static conditions (figure 25b). Also, left panel of the images show that the amount of vimentin is lower in the edge of the ACMs (where the cells invade to the surrounding stroma) when they were maintained in flow/pressure compared to static.

a)

2D	+	-	-
3D	-	+	+
flow/pressure	-	-	+



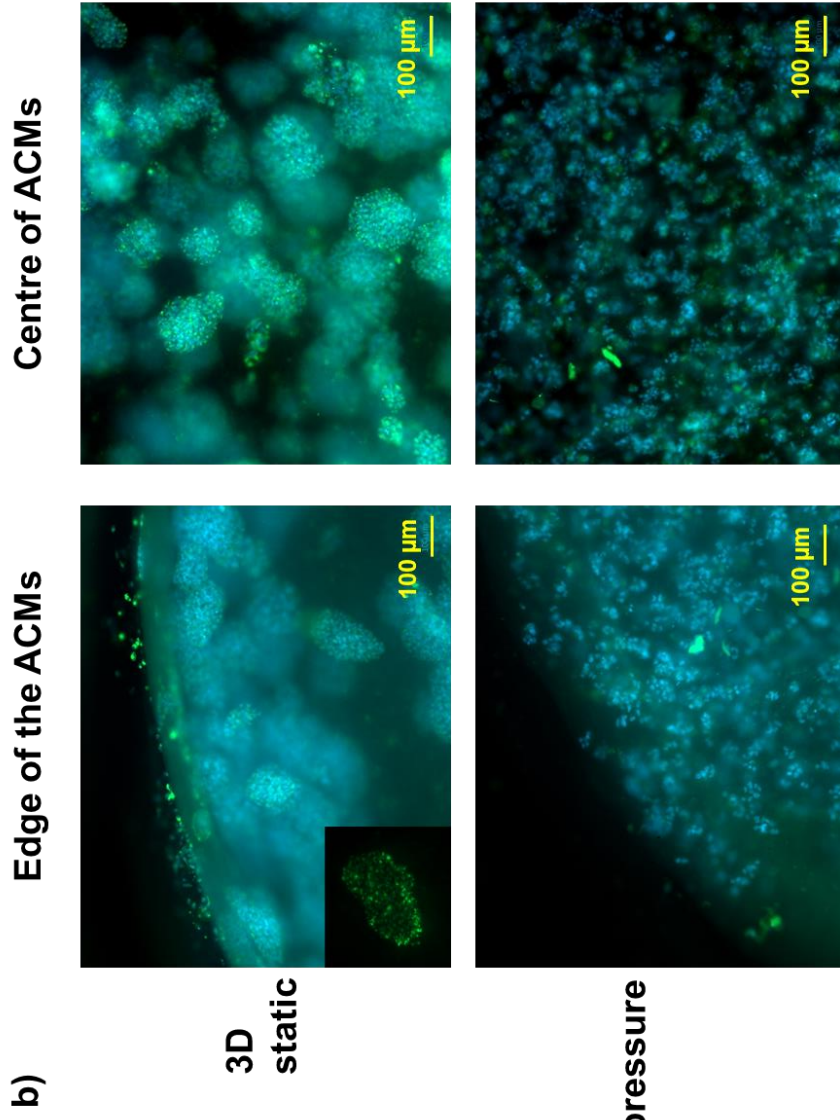


**Figure 25.** Expression of vimentin protein in MDA-MB231 cell maintained in static and flow + pressure conditions for two weeks. a) Western blot analysis of vimentin protein in MDA-MB231 cells grown in 3D (ACM) and maintained in static and flow + pressure conditions. 10 µg protein was loaded in each well. GAPDH antibody was used as loading control. Vimentin protein expression reduced significantly in the presence of flow and pressure compared to static and 2D conditions. b) Immunofluorescent staining of MDA-MB231 grown in ACM using Vimentin antibody (green). Left panel; the edges of ACMs and right panel; the centre the ACMs maintained in static and flow + pressure. The nuclei were stained with DAPI (blue). Images show a significant reduction in Vimentin protein level both at the edge and centre of the ACMs when the cells maintained under flow and pressure condition. Representative images taken from n=2 experiment

### 3.15 Expression of HER2 in SKBR3 cells cultured in 3D/static and 3D/flow/pressure conditions

As indicated in the previous chapter, HER2 mRNA level appeared to increase slightly as a result of cell-ECM interactions in the ACMs. To evaluate the effect of flow and pressure on HER2 expression of SKBR3 cells grown in ACM, 2 ACMs were maintained under flow of 550  $\mu\text{L}/\text{min}$  and pressure of  $\sim 19$  mmHg in the Quasi Vivo system for a week. The cells were harvested from the ACMs and RNA was extracted to be used for cDNA preparation. SKBR3 cells with the same passage number cultured in 3D (ACM) were considered as control group in qRT-PCR analysis and calculation of R (fold change). As shown in Figure 26, HER2 mRNA expression increased by 2.4 fold in flow/pressure compared to static condition and the difference was significant ( $P < 0.05$ ). The results suggest that SKBR3 cells express higher level of HER2 mRNA when they are grown under flow/ pressure conditions.

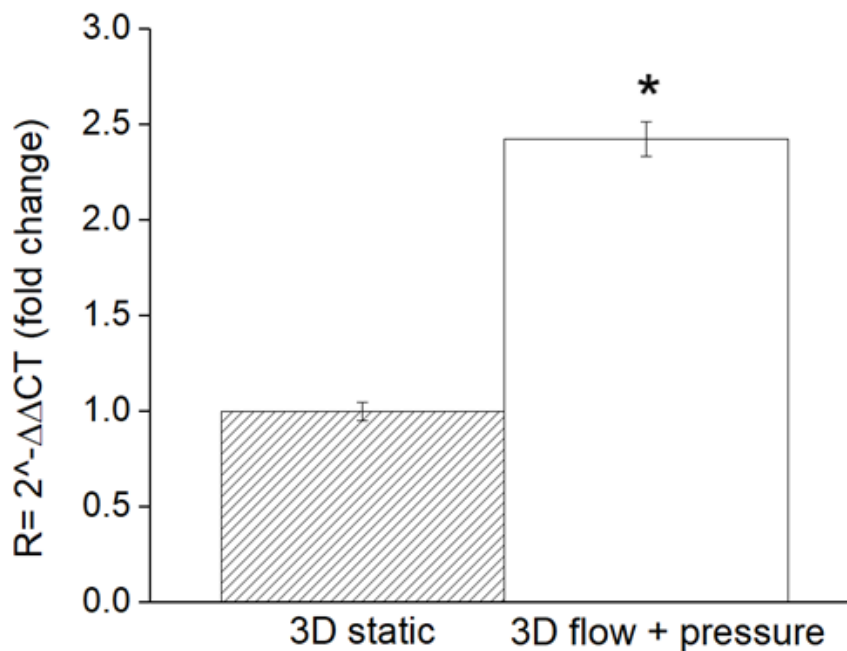


**Figure 26.** Relative quantification of HER2 mRNA expression levels in SKBR3 cells cultured in 3D static and 3D flow + pressure system after a week. The results indicated that HER2 expression upregulated in the presence of flow and pressure compared to static condition. The experiment was performed using quantitative real time PCR technique and mRNA expression levels were normalised against GAPDH.  $\Delta\Delta\text{CT}$  was calculated by subtracting  $\Delta\text{CT}$  static condition (control) from  $\Delta\text{CT}$  of each culture condition.  $R = 2^{-\Delta\Delta\text{CT}}$ , corresponds to the fold change. Data were presented as mean  $\pm$  SD ( $n = 3$ ).

### **3.16 Immunostaining of SKBR3 cells against HER2 antibody**

Following qRT-PCR analysis for HER2 gene expression, ACMs maintained in static and flow/pressure were stained using the anti-HER2 antibody, Figure 27. The fluorescent images obtained from the ACMs showed there was no significant difference between HER2 protein level in SKBR3 cells grown in 3D/static vs those in 3D/flow/pressure conditions.

### **3.17 mRNA expression of apoptosis-related genes in breast cancer cells cultured in 3D/static and 3D/dynamic conditions**

Relative quantification of caspase -3, caspase-9 and BCL2 genes was performed to investigate the effect of flow and pressure on expression of apoptosis-related genes in SKBR3 and MDA-MB231 cells. There was a 60% reduction in the expression of caspase 3 MDA-MB231 cells cultured in flow and pressure compared to static condition. In contrast, flow/pressure condition was associated with a significant increase of 13 fold in the expression of caspase 9 ( $P < 0.05$ ). Although not significant, expression of BCL2 reduced by almost 80% in flow and pressure compared to static condition, Figure 28.

A significant increase in mRNA levels of caspase -3 and -9 was observed in SKBR3 cells grown in flow/pressure condition with 3.5 and 2.5 fold higher expression, respectively, compared to static condition. Overall, the results obtained indicated that introducing flow and pressure on breast cancer cells increases the expression of pro-apoptotic markers (caspase-3 and caspase -9) and reduces the expression of the anti-apoptotic marker BCL2.

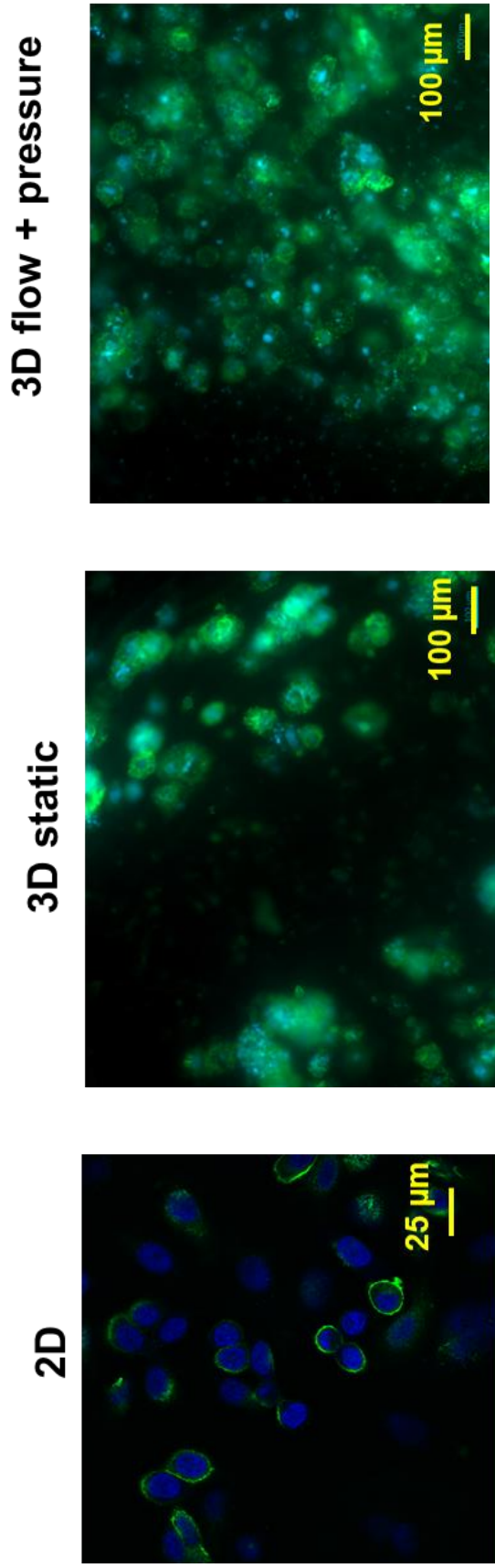


**Figure 27.** Immunofluorescent staining of HER2 proteins in SKBR3 cells grown in different microenvironments: from left to right: 2D, 3D static and 3D flow + pressure. The images show that HER2 protein level remained unchanged in all three conditions. The nuclei were counter-stained with TO-PRO-3 in the case of 2D and DAPI

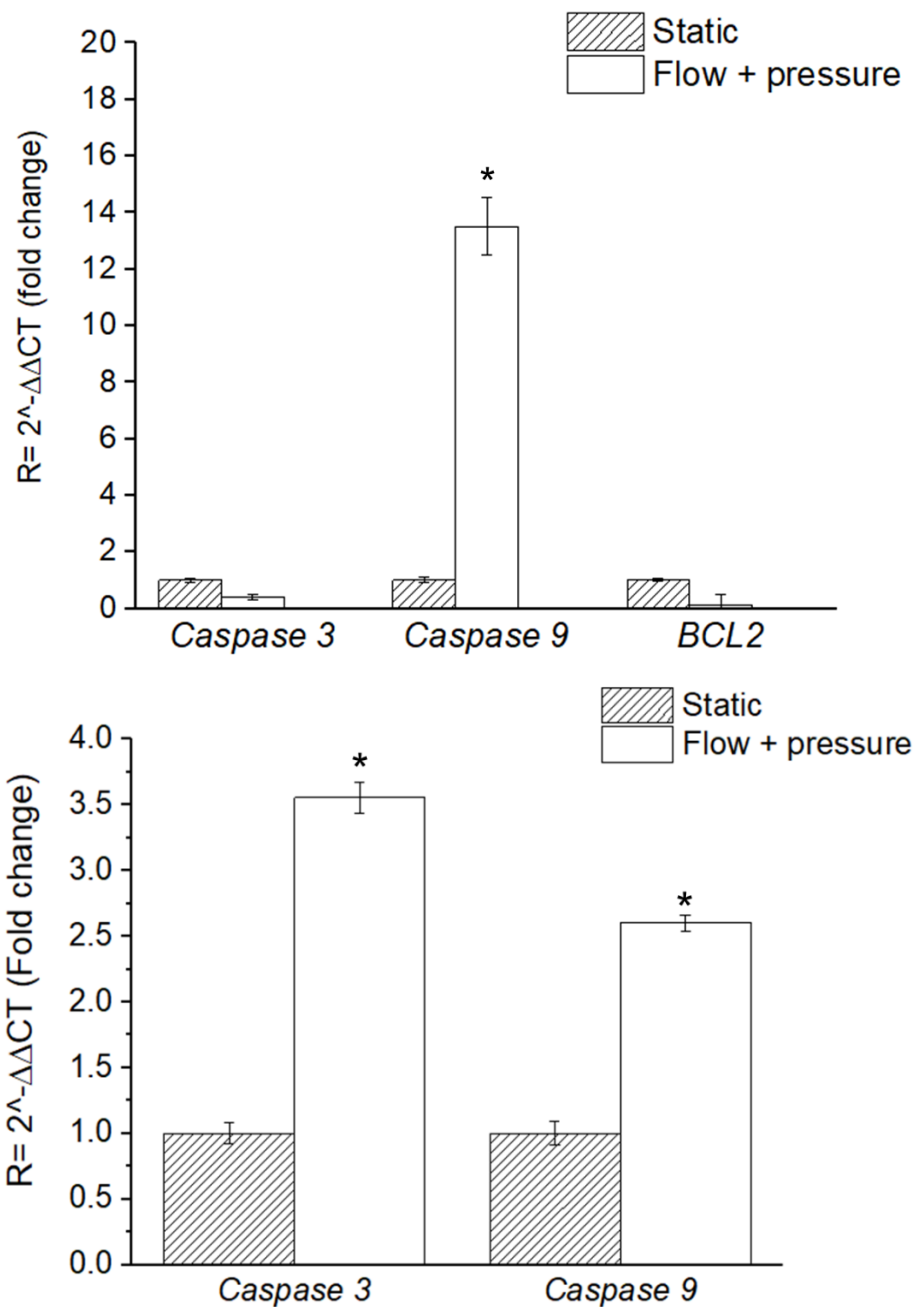


**Figure 28.** Quantification of apoptosis related genes in MDA-MB231 (top graph) and SKBR3 cells (bottom graph) cultured in flow + pressure condition relative to its level in static condition. Caspase 9 mRNA expression increased and BCL2 decreased in both cell types suggesting induction of apoptosis in the presence of flow and pressure. Transcriptional expression of indicated genes was measured by real-time qPCR. mRNA expression levels were normalised against GAPDH.  $\Delta\Delta CT$  was calculated by subtracting  $\Delta CT$  of static (control) from  $\Delta CT$  of each culture condition.  $R = 2^{-\Delta\Delta CT}$ , corresponds to the fold change. Data were presented as mean  $\pm$  SD (n = 3).

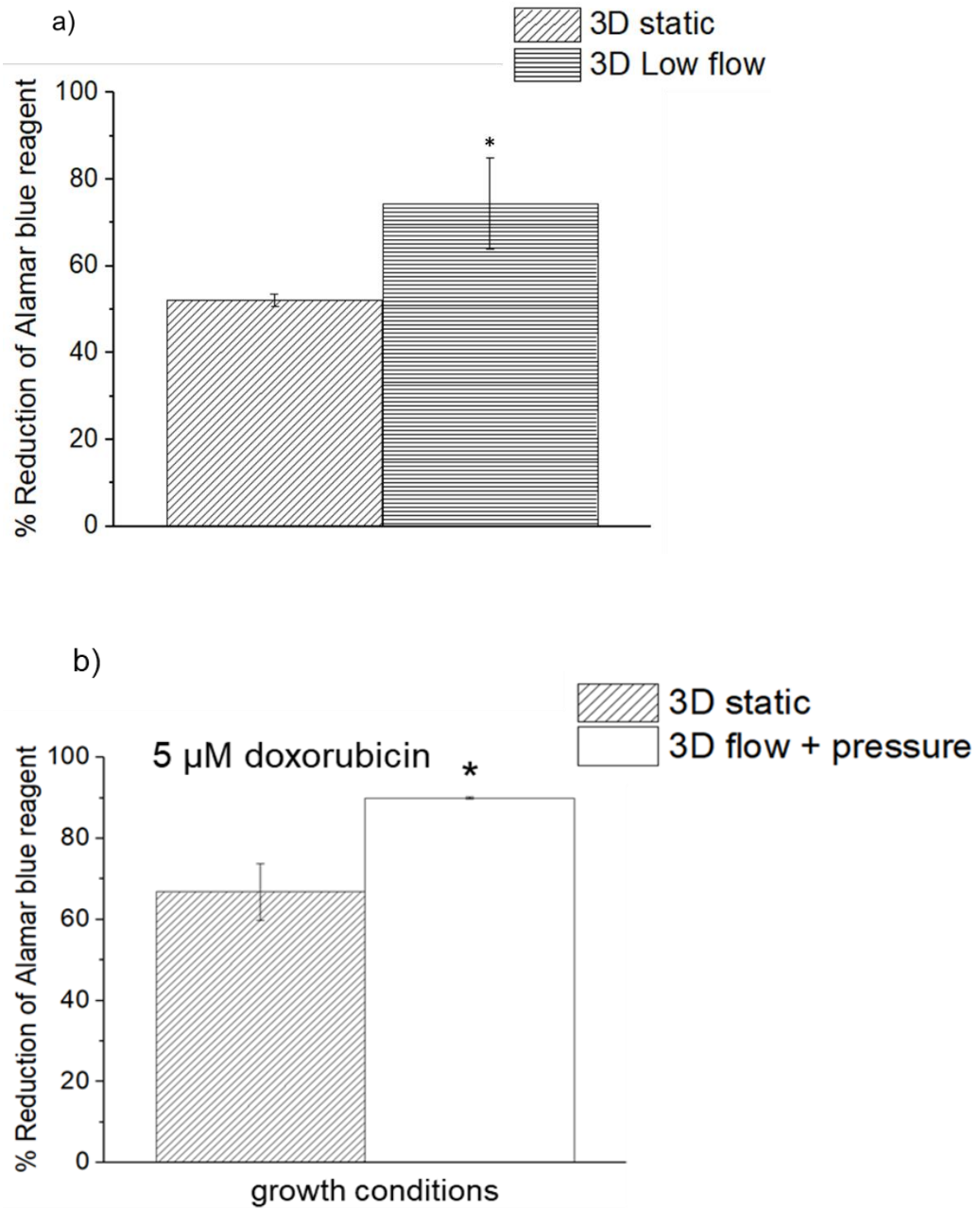
### **3.18 Sensitivity to doxorubicin in breast cancer cells cultured in 3D/static and 3D/dynamic conditions**

Interstitial fluid flow (IFF) and interstitial fluid pressure (IFP) are also important components of the tumor microenvironment and is suggested to influence drug responsiveness of cancer cells. Cytotoxicity effect of doxorubicin on MDA-MB231 and SKBR3 cells grown in collagen (ACM) and maintained in static or under different dynamic conditions in our Quasi Vivo system was assessed using the Alamar blue assay.

As indicted in the methods section, all ACMs were prepared and maintained under static conditions for 5 days to allow cells to acclimatise to the new environment (collagen). On the day 5, the percentage of cell viability was measured in all ACMs to make sure the number of cells seeded in all ACMs was the same. Then, two ACMs were transferred to two Quasi Vivo systems (two in each system, one system for untreated controls and one system for treated ones). All ACMs including those in static and those in flow/pressure (550  $\mu\text{L}/\text{min}$  and 19 mmHg) or only flow (150  $\mu\text{L}/\text{min}$ ) were serum starved for 24 hours prior to being treated with 5  $\mu\text{M}$  doxorubicin for 48 hours. A 5  $\mu\text{M}$  concentration was selected according to the results obtained from the previous experiments on treating cells in 2D and 3D (ACM) using different concentrations of doxorubicin. The viability of the cells was measured using Alamar blue assay after 48 hours.

The cytotoxicity of doxorubicin on the cells cultured in static condition was compared with those in flow/pressure conditions. Figure 29a indicates that low flow (150  $\mu\text{L}/\text{min}$ ) was associated with a 40% decrease in MDA-MB231 cell viability compared to the static condition ( $P < 0.05$ ). Likewise, treating MDA-MB231 cells under flow and pressure conditions, maintained cell viability with a 36% enhancement compared to treating the cells in the static condition, figure 29b. As the result showed, figure 29c, SKBR3 cells were also more sensitive to doxorubicin treatment when they were grown in static compared to flow/pressure conditions. There was a 50% increase in cell viability when

they were grown in 3D/flow/pressure compared to 3D/static condition. These results suggest that flow and pressure in tumour microenvironment can affect cancer cell sensitivity to chemotherapeutic drugs.



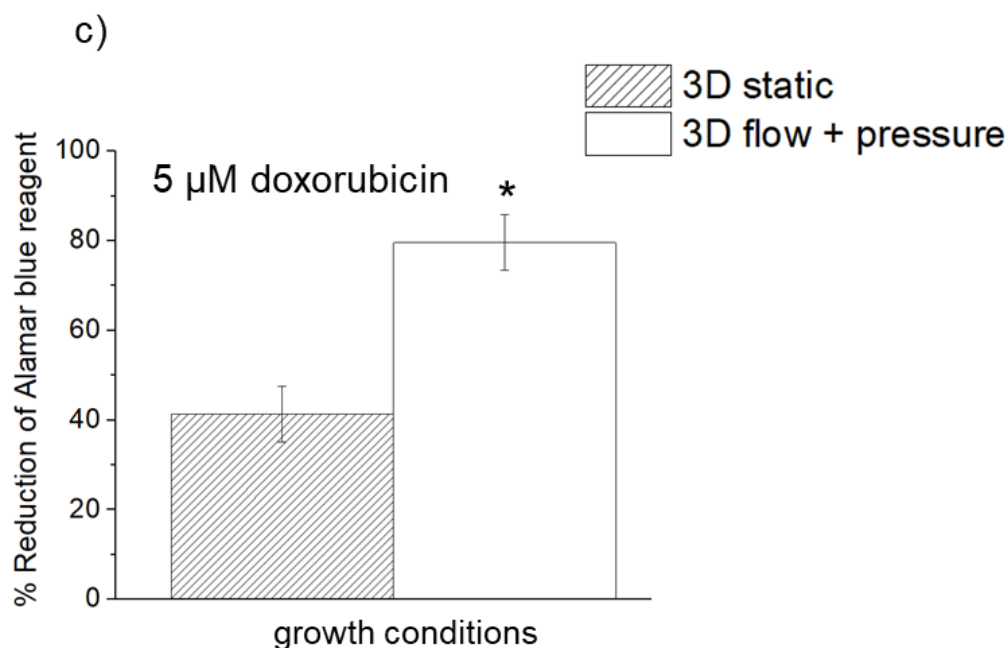


**Figure 29.** Comparing the cytotoxic effect of doxorubicin on MDA-MB231 and SKBR3 cells grown in different conditions. a) Viability of MDA-MB231 ACMs maintained in 3D low flow with those in 3D static condition. b) Comparing viability of MDA-MB231 cells grown in flow/pressure with those grown in static. c) SKBR3 responses to doxorubicin treatment in flow + pressure and static conditions. The results indicated that the cells are less sensitive to doxorubicin treatment when they were grown in the dynamic (flow and pressure) condition compared to static condition. Two wells were assessed for each concentration and the result is from three experiments.

### 3.19 Expression of EMT markers in presence of flow and normal fibroblasts

In the final part of the project, the effects of fibroblast cells grown in 3D scaffolds (ACMs) on induction of EMT in the cancer cells were investigated under flow condition. The fibroblasts grown in a 24-well plate format RAFT gel and a cancer ACM were nested in a series chamber format designed so that the fibroblast chamber was next to the reservoir bottle. Another Quasi Vivo system having only one chamber (ACM) was also run in parallel as control. The growth media was supplemented with 2.5% v/v FBS and a flow of 150

$\mu\text{L}/\text{min}$  was applied for 7 days. The relative quantification of mRNA of EMT markers and Ki67 was performed using qRT-PCR. The initial results from a single experiment showed that MMP14 and snail mRNA expression increased in the presence of fibroblasts while the expression levels of vimentin and cadherin 11 slightly decreased and that the Ki67 mRNA level remained unchanged, Figure 30. However, these experiments require repeats for further validation. The results suggest that fibroblasts produce chemokines and factors that may affect the expression of the genes associated with ECM remodelling and mesenchymal phenotype.

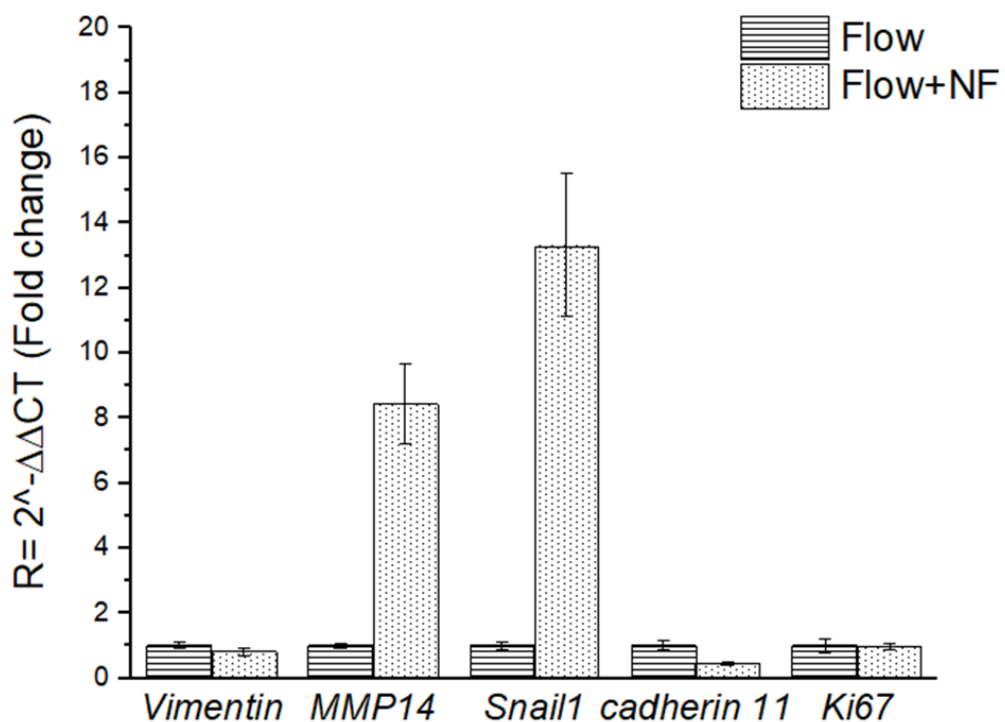


**Figure 30.** Relative quantification of vimentin, MMP14, snail1, cadherin 11 and Ki67 mRNA expression levels in MDA-MB231 cells cultured in 3D flow with and without fibroblasts after a week. MMP14 and snail1 mRNA expression increased in the presence of normal fibroblasts (NFs). The experiment was performed using quantitative real time PCR technique and mRNA expression levels were normalised against GAPDH.  $\Delta\Delta\text{CT}$  was calculated by subtracting  $\Delta\text{CT}$  of flow culture (control) from  $\Delta\text{CT}$  of flow + NF condition.  $R = 2^{-\Delta\Delta\text{CT}}$ ,

corresponds to the fold change. Data is presented as single experiment performed in triplicate.

### **3.20 MDA-MB231 invasion in ACMs with and without normal fibroblasts**

To investigate if addition of normal breast-derived fibroblasts can affect cancer cell invasion, the fibroblast cells were embedded in the stromal collagen in the RAFT system. Three ACMs were imaged for each condition using an inverted light microscope after 7 days, Figure 31.

The images indicate an increase in the number of cancer cells invading from tumour mass to the stroma where normal fibroblasts exist. The migration distance of the MDA-MB231 cells increased in the presence of fibroblasts. The results suggest that even normal breast-derived fibroblasts may affect the invasive behaviours of the cancer cells.

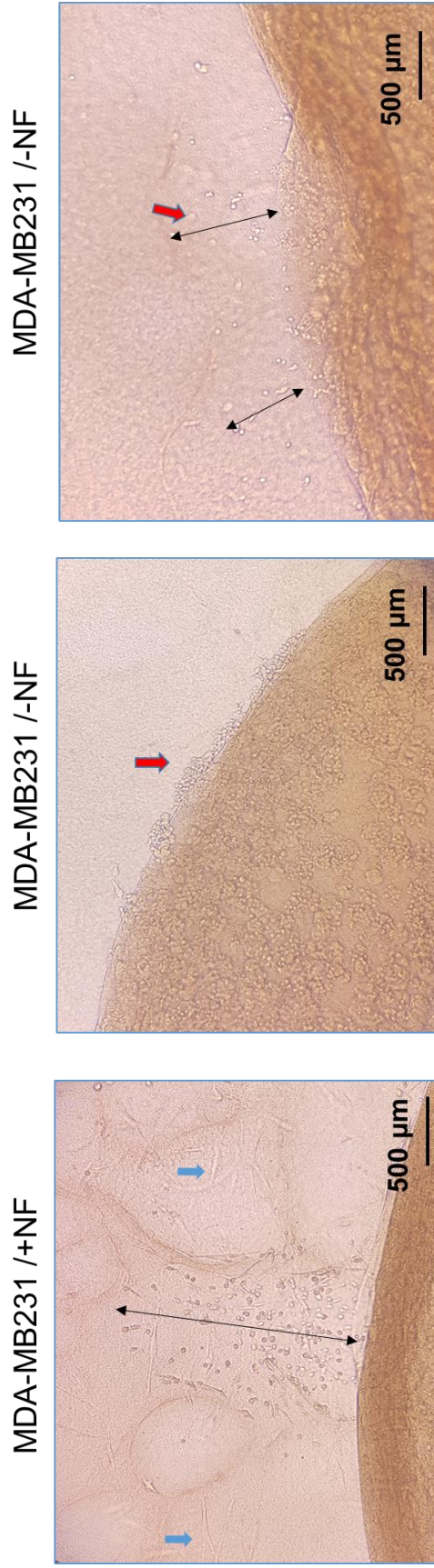


**Figure 31.** MDA-MB231 grown as ACM with and without normal fibroblasts in the stroma. The cancer cells are in the centre of the ACM and surrounded with normal fibroblast cells. The images show cancer cells invasion towards stroma increases in the presence of breast-derived fibroblasts. Blue arrows show normal fibroblasts and red arrows are the cancer cells. Black arrows show the migration distance.

# **CHAPTER 4**

## **DISCUSSION**

## **4.1 Breast cancer cell viability, proliferation and apoptosis**

The effect of different components of tumour microenvironment on cancer cells behaviour has been intensely studied (Wang et al., 2017, Anari et al., 2018). Since cell proliferation and growth are major causative factors in the development and the progression of cancer changes in these parameters have most often been assessed and in particular when cancer cells were exposed to different microenvironments. In this study the viability and proliferation of breast cancer cells was evaluated whilst cells were cultured under different conditions including 2D, 3D, static and dynamic flow and flow/pressure. In addition, to better understand the underlying molecular mechanisms of the observed alterations in cell growth, the expression of a range of markers was also evaluated.

### **4.1.1. Cellular viability in 3D cell culture compared with conventional 2D cell culture**

The first part of this project involved culturing cancer cells in a 3D system, leading to the key question: does 3D culture alter cell proliferation and viability? To address this fundamental question, researchers have conducted diverse projects using various 3D culture methods and cell types. In this project, cell viability, an indicator of cell proliferation/growth was evaluated by assessing the metabolic activity of breast cancer cells grown in 2D monolayers and in 3D as ACMs of 10% w/v collagen type-I. Amongst the diverse cell viability assays available to researchers, the Alamar blue assay was selected owing to the non-toxic properties of this reagent which has allowed the assay to be performed at different time points on the same cells. Unfortunately, the Alamar blue assay was not suited to the analysis of cancer cells grown as 3D spheroids due to lack of reproducibility caused by floating/unattached cells.

Since different numbers of the cells were initially seeded in the 2D and 3D format the rate of increase and/or decrease in cell viability was compared

rather than the actual percentage cell viability at each time point. MDA-MB231 cells were grown for 14 days (data not shown) and SKBR3 were grown for 7 days as a significant decrease in the viability of SKBR3 cells was observed at day 7. Reduced viability rates for MDA-MB231 and SKBR3 cells were observed over the 7-day period when the cells were grown in 3D ACM compared to 2D. In the case of MDA-MB231 cells, there was a significant difference between day 1 and day 3 when cells were grown in 3D compared to 2D,  $P < 0.05$ . Although the (rate of) increase in cell viability was reduced in both culture conditions between days 3 and 7 a significantly lower rate was observed in 3D compared to 2D. The viability of SKBR3 cells increased approximately with a similar rate between day 1 and day 3 and continued to increase slightly on day 7 in 2D while a significant reduction was observed in the 3D culture ( $P < 0.05$ ). To assess whether the observed changes in cell viability, as measured using the Alamar blue assay, were due to an alteration in the proliferation rate of the cells, their metabolic activity and cell death (particularly apoptosis) was determined by measurement of the expression levels of markers of these processes using qRT-PCR.

Ki67 is a proliferation marker associated with dividing cells, its expression varies in different phases of the cell cycle, but it is not detected while cells are in cell cycle arrest; G0 (Juríková et al., 2016). MDA-MB231 and SKBR3 cells exhibited reduced expression levels of Ki67 when they were cultured in the 3D ACM compared to 2D monolayer cultures. These results were consistent with the results of the Alamar blue cell viability assay and suggest that growing the cells in collagen type-I may exhibit a decrease in cell division and, therefore, cell proliferation. However, when the cells were cultured in the ultra-low attachment plates and allowed to form spheroids a significant increase in the Ki67 expression level was observed compared with 2D cell culture ( $P < 0.05$ ). This may be associated with increased cell-cell interactions, a feature of spheroid formation. The increase in Ki67 expression levels in SKBR3 might be associated with the HER2 positivity of this cell line as Ki67 expression has previously been shown to be elevated in HER2 enriched cells compared to the claudin-low breast cancer subtypes (Holliday and Speirs, 2011). Examination

of the levels of other cell-cycle-specific antigens including proliferating cell nuclear antigen (PCNA), and mini-chromosome maintenance (MCM) proteins, may help to further elucidate the molecular alterations involved in tumour cell growth and proliferation that occur when cells are cultured in 3D ACM.

To further understand the behaviour of cells grown in 3D ACM the expression levels of genes coding for proteins involved in intrinsic and extrinsic apoptosis pathways were analysed. The pro-apoptotic markers caspase -3 and caspase -9 were expressed in the cancer cells at approximately the same level irrespective of whether cells were grown in 3D or in 2D cultures. The only exception was the significantly decreased expression-levels of caspase -3 observed when SKBR3 cells cultured in 3D. The expression-levels of the anti-apoptosis marker BCL-2 of both cell lines was elevated when the cells were grown in 3D (ACM) compared to 2D. Taken together, the expression levels of BCL-2/caspase -3 and -9 suggest that the induction of apoptosis may not be the underlying mechanism associated with the reduction in cell viability described above. Analysis of a larger panel of genes and proteins involved in apoptotic processes in conjunction with other assays, for example annexin V and caspase 3/7 activity assays would serve to more fully understand the changes in cancer cell behaviour when grown in 3D.

A further consideration when evaluating the data from the Alamar blue assays is that reduced cellular viability in the collagen scaffolds (ACMs) may result from a decrease in concentration of the Alamar blue reagent (dilution effect) when applied to the collagen matrix, and/or differential uptake of Alamar blue dye by cells which have formed clusters within the collagen.

Previous studies using cancer cell lines have shown that cell proliferation rates depend on both the cell type and the 'matrix' supporting cell growth. In a study of endometrial cancer cell lines, RL95-2, KLE, EN-1078D, Chitcholtan et al (2013) reported a significant decrease in cell proliferation of cells cultured in reconstituted basement membrane (rBM) compared to 2D culture. Similarly, in another study, a panel of colorectal cancer cells including SW-480, HT-29, DLD-1, LOVO, CACO-2, COLO-205 and COLO-206F were grown in Matrigel (3D) and exhibited a decrease in cell viability, measured by MTT assay, and

proliferation, quantified by 5-bromo-2'-deoxyuridine, compared to the cells grown in 2D monolayers (Luca et al., 2013). Conversely, JIMT1 breast cancer cells exhibited a higher proliferation rate when cultured in Matrigel but slower growth in a synthetic, polyHEMA 3D scaffold compared with 2D culture (Hongisto et al., 2013). The viability of C4-2B prostate cancer cells grown in 3D hyaluronic acid hydrogels was not found to be significantly different compared to those cultured in 2D, in a report utilising Trypan blue staining to count the total cells and the dead cells (Gurski et al., 2009). In a recent study, the proliferation of glioma cells lines, U87, U251 and HS683, was evaluated by determining the number of cells within collagen scaffolds and 2D monolayers over a 10-day time course. They concluded that cell growth declined in 3D collagen scaffolds compared to 2D culture and qRT-PCR and Western blot analysis revealed that the expression of Ki67 in the glioma cells reduced when they were grown in collagen scaffolds, compared with the 2D monolayer system (Jia et al., 2018).

In summary, the results presented here indicate that the growth rate of MDA-MB231 and SKBR3 cells collagen type-I matrix compared to growth as conventional 2D monolayers. This reduction in cell growth was associated with decreased metabolic activity and/or arrest of cells in the G0 phase of the cell cycle but not apoptosis and cell death.

#### **4.1.2. Cellular viability and colony morphologies of the cells grown in 3D culture and in the presence of fluid flow**

Biophysical cues from the tumour microenvironment include the stiffness of the ECM, interstitial fluid flow and pressure and these have been shown to have broad-reaching effects on cancer cells (Broders-Bondon et al., 2018). In this part of the study, there were two aims: 1) to investigate if the cells remained viable under the new 3D/dynamic system which was developed in this project and 2) to compare viability and proliferation of the cells grown in dynamic systems with their counterparts in static conditions. Accordingly,

ACMs were maintained under different conditions: static, flow (150  $\mu\text{L}/\text{min}$ ) and flow/pressure (550  $\mu\text{L}/\text{min}$ ,  $\sim 19\text{mmHg}$ ) and cell viability was measured using the Alamar blue assay as described above.

Applying a flow of media over the cells cultured as 3D ACMs resulted in a lower cell viability at a flow rate of 550  $\mu\text{L}/\text{min}$  and pressure of  $\sim 19\text{mmHg}$  compared to cells grown in equivalent but static conditions. After 7 days cell culture, the viability of MDA-MB231 cells was significantly reduced when grown under flow/pressure compared with static conditions. However, between days 7 and 14 a similar (rate of) cell viability was observed, irrespective of the culture conditions. If this tumour model were to be used in drug cytotoxicity testing setting, cancer cells would need to be maintained in the flow model at least for 7 days prior to treatment in order to avoid misinterpretations of the results.

The viability of MDA-MB231 cells exposed to a flow rate of 550  $\mu\text{L}/\text{min}$  without the application of pressure was similar when compared with cells cultured under static conditions (Appendix 6). When a flow rate of 150  $\mu\text{L}/\text{min}$  was applied over the ACMs of MDA-MB231 cells the viability was similar to that observed in flow/pressure (results not shown). These results indicate that applying pressure while using high flow rates, affects the cell viability in the same manner as a low flow rate.

Although there have been several *in vivo* studies with tumour tissue derived samples and animal models of cancer in which fluid flow/pressure have been associated with tumour cell proliferation, invasion and metastasis (Leunig et al., 1992, Hofmann et al., 2006). Only a few *in vitro* studies have demonstrated that cancer cell proliferation is altered in the presence of fluid flow or high interstitial fluid pressure. In an *in vitro* study conducted on SCC-4 and SCC-9 human tongue squamous carcinoma cells, an increase in the extracellular pressure from 15 mm Hg to 30 mm Hg resulted in a significant elevation in cell proliferation and an alteration in expression levels of more than 1800 genes involved in invasion and metastasis (Yu et al., 2013). In another report, increasing the hydrostatic pressure (20, 50, 100 mm Hg) applied to primary osteosarcoma (HOS, U2OS, SaOS2) and two metastatic tumour cell lines

(MCF7 breast, H1299 lung), using an Opticell–HPA cell culture system showed the cancer cells to react differently with regards to their proliferation rate(s) (DiResta et al., 2005).

The results obtained during this project concur with previous research in which it has been reported that the application of sheer stresses to human cancer cells , two osteosarcoma and two oral squamous carcinoma, resulted in G2/M arrest and a decrease in cellular differentiation; with the mad signalling pathway recognised as the underlying molecular mechanism (Chang et al., 2008). It would be intriguing to determine if the smad signalling pathway is activated in the MD-MB231 cells grown in the 3D ACM system utilised in this study.

In contrast to the observations with the MDA-MB321 cells, when SKBR3 cells were used for the preparation of ACMs and maintained under flow and pressure conditions their viability reduced between day 1 and 7 whilst cells maintained under static conditions exhibited a significant increase in cell viability. This is the first report in which SKBR3 cells have been cultured under flow and pressure conditions; it may be the case that breast cancer cells behave differently depending upon their subtype, when maintained in 3D and under fluid flow and pressure.

An investigation aimed at elucidating molecular mechanisms underlying the changes in cell viability evaluated the mRNA expression levels of the proliferation marker Ki67 and apoptosis-related markers caspase -3, caspase -9 and BCL2. MDA-MB231 and SKBR3 cells exhibited a significant increase in the expression level of Ki67 when grown under flow/pressure compared to static conditions. This report is the first of its kind to consider the effect of fluid flow and pressure on the Ki67 expression level in human cancer cells. The only previous report indicating an association between IFP and Ki67 found that lowering the IFP for at least 6 h significantly suppressed Ki67 expression in an epidermoid vulva carcinoma and lung carcinoma tumours of mice (Hofmann et al., 2007). It has been reported, however, that mechanical signals control the shuttling of Yes-associated protein (YAP) to the nucleus where it interacts

with transcriptional enhanced associate domain (TEAD) is associated with increased cellular proliferation (Aragona et al., 2013).

To further understand the behaviour of cells maintained in a microenvironment incorporating fluid flow and pressure, the expression levels of key genes involved in intrinsic and extrinsic apoptosis pathways were analysed. In these experiments caspase -9 expression levels were significantly increased in MDA-MB231 cells grown under flow and pressure, while caspase -3 and BCL2 expression levels were decreased (non-significant) compared with the static 3D cell culture conditions. However, in the case of the SKBR3 cells, significant increase in expression levels of either caspase -3 or caspase -9 were observed. This is the first time that the effect of flow/pressure on the expression of apoptotic markers of cancer cells has been reported.

Microscopic analysis revealed that the cancer cells form colonies when they are maintained in 3D conditions - a feature common to cells cultured under both static and flow conditions as ACMs. MDA-MB231 cells grew in regular-shaped colonies in static conditions but under flow/pressure they displayed a 'grape-like' morphology. In contrast, SKBR-3 cells exhibited a 'grape-like' morphology irrespective of the condition: static or flow/pressure. The types of colonies formed when breast cancers are grown in 3D has been the subject of a number of studies. The morphology of colonies of a large panel of breast cancer cell lines grown in 3D Matrigel, alongside their gene expression profiles was studied. They classified the morphology into four categories; mass, round, stellate and grape-like. The gene expression pattern of the cells was strongly associated with colony morphology. However, it was reported that MDA-MB231 cells exhibited a stellate morphology and SKBR3 cells a grape-like morphology (Kenny et al., 2007). Comparing the results of this study with theirs it can be concluded that: 1) a specific cancer cell line can adopt different colony morphologies in biochemically or biophysically different microenvironments and 2) changes in the gene expression profile of the cells grown under flow/pressure may cause the changes in colony morphology.

In summary, the growth rate of MDA-MB231 and SKBR-3 cells was reduced when the cells were maintained under flow/pressure compared to when they

remained in static conditions. This reduction in cell growth was associated with reduced metabolic activity and increased apoptosis and was not associated with proliferative activity.

## **4.2. Epithelial mesenchymal transition (EMT) of breast cancer cells grown under different conditions**

EMT is a process which occurs during tumour cell invasion and intravasation and the identification of factors that can trigger and sustain EMT is an important aim. EMT-related signalling pathways play an important role in epithelial-mesenchymal switching. Signalling pathways altered during EMT include TGF- $\beta$ , Wnt/ $\beta$ -catenin and NF- $\kappa$ B. Transcription factors, for example STAT3 and snail, slug, Nanog, ZEB1 (Guaita et al., 2002a) and microRNAs have also been implicated in this process (Ren et al., 2017). Factors in the tumour microenvironment have been shown to induce EMT in epithelial cancer cells leading to cellular invasion (and metastasis) (Yang et al., 2018).

In this project, the effect of biochemical and biomechanical components of the tumour microenvironment on the expression of EMT-associated markers was investigated.

### **4.2.1. EMT of breast cancer cells maintained in 3D cell cultures compared with conventional 2D cell culture**

In this part of the study the aim was to investigate whether growing MDA-MB231 cells in 3D dense collagen type-I or in spheroids, rather than conventional 2D culture, would alter expression levels of mesenchymal markers. SKBR3 cells exhibited extremely low expression levels of vimentin, snail, N-cadherin, MMP14 and cadherin 11 when grown in either in 2D and 3D (data was not shown).

Relative quantification of the EMT markers vimentin, MMP14, snail and cadherin-11 was performed using qRT-PCR; an increase in the expression levels of these markers was observed when the cells were cultured in 3D as either ACM or spheroids. The exception was cadherin-11 expression-levels which were observed to decrease when MDA-MB231 cells were cultured in 3D as ACM in type-I collagen.

Vimentin is an important marker of EMT but a significant increase in the expression of this marker in most cells cultured in 3D compared with those in 2D has not been reported. Further analysis of vimentin levels was undertaken by separation of proteins extracted from cells grown in both 2D and 3D by SDS-PAGE followed by Western blotting and by immunofluorescent, confocal, microscopy. MDA-MB231 cells grown in 2D and in 3D as ACM in collagen type-I did not exhibit a significant difference in overall levels of the vimentin protein. The Western blot analysis utilised a primary anti-vimentin antibody (D21H3, Cell Signalling Technology) raised against both the phosphorylated and non-phosphorylated forms of vimentin, accordingly, 2 bands were observed on the Western blots and whilst vimentin mRNA levels in 2D and 3D culture were not different, more of the vimentin filaments appeared phosphorylated when the cancer cells were grown in 3D as ACM.

In contrast to the results obtained in this study, others have shown vimentin expression-levels to be increased when mammary epithelial cells were cultured in 3D collagen scaffolds or as spheroids. For example, the growth of the normal mammary epithelial cell line MCF 10A in 1-1.5 mg/mL collagen was associated with upregulation of vimentin gene-expression (Decarlo et al., 2015). Another study utilising immunohistochemical methodology reported a significant elevation in vimentin levels when MCF7 cells were grown in spheroids compared to 2D culture (Herheliuk et al., 2016). Upregulation of the gene-expression and protein levels of vimentin were also reported when glioma cells were grown on collagen scaffolds with larger pore sizes (Jia et al., 2018). Colorectal cancer cells HT29 and HTC116 were also cultured in the same collagen scaffold as the ACM used in this study. Western blot analysis showed increased levels of vimentin protein in both cell lines when cultured in

the ACM compared with 2D cell culture (Magdeldin et al., 2017). It should be noted that HT29, HTC116, MCF7, MCF-10A and glioma cells do not express high levels of vimentin in 2D cell culture in contrast to MDA-MB231 cells which constitutively express vimentin. The results obtained in this study, therefore, suggest that when cells already express relatively high levels of vimentin, those levels do not alter when the cells are grown in 3D but rather the phosphorylation status of vimentin may be affected by the culture conditions.

MMP14 is a membrane-type matrix metalloproteinase (synonym MT1-MMP) which paves the path for cancer cell migration by cleavage of ECM macromolecules including collagen type-I, type-II, type-III, laminin-1, laminin-5, fibronectin and vitronectin (Itoh, 2006). MMP14 expression-levels were increased significantly when MDA-MB231 cells were grown in 3D as either ACMs or spheroids, compared with 2D culture. These results suggest that MMP14 expression levels in MDA-MB231 cells is affected by the 3D microenvironment irrespective of the presence of macromolecules associated with the ECM, the significance of this paradoxical finding remains unclear. Currently there are few reports concerned with the effect of 3D culture on the levels of MMP14 in cancer cells, although a recent study showed a significant increase in MMP14 expression levels in human mammary fibroblasts grown in 3D collagen scaffolds compared to those grown in 2D (Sung et al., 2013).

As detailed above, signalling pathways and transcription factors are involved in EMT. Amongst the transcription factors activated, snail has emerged factor as an important modulator of EMT, principally via its inhibitory effect on E-cadherin levels (Guaita et al., 2002b). However, snail also controls other factors that are involved in cancer cell survival and invasion. For example, snail has been shown to regulate the glycolytic switch (Warburg effect) repressing levels of fructose-1,6-biphosphatase (FBP1) in basal type breast cancer cells (Dong et al., 2013). This in turn may lead to increased production of reactive oxygen species (ROS) with genotoxic effects (Wang et al., 2013). In addition to modulating soluble factors of the tumour microenvironment which trigger signalling pathways involved in snail activation, ECM molecules, for example collagen and hyaluronic acid, affect snail induction. A recent study

has shown that 3D culture of ovarian cancer cells on collagen type-I scaffolds induced expression of snail and slug through co-activation of TGF $\beta$  and Wnt signalling pathways (Liu et al., 2018). Another study revealed that the growth of pancreatic ductal adenocarcinoma cells in 3D collagen gels induced snail expression. The same study reported that TGF- $\beta$  type-I receptor and its downstream effector molecules, smad3 and smad4, were essential for induction of snail by collagen (Shields et al., 2011). Furthermore, snail expression-levels have emerged as important in the lymph node metastasis of MDA-MB-231 cells (Olmeda et al., 2007). However, to date, little is known about the effect of the collagen type-I matrix in the expression of snail in MDA-MB231 cells. In this study, MDA-MB231 cells were grown on ultra-low attachment surfaces or were embedded in collagen type-I (ACM) - a significant increase in snail mRNA expression-levels was observed in cells cultured in 3D (as ACMs and spheroids) compared with cells grown in 2D monolayers - suggestive that stimulating factors other than collagen may exist in the 3D microenvironment of tumour cells which induce snail activation. These results concur with previous studies utilising other cancer cell lines (Shields et al., 2011, Carey et al., 2017, Liu et al., 2018).

The final EMT related marker evaluated in this study was cadherin-11. Cadherin 'switching' occurs during EMT, a phenomenon described during human embryonic development and also during tumour invasion and metastasis. This 'switching' results in weaker homotypic cadherin interactions and consequently facilitates cell migration and invasion (Theveneau and Mayor, 2012). Higher cadherin-11 gene expression-levels have been reported for cancer cell lines derived from bone and this has led researchers to investigate whether there is a correlation between upregulation of cadherin-11 in certain cancers including some types of prostate and breast cancers, and bone metastases. It has been reported that MDA-MB231 cells from secondary tumours in bone express higher levels of cadherin-11 compared to MDA-MB231 with those metastatic to the brain. They also demonstrated that MDA-MB231 cells re-expressing cadherin-11 are more prone to metastasise to bone (Tamura et al., 2008). Transfection of the BT-20 breast cancer cell line with

cadherin-11 gave rise to a more invasive and motile phenotype compared to parental cells although they remained less motile than cells transfected with N-cadherin (Nieman et al., 1999). In this study, initially, qRT-PCR analysis was performed to evaluate the effect of cellular growth in the 3D microenvironment (collagen and spheroid) on mRNA expression-level of E and N-cadherin and cadherin 11. The results were consistent with those of Nieman *et al.* (1999): MDA-MB231 cells did not express E-cadherin and N-cadherin (results not shown). Therefore, cadherin-11 expression of the cells grown in 3D was measured relative to those grown in 2D. The results showed that cadherin-11 mRNA expression decreased significantly in the cells grown in 3D scaffold while it increased significantly in the cells grown in the ultra-low attachment plates (spheroids). This observation suggests that MDA-MB231 cells downregulate *CDH11* gene upon exposure to collagen type-I, and that floating and unanchored MDA-MB231 cells express higher levels of cadherin-11 mRNA compared to when they are attached to the surface of flask in conventional 2D culture method.

#### **4.2.2. EMT of 3D cell cultures in the presence of fluid flow**

To date, little research has been conducted on the impact of fluid flow and pressure on the induction of EMT in cancer cells. In this part of the project, the aim was to investigate how mechanical stress generated from interstitial fluid flow and pressure may interact with biochemical signals arising from ECM to induce EMT in solid tumours. MDA-MB231 cells grown as ACMs were maintained under static, flow (150  $\mu$ L/min) and flow/pressure (550  $\mu$ L/min, ~19 mmHg) for two weeks. The mRNA expression levels of vimentin, snail and MMP14 in flow and flow/pressure was measured relative to the levels when cells were grown in static conditions. MDA-MB231 cells exhibited increased levels of vimentin, MMP14 and snail in the presence of fluid flow of 150  $\mu$ L/min compared to static conditions. In contrast, when cells were maintained under

flow/pressure (550  $\mu\text{L}/\text{min}$ ,  $\sim 19$  mmHg) conditions, only the MMP14 mRNA expression-levels increased significantly, while vimentin expression-levels significantly decreased, and snail expression-levels remained unchanged. Further analysis of vimentin levels was undertaken by Western blotting and immunofluorescent confocal microscopy. The MDA-MB231 cells grown in 3D collagen as ACMs under flow/pressure exhibited a significant decrease protein levels of vimentin compared to those grown in static conditions. Images obtained following immunostaining of the MDA-MB231 cells cultured in static and flow/pressure for 2 weeks showed reduced levels of vimentin protein in the cell aggregates at the edges of ACMs, where the cells invade to the surrounding stroma, when maintained under flow/pressure compared to their counterparts grown under static conditions. The increased vimentin mRNA expression-levels when ACMs were maintained under lower flow (150  $\mu\text{L}/\text{min}$ ) and pressure ( $\sim 1$  mmHg) may reflect increased levels, or 'pockets', of hypoxia, this may be evaluated by assessment of the hypoxia-inducible factor  $\alpha$  (HIF-1 $\alpha$ ). HIF-1 $\alpha$  has been shown to be involved in induction of EMT in cancer cells. Increased levels of MMP14 mRNA expression in flow and flow/pressure suggest that matrix remodelling, an essential factor for cellular invasion, is induced in the presence of flow and pressure. Overall, when MDA-MB231 cells were cultured in 3D, irrespective of the conditions (static, flow and flow/pressure) increased expression-levels of vimentin, MMP14 and snail were observed, compared to cells maintained as 2D monolayers. The only exception was the reduction of vimentin mRNA expression levels of cells cultured in the flow/pressure system, discussed above. These results indicate that addition of complexity to the cell culture system perturbs expression-levels of genes involved in EMT.

This is the first time the effect of fluid flow and pressure on the expression of EMT-associated genes of breast cancer cells grown in a dense collagen matrix has been reported. Other studies have investigated the impact of microenvironment on breast and ovarian cancer cells behaviour using different types of 3D engineered tumour models and flow systems. For example, it has been shown that applying different IFP profiles alters the expression levels of

EMT markers in MDA -MB231 cells embedded in 4 mg/mL collagen type-I. 3D cultures accommodated within chambers of PDMS were subjected to a hydrostatic pressure gradient between the core and the tip of cell aggregates in a model incorporating hypotension ( $P_{\text{tip}} > P_{\text{base}}$ ), hypertension ( $P_{\text{tip}} < P_{\text{base}}$ ) and control pressure ( $P_{\text{tip}} = P_{\text{base}}$ ) conditions generated by changing the height of the cell growth medium in the reservoirs connected to either sides of the channel. Hypotensive conditions promoted cellular invasion and vimentin/snail expression-levels were significantly increased compared to the other IFP profiles; epithelial markers (E-cadherin and keratin-8) were also upregulated under hypotension (Piotrowski-Daspit et al., 2016). Rizvi *et al.* have maintained the ovarian cancer cell line OVCAR5 in a Matrigel-containing microfluidic system under continuous flow (2.0  $\mu\text{L}/\text{min}$ ) for 7 days: E-cadherin levels were down-regulated whilst vimentin and EGFR expression levels were upregulated under flow conditions compared to static 3D cell culture (Rizvi et al., 2013). Although the flow rate, pressure, ECM (both material and density) and the flow generating system used in our project were different from the previous studies, they all highlight the substantial roles of fluid dynamics in regulating EMT and which cells encounter under pathological and/ or physiological conditions.

#### **4.3. The effect of cell culture conditions on HIF-1 $\alpha$ expression levels in breast cancer**

Since one of the objectives of this study was to develop a tumour model for drug discovery purposes and since increased amounts of HIF-1 $\alpha$  have been associated with drug resistance mechanisms, the effect of different culture conditions on the expression of HIF-1 $\alpha$  in MDA-MB231 and SKBR3 cells was evaluated using the qRT-PCR technique.

#### **4.3.1. HIF-1 $\alpha$ expression of breast cancer cells in 3D cell culture**

The effect of different 3D culture systems (ACM and spheroids) on HIF-1 $\alpha$  expression was assessed. A slight increase in HIF-1 $\alpha$  mRNA expression-levels was observed when MDA-MB231 cells were cultured in collagen scaffolds compared to 2D culture, whereas a significant increase in HIF-1 $\alpha$  was observed in cells grown on the ultra-low attachment plates (spheroids). However, in the case of SKBR3 cells, HIF-1 $\alpha$  expression was significantly elevated in both types of 3D culture (ACMs and spheroids), although there was a greater elevation in spheroids than in ACMs compared to 2D culture. These results suggest 1) the 3D collagen model (ACM) was not associated with the generation of hypoxic conditions for MDA-MB231 cells, 2) MDA-MB231 cells are less sensitive to oxygen-depletion when they are grown in the dense collagen scaffold compared to SKBR3 cells; 3) the cancer cells grown in the spheroid format are exposed to a lower oxygen gradient in the centre of the spheroid which affects the general amount of HIF-1 $\alpha$  expression in all cells and/or 4) HIF-1 $\alpha$  may be associated with the upregulation of the EMT markers including snail, MMP14 and cadherin 11 in the 3D spheroid system. Previous studies have reported an association between hypoxia and expression of EMT markers in tumour cells. For example, it has been demonstrated that hypoxia-stabilised HIF-1 $\alpha$  induces EMT through enhancing snail transcription in hepatocellular carcinoma cells (Zhang et al., 2013). It has also been reported that hypoxic conditions lead to an increase in the levels of HIF-1 $\alpha$ , N-cadherin and vimentin, but repressed the expression of E-cadherin and cytokeratin in pancreatic cancer cells (Zhu and Zhao, 2017).

#### **4.3.2. HIF-1 $\alpha$ expression of 3D cell cultures in the presence of fluid flow**

Increased levels of IFP and hypoxia are a feature of the tumour microenvironment and have been shown to promote tumour cell invasion and

metastasis to local or distant sites (Finger and Giaccia, 2010). However, associations between tumour IFP and hypoxia have rarely been studied. In a study on human melanoma xenografts, tumours with high IFP (IFP >20 mm Hg) exhibited higher central hypoxic fraction compared to those with low IFP (Rofstad et al., 2014). The work reported in this thesis was concerned with the effect of fluid flow and pressure on HIF-1 $\alpha$  expression-levels in tumour cells grown in 3D scaffolds (ACMs). HIF-1 $\alpha$  mRNA expression was assessed to also understand the molecular alterations underlying induction of EMT (in MDA-MB231) and HER2 expression (in SKBR3) as well as drug resistance. The HIF-1 $\alpha$  mRNA expression-levels were increased significantly in both cell lines in the presence of flow of 150  $\mu$ L/min whilst, surprisingly, in the flow/pressure conditions (500  $\mu$ L/min, ~19 mmHg) expression-levels remained nearly unchanged. These results suggest that lower flow rates generate a hypoxic condition in the bioreactor chamber while higher flow rate and pressure do not. Although the induction of hypoxia should be confirmed by other techniques, for example measurement of oxygen pressure inside the flow chamber and staining the cells with pimonidazole, (Varia et al., 1998), the results found during this study demonstrate the importance of assessing the hypoxia status of closed bioreactors and microfluidic systems used for the study of cancer cell behaviour and drug responsiveness under more physiologically relevant conditions.

#### **4.4. The effect of culture conditions on HER2 expression of SKBR3 cells**

HER2 overexpression has been reported in many types of malignancies particularly in breast and gastric cancers. HER2 overexpression occurs in 15-20% of all breast cancer cases and is associated with poor prognosis and metastatic disease. Therefore, several HER2-targeting agents have been identified and established, including; Trastuzumab, Pertuzumab and Lapatinib (Nahta et al., 2004). Despite promising initial outcomes of these therapeutic agents for breast cancer patients, *de novo* and acquired resistance remains

the main complication in the clinic. Hence, further physiologically relevant *in vitro* tumour models are required to identify microenvironmental cues relevant to the drug discovery process. Previous studies have shown that response to HER2 targeting drugs including Trastuzumab and Pertuzumab is highly dependent on whether cells are grown in 2D or 3D culture systems. For example, SKBR3 cells grown as 3D spheroids on Matrigel appeared to be more resistant to trastuzumab compared to those grown in a 2D monolayer system (Weigelt et al., 2010). It has been shown that HER2 overexpressing breast cancer cells stabilise HIF1 $\alpha$  protein through PI3K and AKT pathway in nonhypoxic conditions (Laughner et al., 2001). Hence, in this study the HER2 and HIF1 $\alpha$  expression-levels of SKBR3 cancer cells cultured in 3D formats were compared with those grown in 2D monolayers.

#### **4.4.1. HER2 expression of breast cancer cells in 3D cell culture**

In this study, we compared HER2 expression (at mRNA and protein level) for SKBR3 cells cultured in our 3D collagen engineered system (ACM) and spheroids relative to cells grown in the conventional 2D monolayer. A significant increase in HER2 mRNA expression level was observed for cells grown in 3D collagen and spheroids compared to 2D monolayers. The Western blot analysis showed a slight increase in the HER2 protein level of cells grown in 3D collagen (ACM) compared to those cultured in 2D. Similarly, (qualitative) analysis of confocal images also showed a slight increase in HER2 protein levels when SKBR3 cells were cultured in ACM compared to those grown in 2D monolayers. The results suggest that HER2 expression increases when the epithelial cancer cells aggregate spontaneously in an anchorage-independent manner without the addition of exogenous ECM. In turn, the increased cell-cell interactions during spheroid formation may trigger signals which induce HER2 expression. No alteration in total amounts of HER2 protein levels was reported when SKBR3 cells were grown on polyHEMA coated (low attachment) plates. However, they found a significant increase in

phosphorylation of HER2 in 3D spheroids compared to 2D culture (Pickl and Ries, 2009). This may indicate that if our 3D model is going to be used in the future, one should consider the possible changes in the expression of HER2. Also, it may indicate that the necessity of considering ECM when Trastuzumab dosage and IC50 values are assessed in the drug discovery processes.

## **HER2 expression of 3D cell cultures in the presence of fluid flow**

The analysis of HER2 levels is a diagnostic and prognostic tool used during the clinical management of breast cancer patients. HER2 levels are used to determine those patients likely to benefit from Trastuzumab (Herceptin) therapy. Targeted therapy using Trastuzumab (Herceptin) has been a gold standard therapy for treatment of HER2 positive breast cancer patients. With the application of new *in vitro* tumour models, implementing mechanical aspects of the tumour microenvironment in drug discovery and personalised therapy, it is important to understand whether the target molecules and/or biomarkers themselves undergo conformational and/or transcriptional changes in according to the different microenvironments. Since the tumour model and flow system designed in this study might, in the future, be used to assess SKBR3 response to Trastuzumab an investigation into whether HER2 levels are altered when cells are grown as ACM was undertaken. A further objective was to determine if an increase in the fluid flow and pressure affected the expression of HER2 in HER2 enriched breast cancer cells. This has been studied for the first time in this project and no previous research has been conducted in this area. The results showed that HER2 gene expression-levels increased significantly ( $P < 0.05$ ) when the cells were grown under flow + pressure compared to static conditions. HER2 levels were also investigated using protein and cells using confocal microscopy. Qualitative analysis of the microscopy images showed no increase in HER2 of cells cultured in flow + pressure compared to those grown in the static conditions. These results

suggest that if the *in vitro* tumour model and Quasi Vivo system used in this project were to be employed as a platform for testing HER2 targeting therapeutic agents, changes in the level of HER2 expression should be considered prior to treatment. The results showed that increased fluid flow and pressure in the tumour microenvironment is associated with an increase in the HER2 expression in breast cancer cells.

#### **4.5. Efficacy of doxorubicin under different culture conditions**

The five-year survival following breast cancer has increased from approximately 30% in the 1970s to 80% in 2016 (Cancer research UK, 2017). This has been a result of improved diagnosis and the development of many cancer treatments including chemotherapy, immunotherapy, hormone therapy and radiotherapy. Nevertheless, cancer remains a leading cause of death worldwide and there is a need to understand the treatment responses for individual cancer patients. It is also not uncommon for anti-cancer drugs which have demonstrated promise during the development phase in pre-clinical research to fail during the clinical trial phase. This failure, known as the attrition rate, is in part due to the intrinsic complexity and heterogeneity of tumours; features that are often difficult to recapitulate during the drug discovery phase.

Since the 1970s, cancer cells have been cultured on 2D surfaces as monolayer cultures while biochemical and physical cues found in the TME have often been overlooked. The interaction between tumour cells and the microenvironment triggers reciprocal alterations in their structures and the physiological functions that support tumour growth and invasion, and the TME has been shown to affect cancer cell sensitivity and resistance to treatments (Giancotti and Ruoslahti, 1999).

Conventional monolayer cultures (2D) are simplistic models for testing therapeutic drugs failing to reflect key aspects of tissue architecture. In 2D monolayer cell cultures the cancer cells are in contact only with peripheral

cells, adhering to a plastic or a glass surface, this results in a default apical-basal polarity and cell shape which can alter cell function (Baker and Chen, 2012), in contrast, when cells are cultured in 3D they have a greater surface area for cell-cell attachments and have been shown to have more contacts with neighbouring cells.

When cancer cells are grown as 2D monolayers they are exposed to equal levels of oxygen, nutrients, waste products and therapeutic agents, whilst *in vivo*, a cancer cell mass would be exposed to the gradients of these components across the tumour, a phenomenon which can be recapitulated in 3D cell culture models (Lin and Chang, 2008).

In this project the effect of different microenvironmental conditions on cancer cell viability following treatment of the cells with chemotherapeutic drugs was assessed. Doxorubicin was chosen as it is used as a combination therapy for breast cancer treatment. MDA-M231 and SKBR3 cells were grown in the different culture conditions (2D, 3D static and dynamic) and were treated with doxorubicin hydrochloride. After 48 hours treatment, the viability of the cells was measured using the Alamar blue assay.

#### **4.5.1. Efficacy of doxorubicin when breast cancer cells are cultured in 3D**

Initially, the cytotoxic effect of different concentrations of doxorubicin on cells grown in 2D and 3D cultures was investigated. This experiment was also performed to optimise the concentration of doxorubicin to be used in subsequent experiments. In general, the Alamar blue assay results showed that cells cultured in 3D were less responsive to doxorubicin treatment compared to 2D, this was significant at the concentrations of 1  $\mu\text{M}$  and 5  $\mu\text{M}$  for cells treated in 3D compared 2D culture ( $P < 0.01$ ), figure 18. The increased resistance of cancer cells to the chemotherapeutic agent when they were grown in 3D compared with 2D may be attributed to limited drug diffusion through the collagen matrix; it is relevant to note that the molecular weight of

doxorubicin hydrochloride is 579.98 kDa which is greater than nutrients and/or Resazurin, the main constituent in the Alamar blue reagent. In addition, as reported above (section 3.3), SKBR3 cells exhibited a significant increase in HIF-1 $\alpha$  mRNA expression in the 3D ACM system compared to conventional 2D cell culture. HIF-1 $\alpha$  has been shown to be associated with induction of genes associated with cellular survival (Ziello et al., 2007). Therefore, reduced drug responsiveness in SKBR3 cells grown in 3D (ACM) may be associated with increased expression of HIF-1 $\alpha$ . Furthermore, the increased level of antiapoptotic marker BCL2 in both cell lines grown in 3D (ACM) compared to 2D may also be associated with increased resistance to Doxorubicin treatment.

In the case of MDA-MB231 cells, elevation in the expression of EMT markers MMP14 and snail may also have contributed to the decreased sensitivity to doxorubicin in 3D compared to 2D culture. These results are consistent with previous studies in which cancer cells were treated with chemotherapeutic drugs in 2D and 3D culture conditions. For example, it has been reported that the viability of human epithelial ovarian cancer cells OV-MZ-6 grown as 3D spheroids was 50% greater than the viability of 2D cell monolayers following the same level of exposure to Paclitaxel (Loessner et al., 2010). Another study showed that immortalized human cervical cells, HeLa, had lower toxic response to doxorubicin after 24h exposure when they were grown in collagen type-I compared to 2D monolayer culture (Casey et al., 2016). The sensitivity of colon cancer HT-119 cells to four standard anticancer drugs (melphalan, 5-FU, oxaliplatin, and irinotecan) has been reported to be lower when the cells were grown in 3D culture compared to 2D monolayers (Karlsson et al., 2012). In this study, SKBR3 cells were found to be non-responsive to <1  $\mu$ M doxorubicin when maintained as 2D cell culture whilst MDA-MB231 cells were sensitive to  $\geq 0.1$   $\mu$ M. SKBR3 cells were, however, more sensitive to doxorubicin at concentrations of 5  $\mu$ M and 10  $\mu$ M compared to MDA-MB231 cells treated with the same concentration. The greater sensitivity to doxorubicin may be attributable to the positive HER2 status of SKBR3 cells compared with MDA-MB231 cells which are HER2 negative. In a study of

n=220 breast cancer patients with tumours >2.5 cm diameter, three cycles of doxorubicin was found to be more effective for patients with HER2 positive tumours than HER2 negative patients (Campiglio et al., 2003). Collectively, the results obtained here indicate that conventional 2D monolayer cell culture methods lack fundamental microenvironmental cues as determining factors for drug responsiveness.

#### **4.5.2. Efficacy of doxorubicin when breast cancer cells were cultured in the presence of fluid flow**

Over the last two decades there has been an interest in the potential effect of increased IFF and IFP on efficacy of different cancer therapeutics. It has been argued that elevated IFF and IFP may be associated with treatment failure particularly when therapeutic agents are delivered systemically (Heldin et al., 2004). High molecular-weight drugs such as biological, immunotherapy and nanoparticles are transported and delivered via the circulatory system by moving through the interstitial space by convection (i.e. carried by streaming fluid) whereas small molecules (<1 kDa) mainly diffuse from areas with high concentrations to the area with low concentration (Rippe and Haraldsson, 1994). Increased IFP in the centre of the tumour and the sharp drop in IFP at the edge generates a high-pressure gradient at the periphery of the tumour. However, many modelling data also suggest that there is uniform high pressure over the majority of the tumour mass. Either of these phenomena may contribute to reduced uptake of therapeutic agents by the tumour cells and a non-uniform distribution of drugs in the tumour mass (Welter and Rieger, 2013). A further important factor is the observation that anti-cancer drugs may be sequestered by the tumour cells or may bind to molecules in the extracellular matrix, hindering drug penetration deep into the tumour (Berk et al., 1997). Increased IFP has been shown to be a significant barrier against

delivering therapeutic drugs such as chemotherapeutic agents into the centre of a tumour mass (Heldin et al., 2004). In another study, high IFP found to be associated with low diffusion of anti EpCAM MOC31 antibody into xenograft tumour models of HT29 colorectal cancer cells (Heine et al., 2012). Studies concerned with the role of IFP of tumours in the response of patients to cancer treatment have reported that decreasing IFP using Imatinib, an inhibitor of platelet-derived growth factor receptor, resulted in improved treatment response to chemotherapeutic drugs (Taxol and 5-FU) in mice bearing thyroid carcinoma tumours (Pietras et al., 2002).

In this project the cytotoxic effects of doxorubicin on SKBR3 and MDA-MB231 cells grown and treated under dynamic conditions was compared with its effect on cells treated under static conditions. The results showed a significant increase in the viability of the cells (survival) under dynamic conditions for both cell lines compared to static conditions. Sensitivity of MDA-MB321 cells to doxorubicin decreased significantly when cells were treated under flow/pressure or flow (150  $\mu$ L/min) conditions compared to static condition. SKBR3 cells also exhibited significantly higher resistance to doxorubicin treatment under flow and pressure compared to static condition ( $P < 0.05$ ). The reduction of sensitivity to doxorubicin treatment in dynamic compared to the static conditions may be associated with various molecular events within the ECM or cancer cells themselves. For instance, flow and/or pressure may induce ECM matrix remodelling and alter collagen network deposition and/or stiffness resulting in stimulation of integrin signalling and cancer cell proliferation and survival (Paszek et al., 2005).

Our findings are consistent with the results obtained in other studies. For example, MCF7 and MDA-MB231 cells exhibited much greater resistance to doxorubicin and paclitaxel when they were grown under flow compared to static conditions (Pradhan et al., 2018). In that study, the cancer cells encapsulated with BJ-5ta normal human foreskin immortalized fibroblasts within PEG-fibrinogen (PF) hydrogels and housed in a microfluidic chip and a continuous flow of (0.1  $\mu$ L/min) was generated using syringe pump. Endothelial cells had also been lumenised in the microvasculature of the chips

prior to housing the cells and matrix inside the chamber to recapitulate vascular network surrounding the tumour. The 3D static condition contained the same components as the flow except for endothelial cells and dynamic flow (Pradhan et al., 2018).

Overall, the results obtained in this study indicate 1) the necessity of incorporating other pathophysiological complexities into tumour models used in drug testing processes; 2) the importance of assessment of biophysical characteristics of the solid tumours before selecting the treatment regimen for a patient.

#### **4.6. Addition of fibroblasts to breast cancer cell cultures**

Fibroblasts are the main stromal cells in breast, prostate and pancreatic carcinoma (Alkasalias et al., 2018). During tumourigenesis, normal fibroblasts become activated and undergo a phenotypic modification and transform to cancer associated fibroblasts (CAFs). Although CAFs can originate from other types of cells including adipocytes, epithelial cells, endothelial cells (Zeisberg et al., 2007), bone marrow derived mesenchymal stem cells (Quante et al., 2011), and hematopoietic stem cells, it has been shown that cancer cells induce the conversion of resident fibroblasts to CAFs by secreting cytokines. In turn, CAFs positively promote survival and proliferation of cancer cells by secreting growth factors and cytokines including CXCL12 (Orimo et al., 2005, Yu et al., 2014b), CCL7 (Jung et al., 2010), TGF $\beta$ s (Zhuang et al., 2015), fibroblast growth factors (FGFs) (Bai et al., 2015), HGF (Tyan et al., 2011), periostin (Ratajczak-Wielgomas et al., 2016) and TN-C (O'Connell et al., 2011). To date, the impact of fibroblasts on cancer cells has been studied either by various co-culture methods (2D and 3D) or by growing cancer cells on fibroblast conditioned medium. In this study, normal fibroblasts were grown in collagen type-I (RAFT) and flow condition, while they were connected to cancer cells (ACMs) in a series set up in the Quasi Vivo system. This method has not been used in any previous study of fibroblast-cancer cell interaction.

This closed system allowed to mimic the paracrine signalling that occurs between cancer cells and fibroblasts. The aim was to investigate if normal breast-derived fibroblasts grown under flow conditions alter the expression of EMT related and proliferation-associated genes in the cancer cells.

The initial qRT-PCR results for expression of EMT markers and Ki67 genes showed that mRNA expression levels of MMP14 and snail increased while vimentin and Ki67 remained unchanged and cadherin 11 decreased in MDA-MB231 cell grown under flow in the presence of normal breast-derived fibroblasts. These findings suggest that normal fibroblasts may be converted to CAFs under flow condition and affect invasion of cancer cells by increasing the expression of matrix metalloproteinase.

To investigate the effect of fibroblasts on invasion distance of cancer cells, fibroblasts were co-cultured with cancer cells in ACM, embedding fibroblasts in the stromal collagen surrounding the cancer cells. The initial images and qualitative analysis of invasion distances showed that MDA-MB231 cells invade over further distance when they are co-cultured with fibroblasts compared to those in the absence of fibroblasts. These findings suggest that normal fibroblasts increase cancer cell invasion to stroma. However, the signalling pathways underlying this phenomenon need to be further investigated.

## Future perspectives

In this project, a bioengineered tumour model was combined with a Quasi Vivo bioreactor system for the first time to produce a biomimetic breast tumour. The findings were encouraging, indicating that dynamic flow conditions modulate cancer cell behaviour and response to treatment. However, further investigations can be carried out in a number of different areas. Such future work might be considered in four broad areas:

The first area would focus on further refinement of the bioengineered tumour model by addition of other biochemical components of tumour environment. The results indicated that dynamic flow conditions modulate cancer cell behaviour and response to treatment. However, apart from cancer cells, the biochemical phase of the tumour microenvironment is also affected by flow conditions. Therefore, addition of other biochemical components of the ECM including laminin, fibronectin and hyaluronic acid would serve to provide more complexity to the bioengineered 3D system and would better recapitulate the *in vivo* condition. In addition, to investigate the regulatory effects of stromal cells including fibroblasts (HDFs or CAFs) on inducing EMT and invasion of cancer cells in the presence or absence of flow and pressure, these cells can be added to the stromal collagen surrounding the cancer cells. Since immunotherapy is an emerging approach in cancer treatment, the immune cells including neutrophils, macrophages and lymphocytes could usefully be added to the stromal collagen to investigate the interplay between these cells and the cancer cells. Endothelial cells may also be added to stromal collagen to create a microvasculature network within the ACMs, enabling to study the interaction between endothelial cells and the cancer cells.

The second phase would be to expand and validate the present tumour model using a larger panel of breast cancer cell lines and/or different types of cancer cells. Breast cancer subtypes are highly heterogenous and may behave differently in our bioengineered model and under flow condition(s). Furthermore, investigating how stem cells and cancer cells other than

epithelial cells behave and respond to treatment in the model would also open new avenues for creating a physiologically relevant model for studying cell behaviour(s).

The third area would concentrate on various applications of this *in vitro* tumour model in cancer research. Primary renal carcinoma cells have been grown in RAFT culture system successfully (Prof. Loizidou, unpublished data). Primary cancer cells isolated from breast cancer patients might be usefully grown in this model and under the flow conditions. This would allow for drug responsiveness of the tumour cells isolated from each patient to be tested in the biomimetic microenvironment which ultimately would facilitate patient stratification, currently incorporating in clinical trials.

Another application would be using the Quasi Vivo circuit system to provide a co-culture system where the cancer cells grown in 3D culture in one chamber connect to the other chamber containing cells from other organs which are most likely to be the sites of distant metastases. This approach might help to elucidate mechanisms underlying metastasis and might offer potential in terms of prediction of the potential likely site for distant metastasis for patients.

The final priority for future work would be to investigate the molecular mechanisms and signalling pathways as well as matrix remodelling which may be induced under the flow and pressure condition used in this study. For example, changes in collagen orientations might be studied using scanning electron microscopy. An investigation into how tissue stiffness and flow modulate penetrance and delivery of drugs through 3D volumes, nanoparticle-conjugated drugs with imaging capacities can be used. Mathematical modelling concentrating on developing prediction algorithms based on the physical characteristics of the drugs and the environmental parameters would also further develop our current tumour model.

## Conclusion

This study has provided evidence that cancer cells behave differently in response to changes in the tumour microenvironment. Growing cancer cells in a more complex bioengineered tumour model containing components of tumour microenvironment including ECM and fluid flow and pressure resulted in a reduction of cell viability compared to conventional 2D culture. Molecular mechanisms underlying this reduction in cell viability include changes in proliferation and the apoptotic capacities of the cancer cells in the new microenvironment. The results indicated that biochemical and mechanical components of tumour microenvironment affect the expression of the genes involved in EMT of cancer cells. Growing breast cancer cells in a 3D format under flow conditions altered expression levels of genes related to hypoxia which might be due to differential distribution of oxygen in the more complex tumour model system developed during this project.

A unique finding of this study has been the observation that when cells are cultured in 3D scaffolds, they adopt a different colony morphology under flow and pressure conditions compared to static conditions. The sensitivity of breast cancer cells to doxorubicin treatment decreased when the cells were maintained in 3D culture compared to 2D culture and in flow/pressure compared to static conditions.

Collectively, the results obtained in this project indicate the substantial role of biochemical and mechanical cues of the tumour microenvironment on cancer cell behaviour and highlight the importance of incorporating complexity into *in vitro* tumour models used for studying cancer and used for preclinical phases of the drug discovery process.

## References

- ALKASALIAS, T., MOYANO-GALCERAN, L., ARSENIAN-HENRIKSSON, M. & LEHTI, K. 2018. Fibroblasts in the tumor microenvironment: shield or spear? *International journal of molecular sciences*, 19, 1532.
- ALTIERI, D. C. 2008. Survivin, cancer networks and pathway-directed drug discovery. *Nature Reviews Cancer*, 8, 61.
- ANARI, F., RAMAMURTHY, C. & ZIBELMAN, M. 2018. Impact of tumor microenvironment composition on therapeutic responses and clinical outcomes in cancer. *Future Oncology*, 14, 1409-1421.
- ANDERSON, W. F., CHATTERJEE, N., ERSHLER, W. B. & BRAWLEY, O. W. 2002. Estrogen receptor breast cancer phenotypes in the Surveillance, Epidemiology, and End Results database. *Breast cancer research and treatment*, 76, 27-36.
- ARAGONA, M., PANCIERA, T., MANFRIN, A., GIULITTI, S., MICHIELIN, F., ELVASSORE, N., DUPONT, S. & PICCOLO, S. 2013. A mechanical checkpoint controls multicellular growth through YAP/TAZ regulation by actin-processing factors. *Cell*, 154, 1047-1059.
- ARCAMONE, F., CASSINELLI, G., FANTINI, G., GREIN, A., OREZZI, P., POL, C. & SPALLA, C. 1969. Adriamycin, 14-hydroxydaimomycin, a new antitumor antibiotic from *S. Peucetius* var. *caesius*. *Biotechnology and bioengineering*, 11, 1101-1110.
- BAI, Y. P., SHANG, K., CHEN, H., DING, F., WANG, Z., LIANG, C., XU, Y., SUN, M. H. & LI, Y. Y. 2015. FGF-1/-3/FGFR 4 signaling in cancer-associated fibroblasts promotes tumor progression in colon cancer through Erk and MMP-7. *Cancer science*, 106, 1278-1287.
- BAKER, B. M. & CHEN, C. S. 2012. Deconstructing the third dimension—how 3D culture microenvironments alter cellular cues. *J Cell Sci*, 125, 3015-3024.
- BARRALLO-GIMENO, A. & NIETO, M. A. 2005. The Snail genes as inducers of cell movement and survival: implications in development and cancer. *Development*, 132, 3151-3161.
- BAXTER, L. T. & JAIN, R. K. 1989. Transport of fluid and macromolecules in tumors. I. Role of interstitial pressure and convection. *Microvascular research*, 37, 77-104.
- BERK, D. A., YUAN, F., LEUNIG, M. & JAIN, R. K. 1997. Direct in vivo measurement of targeted binding in a human tumor xenograft. *Proceedings of the National Academy of Sciences*, 94, 1785-1790.
- BØRRESEN-DALE, A. L. 2003. TP53 and breast cancer. *Human mutation*, 21, 292-300.

- BOUCHER, Y., BAXTER, L. T. & JAIN, R. K. 1990. Interstitial pressure gradients in tissue-isolated and subcutaneous tumors: implications for therapy. *Cancer research*, 50, 4478-4484.
- BOUCHER, Y., SALEHI, H., WITWER, B., HARSH IV, G. & JAIN, R. 1997. Interstitial fluid pressure in intracranial tumours in patients and in rodents. *British journal of cancer*, 75, 829.
- BRODERS-BONDON, F., HO-BOULDOIRES, T. H. N., FERNANDEZ-SANCHEZ, M.-E. & FARGE, E. 2018. Mechanotransduction in tumor progression: the dark side of the force. *J Cell Biol*, 217, 1571-1587.
- BUCHSBAUM, R. J. & OH, S. Y. 2016. Breast cancer-associated fibroblasts: where we are and where we need to go. *Cancers*, 8, 19.
- BUTLER, T. P., GRANTHAM, F. H. & GULLINO, P. M. 1975. Bulk transfer of fluid in the interstitial compartment of mammary tumors. *Cancer Research*, 35, 3084-3088.
- CAMPBELL, I. D. & HUMPHRIES, M. J. 2011. Integrin structure, activation, and interactions. *Cold Spring Harbor perspectives in biology*, 3, a004994.
- CAMPIGLIO, M., SOMENZI, G., OLGIATI, C., BERETTA, G., BALSARI, A., ZAFFARONI, N., VALAGUSSA, P. & MÉNARD, S. 2003. Role of proliferation in HER2 status predicted response to doxorubicin. *International journal of cancer*, 105, 568-573.
- CANCER RESEARCH UK. 2017. *Breast cancer statistics* [Online]. Available: <https://www.cancerresearchuk.org/health-professional/cancer-statistics/statistics-by-cancer-type/breast-cancer#heading-Three> [Accessed 11, August, 2018].
- CAREY, S. P., MARTIN, K. E. & REINHART-KING, C. A. 2017. Three-dimensional collagen matrix induces a mechanosensitive invasive epithelial phenotype. *Scientific reports*, 7, 42088.
- CASEY, A., GARGOTTI, M., BONNIER, F. & BYRNE, H. J. 2016. Chemotherapeutic efficiency of drugs in vitro: Comparison of doxorubicin exposure in 3D and 2D culture matrices. *Toxicology in Vitro*, 33, 99-104.
- CHANG, S.-F., CHANG, C. A., LEE, D.-Y., LEE, P.-L., YEH, Y.-M., YEH, C.-R., CHENG, C.-K., CHIEN, S. & CHIU, J.-J. 2008. Tumor cell cycle arrest induced by shear stress: Roles of integrins and Smad. *Proceedings of the National Academy of Sciences*, 105, 3927-3932.
- CHARAMES, G. S. & BAPAT, B. 2003. Genomic instability and cancer. *Current molecular medicine*, 3, 589-596.
- CHEANG, M. C., CHIA, S. K., VODUC, D., GAO, D., LEUNG, S., SNIDER, J., WATSON, M., DAVIES, S., BERNARD, P. S. & PARKER, J. S. 2009. Ki67 index, HER2 status, and prognosis of patients with luminal B breast cancer. *JNCI: Journal of the National Cancer Institute*, 101, 736-750.
- CHOI, Y.-L., OH, E., PARK, S., KIM, Y., PARK, Y.-H., SONG, K., CHO, E. Y., HONG, Y.-C., CHOI, J. S. & LEE, J. E. 2010. Triple-negative, basal-like, and

- quintuple-negative breast cancers: better prediction model for survival. *BMC cancer*, 10, 507.
- CHU, K., CHENG, C.-J., YE, X., LEE, Y.-C., ZURITA, A. J., CHEN, D.-T., YU-LEE, L.-Y., ZHANG, S., YEH, E. T. & HU, M. C. 2008. Cadherin-11 promotes the metastasis of prostate cancer cells to bone. *Molecular Cancer Research*, 6, 1259-1267.
- CLARK, A. G. & VIGNJEVIC, D. M. 2015. Modes of cancer cell invasion and the role of the microenvironment. *Current opinion in cell biology*, 36, 13-22.
- CURTI, B. D., URBA, W. J., ALVORD, W. G., JANIK, J. E., SMITH, J. W., MADARA, K. & LONGO, D. L. 1993. Interstitial pressure of subcutaneous nodules in melanoma and lymphoma patients: changes during treatment. *Cancer research*, 53, 2204-2207.
- DAFNI, H., COHEN, B., ZIV, K., ISRAELY, T., GOLDSHMIDT, O., NEVO, N., HARMELIN, A., VLODAVSKY, I. & NEEMAN, M. 2005a. The role of heparanase in lymph node metastatic dissemination: dynamic contrast-enhanced MRI of Eb lymphoma in mice. *Neoplasia*, 7, 224-233.
- DAFNI, H., COHEN, B., ZIV, K., ISRAELY, T., GOLDSHMIDT, O., NEVO, N., HARMELIN, A., VLODAVSKY, I. & NEEMAN, M. J. N. 2005b. The role of heparanase in lymph node metastatic dissemination: dynamic contrast-enhanced MRI of Eb lymphoma in mice. 7, 224-233.
- DAI, X., LI, T., BAI, Z., YANG, Y., LIU, X., ZHAN, J. & SHI, B. 2015. Breast cancer intrinsic subtype classification, clinical use and future trends. *American journal of cancer research*, 5, 2929.
- DAI, X., XIANG, L., LI, T. & BAI, Z. 2016. Cancer hallmarks, biomarkers and breast cancer molecular subtypes. *Journal of Cancer*, 7, 1281.
- DE WEVER, O., WESTBROEK, W., VERLOES, A., BLOEMEN, N., BRACKE, M., GESPACH, C., BRUYNEEL, E. & MAREEL, M. 2004. Critical role of N-cadherin in myofibroblast invasion and migration in vitro stimulated by colon-cancer-cell-derived TGF- $\beta$  or wounding. *Journal of cell science*, 117, 4691-4703.
- DEBNATH, J. & BRUGGE, J. S. 2005. Modelling glandular epithelial cancers in three-dimensional cultures. *Nature Reviews Cancer*, 5.
- DECARLO, L., MESTEL, C., BARCELLOS-HOFF, M.-H. & SCHNEIDER, R. J. 2015. eIF4E is a Feed-forward translational coactivator of TGF $\beta$  early pro-transforming events in breast epithelial cells. *Molecular and Cellular Biology*, MCB. 00324-15.
- DERYUGINA, E. I. & QUIGLEY, J. P. 2006. Matrix metalloproteinases and tumor metastasis. *Cancer and Metastasis Reviews*, 25, 9-34.
- DESANTIS, C., MA, J., BRYAN, L. & JEMAL, A. 2014. Breast cancer statistics, 2013. *CA: a cancer journal for clinicians*, 64, 52-62.
- DHIMAN, H. K., RAY, A. R. & PANDA, A. K. 2004. Characterization and evaluation of chitosan matrix for in vitro growth of MCF-7 breast cancer cell lines. *Biomaterials*, 25, 5147-5154.

- DIRESTA, G. R., NATHAN, S. S., MANOSO, M. W., CASAS-GANEM, J., WYATT, C., KUBO, T., BOLAND, P. J., ATHANASIAN, E. A., MIODOWNIK, J. & GORLICK, R. 2005. Cell proliferation of cultured human cancer cells are affected by the elevated tumor pressures that exist in vivo. *Annals of biomedical engineering*, 33, 1270-1280.
- DITTMER, J. & LEYH, B. The impact of tumor stroma on drug response in breast cancer. *Seminars in cancer biology*, 2015. Elsevier, 3-15.
- DONG, C., YUAN, T., WU, Y., WANG, Y., FAN, T. W., MIRIYALA, S., LIN, Y., YAO, J., SHI, J. & KANG, T. 2013. Loss of FBP1 by Snail-mediated repression provides metabolic advantages in basal-like breast cancer. *Cancer cell*, 23, 316-331.
- DUMONT, N., LIU, B., DEFILIPPIS, R. A., CHANG, H., RABBAN, J. T., KARNEZIS, A. N., TJOE, J. A., MARX, J., PARVIN, B. & TLSTY, T. D. 2013. Breast fibroblasts modulate early dissemination, tumorigenesis, and metastasis through alteration of extracellular matrix characteristics. *Neoplasia*, 15, 249-262.
- DUNNWALD, L. K., ROSSING, M. A. & LI, C. I. 2007. Hormone receptor status, tumor characteristics, and prognosis: a prospective cohort of breast cancer patients. *Breast cancer research*, 9, R6.
- ECKELMAN, B. P., SALVESEN, G. S. & SCOTT, F. L. 2006. Human inhibitor of apoptosis proteins: why XIAP is the black sheep of the family. *EMBO reports*, 7, 988-994.
- EGEBLAD, M., RASCH, M. G. & WEAVER, V. M. 2010a. Dynamic interplay between the collagen scaffold and tumor evolution. *Current opinion in cell biology*, 22, 697-706.
- EGEBLAD, M., RASCH, M. G. & WEAVER, V. M. J. C. O. I. C. B. 2010b. Dynamic interplay between the collagen scaffold and tumor evolution. 22, 697-706.
- EJLERTSEN, B., JENSEN, M.-B., NIELSEN, K. V., BALSLEV, E., RASMUSSEN, B. B., WILLEMÖE, G. L., HERTEL, P. B., KNOOP, A. S., MOURIDSEN, H. T. & BRÜNNER, N. 2009. HER2, TOP2A, and TIMP-1 and responsiveness to adjuvant anthracycline-containing chemotherapy in high-risk breast cancer patients. *Journal of Clinical Oncology*, 28, 984-990.
- EL-DEIRY, W. 1998. p21/p53, cellular growth control and genomic integrity. *Cyclin dependent kinase (CDK) inhibitors*. Springer.
- ELMORE, S. 2007. Apoptosis: a review of programmed cell death. *Toxicologic pathology*, 35, 495-516.
- EROLE, P., BOSCH, A., PÉREZ-FIDALGO, J. A. & LLUCH, A. 2012. Molecular biology in breast cancer: intrinsic subtypes and signaling pathways. *Cancer treatment reviews*, 38, 698-707.
- FADNES, H., REED, R. & AUKLAND, K. 1977. Interstitial fluid pressure in rats measured with a modified wick technique. *Microvascular research*, 14, 27-36.
- FARAHANI, E., PATRA, H. K., JANGAMREDDY, J. R., RASHEDI, I., KAWALEC, M., RAO PARITI, R. K., BATAKIS, P. & WIECHEC, E. 2014.

- Cell adhesion molecules and their relation to (cancer) cell stemness. *Carcinogenesis*, 35, 747-759.
- FARNSWORTH, R. H., ACHEN, M. G. & STACKER, S. A. 2006. Lymphatic endothelium: an important interactive surface for malignant cells. *Pulmonary pharmacology & therapeutics*, 19, 51-60.
- FENNEMA, E., RIVRON, N., ROUWKEMA, J., VAN BLITTERSWIJK, C. & DE BOER, J. 2013. Spheroid culture as a tool for creating 3D complex tissues. *Trends in biotechnology*, 31, 108-115.
- FINGER, E. C. & GIACCIA, A. J. 2010. Hypoxia, inflammation, and the tumor microenvironment in metastatic disease. *Cancer and Metastasis Reviews*, 29, 285-293.
- FRANKEL, A., BUCKMAN, R. & KERBEL, R. S. 1997. Abrogation of taxol-induced G2-M arrest and apoptosis in human ovarian cancer cells grown as multicellular tumor spheroids. *Cancer research*, 57, 2388-2393.
- FRANKLIN, M. C., CAREY, K. D., VAJDOS, F. F., LEAHY, D. J., DE VOS, A. M. & SLIWKOWSKI, M. X. 2004. Insights into ErbB signaling from the structure of the ErbB2-pertuzumab complex. *Cancer cell*, 5, 317-328.
- FRANTZ, C., STEWART, K. M. & WEAVER, V. M. 2010. The extracellular matrix at a glance. *J Cell Sci*, 123, 4195-4200.
- FRIEDL, P. & WOLF, K. 2009. Plasticity of cell migration: a multiscale tuning model. *The Journal of cell biology*, jcb. 200909003.
- FULDA, S. 2009. Tumor resistance to apoptosis. *International journal of cancer*, 124, 511-515.
- GARCÍA-TEJIDO, P., CABAL, M. L., FERNÁNDEZ, I. P. & PÉREZ, Y. F. 2016. Tumor-infiltrating lymphocytes in triple negative breast cancer: the future of immune targeting. *Clinical Medicine Insights: Oncology*, 10, CMO. S34540.
- GHOUREB, G. 1992. Oncogenes in cancer. *Advances in clinical chemistry*. Elsevier.
- GIAMPIERI, S., MANNING, C., HOOPER, S., JONES, L., HILL, C. S. & SAHAI, E. 2009. Localized and reversible TGF $\beta$  signalling switches breast cancer cells from cohesive to single cell motility. *Nature cell biology*, 11, 1287.
- GIANCOTTI, F. G. & RUOSLAHTI, E. 1999. Integrin signaling. *Science*, 285, 1028-1033.
- GOEL, S., DUDA, D. G., XU, L., MUNN, L. L., BOUCHER, Y., FUKUMURA, D. & JAIN, R. K. 2011. Normalization of the vasculature for treatment of cancer and other diseases. *Physiological reviews*, 91, 1071-1121.
- GOTTFRIED, E., KUNZ-SCHUGHART, L. A., ANDREESEN, R. & KREUTZ, M. 2006. Brave little world: spheroids as an in vitro model to study tumor-immune-cell interactions. *Cell Cycle*, 5, 691-695.
- GUAITA, S., PUIG, I., FRANCÍ, C., GARRIDO, M., DOMÍNGUEZ, D., BATLLE, E., SANCHO, E., DEDHAR, S., DE HERREROS, A. G. A. & BAULIDA, J. 2002a. Snail induction of epithelial to mesenchymal transition in tumor cells

is accompanied by MUC1 repression and ZEB1 expression. *Journal of Biological Chemistry*, 277, 39209-39216.

- GUAITA, S., PUIG, I., FRANCÍ, C., GARRIDO, M., DOMÍNGUEZ, D., BATLLE, E., SANCHO, E., DEDHAR, S., DE HERREROS, A. G. A. & BAULIDA, J. J. O. B. C. 2002b. Snail induction of epithelial to mesenchymal transition in tumor cells is accompanied by MUC1 repression and ZEB1 expression. 277, 39209-39216.
- GUO, W., PYLAYEVA, Y., PEPE, A., YOSHIOKA, T., MULLER, W. J., INGHIRAMI, G. & GIANCOTTI, F. G. 2006.  $\beta$ 4 integrin amplifies ErbB2 signaling to promote mammary tumorigenesis. *Cell*, 126, 489-502.
- GURSKI, L. A., JHA, A. K., ZHANG, C., JIA, X. & FARACH-CARSON, M. C. 2009. Hyaluronic acid-based hydrogels as 3D matrices for in vitro evaluation of chemotherapeutic drugs using poorly adherent prostate cancer cells. *Biomaterials*, 30, 6076-6085.
- GUYTON, A. C., FRANK, M. & ABERNATHY, B. 1963. A concept of negative interstitial pressure based on pressures in implanted perforated capsules. *Circulation research*, 12, 399-414.
- HAESSLER, U., TEO, J. C., FORETAY, D., RENAUD, P. & SWARTZ, M. A. 2012. Migration dynamics of breast cancer cells in a tunable 3D interstitial flow chamber. *Integrative Biology*, 4, 401-409.
- HANAHAN, D. & WEINBERG, R. A. 2011. Hallmarks of cancer: the next generation. *cell*, 144, 646-674.
- HARGENS, A. R. 1981. *Tissue fluid pressure and composition*, Williams & Wilkins.
- HASSAN, M., WATARI, H., ABUALMAATY, A., OHBA, Y. & SAKURAGI, N. 2014. Apoptosis and molecular targeting therapy in cancer. *BioMed research international*, 2014.
- HATSELL, S., ROWLANDS, T., HIREMATH, M. & COWIN, P. 2003.  $\beta$ -Catenin and Tcfs in mammary development and cancer. *Journal of mammary gland biology and neoplasia*, 8, 145-158.
- HEBBARD, L. W., GARLATTI, M., YOUNG, L. J., CARDIFF, R. D., OSHIMA, R. G. & RANSCHT, B. 2008. T-cadherin supports angiogenesis and adiponectin association with the vasculature in a mouse mammary tumor model. *Cancer research*, 68, 1407-1416.
- HEINE, M., FREUND, B., NIELSEN, P., JUNG, C., REIMER, R., HOHENBERG, H., ZANGEMEISTER-WITTKE, U., WESTER, H.-J., LÜERS, G. H. & SCHUMACHER, U. 2012. High interstitial fluid pressure is associated with low tumour penetration of diagnostic monoclonal antibodies applied for molecular imaging purposes. *PloS one*, 7, e36258.
- HELDIN, C.-H., RUBIN, K., PIETRAS, K. & ÖSTMAN, A. 2004. High interstitial fluid pressure—an obstacle in cancer therapy. *Nature Reviews Cancer*, 4, 806.
- HERHELIUK, T., PEREPELYTSINA, O., YURCHENKO, N., SYDORENKO, M. & OSTAPCHENKO, L. J. E. H. S. 2016. EXPRESSION OF TUMOR ASSOCIATED AND EPITHELIAL-MESENCHYMAL TRANSITION

- MARKERS IN 2D AND 3D CELL CULTURES OF MCF-7. *Health Sciences*, 37-44.
- HERNANDEZ-AYA, L. F. & GONZALEZ-ANGULO, A. M. 2013. Adjuvant systemic therapies in breast cancer. *Surgical Clinics*, 93, 473-491.
- HOARAU-VÉCHOT, J., RAFII, A., TOUBOUL, C. & PASQUIER, J. 2018. Halfway between 2D and animal models: are 3D cultures the ideal tool to study cancer-microenvironment interactions? *International journal of molecular sciences*, 19, 181.
- HOFMANN, M., GUSCHEL, M., BERND, A., BEREITER-HAHN, J., KAUFMANN, R., TANDI, C., WIIG, H. & KIPPENBERGER, S. 2006. Lowering of tumor interstitial fluid pressure reduces tumor cell proliferation in a xenograft tumor model. *Neoplasia*, 8, 89-95.
- HOFMANN, M., SCHULTZ, M., BERND, A., BEREITER-HAHN, J., KAUFMANN, R. & KIPPENBERGER, S. 2007. Long-term lowering of tumour interstitial fluid pressure reduces Ki-67 expression. *Journal of biomechanics*, 40, 2324-2329.
- HOLLIDAY, D. L. & SPEIRS, V. 2011. Choosing the right cell line for breast cancer research. *Breast cancer research*, 13, 215.
- HOMPLAND, T., ELLINGSEN, C., ØVREBØ, K. M. & ROFSTAD, E. K. 2012. Interstitial fluid pressure and associated lymph node metastasis revealed in tumors by dynamic contrast-enhanced MRI. *Cancer research*, 72, 4899-4908.
- HONGISTO, V., JERNSTRÖM, S., FEY, V., MPINDI, J.-P., SAHLBERG, K. K., KALLIONIEMI, O. & PERÄLÄ, M. 2013. High-throughput 3D screening reveals differences in drug sensitivities between culture models of JIMT1 breast cancer cells. *PloS one*, 8, e77232.
- HORTOBAGYI, G. N., DE LA GARZA SALAZAR, J., PRITCHARD, K., AMADORI, D., HAIDINGER, R., HUDIS, C. A., KHALED, H., LIU, M.-C., MARTIN, M. & NAMER, M. 2005. The global breast cancer burden: variations in epidemiology and survival. *Clinical breast cancer*, 6, 391-401.
- HOTARY, K., LI, X.-Y., ALLEN, E., STEVENS, S. L. & WEISS, S. J. 2006. A cancer cell metalloprotease triad regulates the basement membrane transmigration program. *Genes & development*, 20, 2673-2686.
- HU, R., DAWOOD, S., HOLMES, M. D., COLLINS, L. C., SCHNITT, S. J., COLE, K., MAROTTI, J., HANKINSON, S. E., COLDITZ, G. & TAMIMI, R. M. 2011. Androgen receptor expression and breast cancer survival in postmenopausal women. *Clinical cancer research*, clincanres. 2021.2010.
- HUANG, C.-F., LIRA, C., CHU, K., BILEN, M. A., LEE, Y.-C., YE, X., KIM, S. M., ORTIZ, A., WU, F.-L. L. & LOGOTHETIS, C. J. 2010. Cadherin-11 increases migration and invasion of prostate cancer cells and enhances their interaction with osteoblasts. *Cancer research*, 0008-5472. CAN-09-3016.
- HUBER, M. A., KRAUT, N. & BEUG, H. 2005. Molecular requirements for epithelial–mesenchymal transition during tumor progression. *Current opinion in cell biology*, 17, 548-558.

- HUDIS, C. A. 2007. Trastuzumab—mechanism of action and use in clinical practice. *New England Journal of Medicine*, 357, 39-51.
- HUH, D., HAMILTON, G. A. & INGBER, D. E. 2011. From 3D cell culture to organs-on-chips. *Trends in cell biology*, 21, 745-754.
- HUIJBERS, I. J., IRAVANI, M., POPOV, S., ROBERTSON, D., AL-SARRAJ, S., JONES, C. & ISACKE, C. M. 2010. A role for fibrillar collagen deposition and the collagen internalization receptor endo180 in glioma invasion. *PLoS one*, 5, e9808.
- HUNTER, A. M., LACASSE, E. C. & KORNELUK, R. G. 2007. The inhibitors of apoptosis (IAPs) as cancer targets. *Apoptosis*, 12, 1543-1568.
- HUNTER, K. W., CRAWFORD, N. P. & ALSARRAJ, J. 2008. Mechanisms of metastasis. *Breast Cancer Research*, 10, S2.
- ITOH, Y. 2006. MT1-MMP: A key regulator of cell migration in tissue. *IUBMB life*, 58, 589-596.
- JASTRZEBSKA, K., KUCHARCZYK, K., FLORCZAK, A., DONDAJEWSKA, E., MACKIEWICZ, A. & DAMS-KOZLOWSKA, H. 2015. Silk as an innovative biomaterial for cancer therapy. *Reports of Practical Oncology & Radiotherapy*, 20, 87-98.
- JIA, W., JIANG, X., LIU, W., WANG, L., ZHU, B., ZHU, H., LIU, X., ZHONG, M., XIE, D. & HUANG, W. 2018. Effects of three-dimensional collagen scaffolds on the expression profiles and biological functions of glioma cells. *International journal of oncology*, 52, 1787-1800.
- JIANG, W. G., DAVIES, G., MARTIN, T. A., PARR, C., WATKINS, G., MASON, M. D. & MANSEL, R. E. 2006. Expression of membrane type-1 matrix metalloproteinase, MT1-MMP in human breast cancer and its impact on invasiveness of breast cancer cells. *International journal of molecular medicine*, 17, 583-590.
- JUNG, D. W., CHE, Z. M., KIM, J., KIM, K., KIM, K. Y., WILLIAMS, D. & KIM, J. 2010. Tumor-stromal crosstalk in invasion of oral squamous cell carcinoma: a pivotal role of CCL7. *International journal of cancer*, 127, 332-344.
- JURÍKOVÁ, M., DANIHEL, Ľ., POLÁK, Š. & VARGA, I. 2016. Ki67, PCNA, and MCM proteins: Markers of proliferation in the diagnosis of breast cancer. *Acta histochemica*, 118, 544-552.
- KALLURI, R. & WEINBERG, R. A. 2009. The basics of epithelial-mesenchymal transition. *The Journal of clinical investigation*, 119, 1420-1428.
- KAMIYA, A., ANDO, J., SHIBATA, M. & MASUDA, H. 1988. Roles of fluid shear stress in physiological regulation of vascular structure and function. *Biorheology*, 25, 271-278.
- KARLSSON, H., FRYKNÄS, M., LARSSON, R. & NYGREN, P. 2012. Loss of cancer drug activity in colon cancer HCT-116 cells during spheroid formation in a new 3-D spheroid cell culture system. *Experimental cell research*, 318, 1577-1585.

- KAUPPILA, S., STENBÄCK, F., RISTELI, J., JUUKOLA, A. & RISTELI, L. 1998. Aberrant type I and type III collagen gene expression in human breast cancer in vivo. *The Journal of pathology*, 186, 262-268.
- KENNY, P. A., LEE, G. Y., MYERS, C. A., NEVE, R. M., SEMEIKS, J. R., SPELLMAN, P. T., LORENZ, K., LEE, E. H., BARCELLOS-HOFF, M. H. & PETERSEN, O. W. 2007. The morphologies of breast cancer cell lines in three-dimensional assays correlate with their profiles of gene expression. *Molecular oncology*, 1, 84-96.
- KERR, D., WHELDON, T., KERR, A., FRESHNEY, R. & KAYE, S. 1986. The effect of adriamycin and 4'-deoxydoxorubicin on cell survival of human lung tumour cells grown in monolayer and as spheroids. *British journal of cancer*, 54, 423.
- KERR, J. F., WYLLIE, A. H. & CURRIE, A. R. 1972. Apoptosis: a basic biological phenomenon with wideranging implications in tissue kinetics. *British journal of cancer*, 26, 239.
- KIDD, M. E., SHUMAKER, D. K. & RIDGE, K. M. 2014. The role of vimentin intermediate filaments in the progression of lung cancer. *American journal of respiratory cell and molecular biology*, 50, 1-6.
- KITTANEH, M., MONTERO, A. J. & GLÜCK, S. 2013. Molecular profiling for breast cancer: a comprehensive review. *Biomarkers in cancer*, 5, BIC. S9455.
- KOBAYASHI, H., MAN, S., GRAHAM, C. H., KAPITAIN, S. J., TEICHER, B. A. & KERBEL, R. S. 1993. Acquired multicellular-mediated resistance to alkylating agents in cancer. *Proceedings of the National Academy of Sciences*, 90, 3294-3298.
- KUNZ-SCHUGHART, L. A., SCHROEDER, J. A., WONDRAK, M., VAN REY, F., LEHLE, K., HOFSTAEDTER, F. & WHEATLEY, D. N. 2006. Potential of fibroblasts to regulate the formation of three-dimensional vessel-like structures from endothelial cells in vitro. *American Journal of Physiology-Cell Physiology*, 290, C1385-C1398.
- KWOK, C. K., UEDA, Y., KADARI, A., GÜNTHER, K., ERGÜN, S., HERON, A., SCHNITZLER, A. C., ROOK, M. & EDENHOFER, F. 2018. Scalable stirred suspension culture for the generation of billions of human induced pluripotent stem cells using single-use bioreactors. *Journal of tissue engineering and regenerative medicine*, 12, e1076-e1087.
- LAMBERT, A. W., OZTURK, S. & THIAGALINGAM, S. 2012. Integrin signaling in mammary epithelial cells and breast cancer. *ISRN oncology*, 2012.
- LAO, J., MADANI, J., PUÉRTOLAS, T., ÁLVAREZ, M., HERNÁNDEZ, A., PAZO-CID, R., ARTAL, Á. & ANTÓN TORRES, A. 2013. Liposomal doxorubicin in the treatment of breast cancer patients: a review. *Journal of drug delivery*, 2013.
- LAUGHNER, E., TAGHAVI, P., CHILES, K., MAHON, P. C. & SEMENZA, G. L. 2001. HER2 (neu) signaling increases the rate of hypoxia-inducible factor 1 $\alpha$  (HIF-1 $\alpha$ ) synthesis: novel mechanism for HIF-1-mediated vascular endothelial growth factor expression. *Molecular and cellular biology*, 21, 3995-4004.

- LEE, Y.-C., BILEN, M. A., YU, G., LIN, S.-C., HUANG, C.-F., ORTIZ, A., CHO, H., SONG, J. H., SATCHER, R. L. & KUANG, J. 2013. Inhibition of cell adhesion by an anti-cadherin 11 antibody prevents bone metastasis. *Molecular Cancer Research*, molcanres. 0108.2013.
- LEHMANN, B. D., BAUER, J. A., CHEN, X., SANDERS, M. E., CHAKRAVARTHY, A. B., SHYR, Y. & PIETENPOL, J. A. 2011. Identification of human triple-negative breast cancer subtypes and preclinical models for selection of targeted therapies. *The Journal of clinical investigation*, 121, 2750.
- LEUNIG, M., YUAN, F., MENGER, M. D., BOUCHER, Y., GOETZ, A. E., MESSMER, K. & JAIN, R. K. 1992. Angiogenesis, microvascular architecture, microhemodynamics, and interstitial fluid pressure during early growth of human adenocarcinoma LS174T in SCID mice. *Cancer research*, 52, 6553-6560.
- LEWIS-WAMBI, J. S. & JORDAN, V. C. 2009. Estrogen regulation of apoptosis: how can one hormone stimulate and inhibit? *Breast cancer research*, 11, 206.
- LI, D.-W., LEI, X., HE, F.-L., HE, J., LIU, Y.-L., YE, Y.-J., DENG, X., DUAN, E. & YIN, D.-C. 2017. Silk fibroin/chitosan scaffold with tunable properties and low inflammatory response assists the differentiation of bone marrow mesenchymal stem cells. *International journal of biological macromolecules*, 105, 584-597.
- LI, Y. M., ZHOU, B. P., DENG, J., PAN, Y., HAY, N. & HUNG, M.-C. 2005. A hypoxia-independent hypoxia-inducible factor-1 activation pathway induced by phosphatidylinositol-3 kinase/Akt in HER2 overexpressing cells. *Cancer Research*, 65, 3257-3263.
- LIN, R. Z. & CHANG, H. Y. 2008. Recent advances in three-dimensional multicellular spheroid culture for biomedical research. *Biotechnology Journal: Healthcare Nutrition Technology*, 3, 1172-1184.
- LIU, L. J., BROWN, S. L., EWING, J. R., ALA, B. D., SCHNEIDER, K. M. & SCHLESINGER, M. 2016. Estimation of Tumor Interstitial Fluid Pressure (TIFP) Noninvasively. *PloS one*, 11, e0140892.
- LIU, M., ZHANG, X., LONG, C., XU, H., CHENG, X., CHANG, J., ZHANG, C., ZHANG, C. & WANG, X. 2018. Collagen-based three-dimensional culture microenvironment promotes epithelial to mesenchymal transition and drug resistance of human ovarian cancer in vitro. *RSC Advances*, 8, 8910-8919.
- LOESSNER, D., STOK, K. S., LUTOLF, M. P., HUTMACHER, D. W., CLEMENTS, J. A. & RIZZI, S. C. 2010. Bioengineered 3D platform to explore cell-ECM interactions and drug resistance of epithelial ovarian cancer cells. *Biomaterials*, 31, 8494-8506.
- LOI, S., HAIBE-KAINS, B., DESMEDT, C., LALLEMAND, F., TUTT, A. M., GILLET, C., ELLIS, P., HARRIS, A., BERGH, J. & FOEKENS, J. A. 2007. Definition of clinically distinct molecular subtypes in estrogen receptor-positive breast carcinomas through genomic grade. *Journal of clinical oncology*, 25, 1239.

- LØNNING, P., KNAPPSKOG, S., STAALESEN, V., CHRISANTHAR, R. & LILLEHAUG, J. 2007. Breast cancer prognostication and prediction in the postgenomic era. *Annals of Oncology*, 18, 1293-1306.
- LOVITT, C. J., SHELPER, T. B. & AVERY, V. M. 2018. Doxorubicin resistance in breast cancer cells is mediated by extracellular matrix proteins. *BMC cancer*, 18, 41.
- LUCA, A. C., MERSCH, S., DEENEN, R., SCHMIDT, S., MESSNER, I., SCHÄFER, K.-L., BALDUS, S. E., HUCKENBECK, W., PIEKORZ, R. P. & KNOEFEL, W. T. 2013. Impact of the 3D microenvironment on phenotype, gene expression, and EGFR inhibition of colorectal cancer cell lines. *PloS one*, 8, e59689.
- LUO, H., TU, G., LIU, Z. & LIU, M. 2015. Cancer-associated fibroblasts: a multifaceted driver of breast cancer progression. *Cancer letters*, 361, 155-163.
- MA, J. & JEMAL, A. 2013. Breast cancer statistics. *Breast Cancer Metastasis and Drug Resistance*. Springer.
- MACFARLANE, R. J. & GELMON, K. A. 2011. Lapatinib for breast cancer: a review of the current literature. *Expert opinion on drug safety*, 10, 109-121.
- MAGDELDIN, T., LÓPEZ-DÁVILA, V., PAPE, J., CAMERON, G. W., EMBERTON, M., LOIZIDOU, M. & CHEEMA, U. 2017. Engineering a vascularised 3D in vitro model of cancer progression. *Scientific reports*, 7, 44045.
- MALANEY, P., NICOSIA, S. V. & DAVÉ, V. 2014. One mouse, one patient paradigm: New avatars of personalized cancer therapy. *Cancer letters*, 344, 1-12.
- MARANGONI, E. & POUPON, M.-F. 2014. Patient-derived tumour xenografts as models for breast cancer drug development. *Current opinion in oncology*, 26, 556-561.
- MATSUOKA, J., YASHIRO, M., DOI, Y., FUYUHIRO, Y., KATO, Y., SHINTO, O., NODA, S., KASHIWAGI, S., AOMATSU, N. & HIRAKAWA, T. 2013. Hypoxia stimulates the EMT of gastric cancer cells through autocrine TGF $\beta$  signaling. *PloS one*, 8, e62310.
- MCILWAIN, D. R., BERGER, T. & MAK, T. W. 2013. Caspase functions in cell death and disease. *Cold Spring Harbor perspectives in biology*, 5, a008656.
- MICHEAU, O. 2003. Cellular FLICE-inhibitory protein: an attractive therapeutic target? *Expert opinion on therapeutic targets*, 7, 559-573.
- MILOSEVIC, M., FYLES, A., HEDLEY, D., PINTILIE, M., LEVIN, W., MANCHUL, L. & HILL, R. 2001. Interstitial fluid pressure predicts survival in patients with cervix cancer independent of clinical prognostic factors and tumor oxygen measurements. *Cancer research*, 61, 6400-6405.
- MUELLER, B. M. & REISFELD, R. A. 1991. Potential of the scid mouse as a host for human tumors. *Cancer and Metastasis Reviews*, 10, 193-200.

- NAHTA, R., HUNG, M.-C. & ESTEVA, F. J. 2004. The HER-2-targeting antibodies trastuzumab and pertuzumab synergistically inhibit the survival of breast cancer cells. *Cancer research*, 64, 2343-2346.
- NANDA, R. 2014. A phase Ib study of pembrolizumab (MK-3475) in patients with advanced triple-negative breast cancer. *San Antonio Breast Cancer Symposium (SABCS)*, San Antonio.
- NARDELLA, C., LUNARDI, A., PATNAIK, A., CANTLEY, L. C. & PANDOLFI, P. P. 2011. The APL paradigm and the “co-clinical trial” project. *AACR*.
- NG, C. P., HINZ, B. & SWARTZ, M. A. 2005. Interstitial fluid flow induces myofibroblast differentiation and collagen alignment in vitro. *Journal of cell science*, 118, 4731-4739.
- NIEMAN, M. T., PRUDOFF, R. S., JOHNSON, K. R. & WHEELOCK, M. J. 1999. N-cadherin promotes motility in human breast cancer cells regardless of their E-cadherin expression. *The Journal of cell biology*, 147, 631-644.
- NIEMIEC, J. A., ADAMCZYK, A., AMBICKA, A., MUCHA-MALECKA, A., WYSOCKI, W. M. & RYS, J. 2014. Triple-negative, basal marker-expressing, and high-grade breast carcinomas are characterized by high lymphatic vessel density and the expression of podoplanin in stromal fibroblasts. *Applied Immunohistochemistry & Molecular Morphology*, 22, 10-16.
- NOWELL, P. C. 1976. The clonal evolution of tumor cell populations. *Science*, 194, 23-28.
- NUCIFORO, P., RADOSEVIC-ROBIN, N., NG, T. & SCALTRITI, M. 2015. Quantification of HER family receptors in breast cancer. *Breast cancer research*, 17, 53.
- O'CONNELL, J. T., SUGIMOTO, H., COOKE, V. G., MACDONALD, B. A., MEHTA, A. I., LEBLEU, V. S., DEWAR, R., ROCHA, R. M., BRENTANI, R. R. & RESNICK, M. B. 2011. VEGF-A and Tenascin-C produced by S100A4+ stromal cells are important for metastatic colonization. *Proceedings of the National Academy of Sciences*, 108, 16002-16007.
- OGAWA, Y., HAI, E., MATSUMOTO, K., IKEDA, K., TOKUNAGA, S., NAGAHARA, H., SAKURAI, K., INOUE, T. & NISHIGUCHI, Y. 2008. Androgen receptor expression in breast cancer: relationship with clinicopathological factors and biomarkers. *International journal of clinical oncology*, 13, 431-435.
- OKAZAKI, M., TAKESHITA, S., KAWAI, S., KIKUNO, R., TSUJIMURA, A., KUDO, A. & AMANN, E. 1994. Molecular cloning and characterization of OB-cadherin, a new member of cadherin family expressed in osteoblasts. *Journal of Biological Chemistry*, 269, 12092-12098.
- OLMEDA, D., MORENO-BUENO, G., FLORES, J. M., FABRA, A., PORTILLO, F. & CANO, A. 2007. SNAI1 is required for tumor growth and lymph node metastasis of human breast carcinoma MDA-MB-231 cells. *Cancer research*, 67, 11721-11731.

- ONCOLOGY, A. S. O. C. 2018. *TAILORx: Most Women With Early-Stage Breast Cancer Can Forgo Chemotherapy When Guided by a Diagnostic Test* [Online]. Available: <http://www.ascopost.com/News/58904> [Accessed 6 August,2018].
- ORIMO, A., GUPTA, P. B., SGROI, D. C., ARENZANA-SEISDEDOS, F., DELAUNAY, T., NAEEM, R., CAREY, V. J., RICHARDSON, A. L. & WEINBERG, R. A. 2005. Stromal fibroblasts present in invasive human breast carcinomas promote tumor growth and angiogenesis through elevated SDF-1/CXCL12 secretion. *Cell*, 121, 335-348.
- OSKARSSON, T. 2013. Extracellular matrix components in breast cancer progression and metastasis. *The Breast*, 22, S66-S72.
- OZERDEM, U. & HARGENS, A. R. 2005. A simple method for measuring interstitial fluid pressure in cancer tissues. *Microvascular research*, 70, 116-120.
- PALMIERI, C., ROBERTS-CLARK, D., ASSADI-SABET, A., COOPE, R., O'HARE, M., SUNTERS, A., HANBY, A., SLADE, M., GOMM, J. & LAM, E. 2003. Fibroblast growth factor 7, secreted by breast fibroblasts, is an interleukin-1beta-induced paracrine growth factor for human breast cells. *Journal of Endocrinology*, 177, 65-81.
- PASZEK, M. J., ZAHIR, N., JOHNSON, K. R., LAKINS, J. N., ROZENBERG, G. I., GEFEN, A., REINHART-KING, C. A., MARGULIES, S. S., DEMBO, M. & BOETTIGER, D. 2005. Tensional homeostasis and the malignant phenotype. *Cancer cell*, 8, 241-254.
- PATHAK, A. P., ARTEMOV, D., NEEMAN, M. & BHUJWALLA, Z. M. 2006. Lymph node metastasis in breast cancer xenografts is associated with increased regions of extravascular drain, lymphatic vessel area, and invasive phenotype. *Cancer research*, 66, 5151-5158.
- PATSIALOU, A., BRAVO-CORDERO, J. J., WANG, Y., ENTENBERG, D., LIU, H., CLARKE, M. & CONDEELIS, J. S. 2013. Intravital multiphoton imaging reveals multicellular streaming as a crucial component of in vivo cell migration in human breast tumors. *Intravital*, 2, e25294.
- PDQPTE, B. 2002. Childhood non-hodgkin lymphoma treatment (PDQ (R)): health professional version. *PDQ Cancer Information Summaries*.
- PEDERSEN, J. A., LICHTER, S. & SWARTZ, M. A. 2010. Cells in 3D matrices under interstitial flow: effects of extracellular matrix alignment on cell shear stress and drag forces. *Journal of biomechanics*, 43, 900-905.
- PICKL, M. & RIES, C. 2009. Comparison of 3D and 2D tumor models reveals enhanced HER2 activation in 3D associated with an increased response to trastuzumab. *Oncogene*, 28, 461.
- PIETRAS, K., RUBIN, K., SJÖBLM, T., BUCHDUNGER, E., SJÖQUIST, M., HELDIN, C.-H. & ÖSTMAN, A. 2002. Inhibition of PDGF receptor signaling in tumor stroma enhances antitumor effect of chemotherapy. *Cancer research*, 62, 5476-5484.

- PIOTROWSKI-DASPIT, A. S., TIEN, J. & NELSON, C. M. 2016. Interstitial fluid pressure regulates collective invasion in engineered human breast tumors via Snail, vimentin, and E-cadherin. *Integrative Biology*, 8, 319-331.
- PRADHAN, S., SMITH, A. M., GARSON, C. J., HASSANI, I., SEETO, W. J., PANT, K., ARNOLD, R. D., PRABHAKARPANDIAN, B. & LIPKE, E. A. 2018. A microvascularized tumor-mimetic platform for assessing anti-cancer drug efficacy. *Scientific reports*, 8, 3171.
- PRAT, A. & PEROU, C. M. 2011. Deconstructing the molecular portraits of breast cancer. *Molecular oncology*, 5, 5-23.
- QIAN, B.-Z. & POLLARD, J. W. 2010. Macrophage diversity enhances tumor progression and metastasis. *cell*, 141, 39-51.
- QUANTE, M., TU, S. P., TOMITA, H., GONDA, T., WANG, S. S., TAKASHI, S., BAIK, G. H., SHIBATA, W., DIPRETE, B. & BETZ, K. S. 2011. Bone marrow-derived myofibroblasts contribute to the mesenchymal stem cell niche and promote tumor growth. *Cancer cell*, 19, 257-272.
- RAKHA, E. A., EL-SAYED, M. E., GREEN, A. R., PAISH, E. C., POWE, D. G., GEE, J., NICHOLSON, R. I., LEE, A. H., ROBERTSON, J. F. & ELLIS, I. O. 2007. Biologic and clinical characteristics of breast cancer with single hormone receptor-positive phenotype. *Journal of Clinical Oncology*, 25, 4772-4778.
- RATAJCZAK-WIELGOMAS, K., GRZEGRZOLKA, J., PIOTROWSKA, A., GOMULKIEWICZ, A., WITKIEWICZ, W. & DZIEGIEL, P. 2016. Periostin expression in cancer-associated fibroblasts of invasive ductal breast carcinoma. *Oncology reports*, 36, 2745-2754.
- RATHOS, M. J., KHANWALKAR, H., JOSHI, K., MANOHAR, S. M. & JOSHI, K. S. 2013. Potentiation of in vitro and in vivo antitumor efficacy of doxorubicin by cyclin-dependent kinase inhibitor P276-00 in human non-small cell lung cancer cells. *BMC cancer*, 13, 29.
- REN, D., YANG, Q., DAI, Y., GUO, W., DU, H., SONG, L. & PENG, X. 2017. Oncogenic miR-210-3p promotes prostate cancer cell EMT and bone metastasis via NF- $\kappa$ B signaling pathway. *Molecular cancer*, 16, 117.
- RENAUD, S., GUENOT, D., FALCOZ, P.-E., MASSARD, G. & BEAU-FALLER, M. 2014. Role of hypoxia in epithelial-to-mesenchymal transition (EMT) in non-small cell lung cancer (NSCLC). *European Respiratory Journal*, 44, P814.
- REYMOND, N., D'ÁGUA, B. B. & RIDLEY, A. J. 2013. Crossing the endothelial barrier during metastasis. *Nature Reviews Cancer*, 13, 858.
- RIJAL, G. & LI, W. 2016. 3D scaffolds in breast cancer research. *Biomaterials*, 81, 135-156.
- RIPPE, B. & HARALDSSON, B. 1994. Transport of macromolecules across microvascular walls: the two-pore theory. *Physiological reviews*, 74, 163-219.
- RIZVI, I., GURKAN, U. A., TASOGLU, S., ALAGIC, N., CELLI, J. P., MENSAH, L. B., MAI, Z., DEMIRCI, U. & HASAN, T. 2013. Flow induces epithelial-

- mesenchymal transition, cellular heterogeneity and biomarker modulation in 3D ovarian cancer nodules. *Proceedings of the National Academy of Sciences*, 110, E1974-E1983.
- ROFSTAD, E. K., GALAPPATHI, K. & MATHIESEN, B. S. 2014. Tumor interstitial fluid pressure—a link between tumor hypoxia, microvascular density, and lymph node metastasis. *Neoplasia*, 16, 586-594.
- ROFSTAD, E. K., TUNHEIM, S. H., MATHIESEN, B., GRAFF, B. A., HALSØR, E. F., NILSEN, K. & GALAPPATHI, K. 2002. Pulmonary and lymph node metastasis is associated with primary tumor interstitial fluid pressure in human melanoma xenografts. *Cancer research*, 62, 661-664.
- RUSSO, J., HU, Y.-F., YANG, X. & RUSSO, I. H. 2000. Chapter 1: Developmental, cellular, and molecular basis of human breast cancer. *JNCI Monographs*, 2000, 17-37.
- SAELENS, X., FESTJENS, N., WALLE, L. V., VAN GURP, M., VAN LOO, G. & VANDENABEELE, P. 2004. Toxic proteins released from mitochondria in cell death. *Oncogene*, 23, 2861.
- SAINI, S., TULLA, K., MAKER, A. V., BURMAN, K. D. & PRABHAKAR, B. S. 2018. Therapeutic advances in anaplastic thyroid cancer: a current perspective. *Molecular cancer*, 17, 154.
- SARRIÓ, D., RODRIGUEZ-PINILLA, S. M., HARDISSON, D., CANO, A., MORENO-BUENO, G. & PALACIOS, J. 2008. Epithelial-mesenchymal transition in breast cancer relates to the basal-like phenotype. *Cancer research*, 68, 989-997.
- SATCHER, R. L., PAN, T., CHENG, C.-J., LEE, Y.-C., LIN, S.-C., YU, G., LI, X., HOANG, A. G., TAMBOLI, P. & JONASCH, E. 2014. Cadherin-11 in renal cell carcinoma bone metastasis. *PloS one*, 9, e89880.
- SCHMITTGEN, T. D. & LIVAK, K. J. J. N. P. 2008. Analyzing real-time PCR data by the comparative C T method. 3, 1101.
- SCHOLANDER, P., HARGENS, A. R. & MILLER, S. L. 1968. Negative pressure in the interstitial fluid of animals. *Science*, 161, 321-328.
- SCHOUMACHER, M., GOLDMAN, R. D., LOUVARD, D. & VIGNJEVIC, D. M. 2010. Actin, microtubules, and vimentin intermediate filaments cooperate for elongation of invadopodia. *The Journal of cell biology*, 189, 541-556.
- SHIEH, A. C., ROZANSKY, H. A., HINZ, B. & SWARTZ, M. A. 2011. Tumor cell invasion is promoted by interstitial flow-induced matrix priming by stromal fibroblasts. *Cancer research*.
- SHIELDS, J. D., FLEURY, M. E., YONG, C., TOMEI, A. A., RANDOLPH, G. J. & SWARTZ, M. A. 2007. Autologous chemotaxis as a mechanism of tumor cell homing to lymphatics via interstitial flow and autocrine CCR7 signaling. *Cancer cell*, 11, 526-538.
- SHIELDS, M. A., DANGI-GARIMELLA, S., KRANTZ, S. B., BENTREM, D. J. & MUNSHI, H. G. 2011. Pancreatic cancer cells respond to type I collagen by inducing snail expression to promote membrane type 1 matrix

- metalloproteinase-dependent collagen invasion. *Journal of Biological Chemistry*, 286, 10495-10504.
- SIOW, Z. R., DE BOER, R. H., LINDEMAN, G. J. & MANN, G. B. 2018. Spotlight on the utility of the Oncotype DX® breast cancer assay. *International journal of women's health*, 10, 89.
- SJÖGREN, S., INGANÄS, M., LINDGREN, A., HOLMBERG, L. & BERGH, J. 1998. Prognostic and predictive value of c-erbB-2 overexpression in primary breast cancer, alone and in combination with other prognostic markers. *Journal of Clinical Oncology*, 16, 462-469.
- SOLINAS, G., GERMANO, G., MANTOVANI, A. & ALLAVENA, P. 2009. Tumor-associated macrophages (TAM) as major players of the cancer-related inflammation. *Journal of leukocyte biology*, 86, 1065-1073.
- SOMMERS, C. L., WALKER-JONES, D., HECKFORD, S. E., WORLAND, P., VALVERIUS, E., CLARK, R., MCCORMICK, F., STAMPFER, M., ABULARACH, S. & GELMANN, E. P. 1989. Vimentin rather than keratin expression in some hormone-independent breast cancer cell lines and in oncogene-transformed mammary epithelial cells. *Cancer research*, 49, 4258-4263.
- SOON, P. S., KIM, E., PON, C. K., GILL, A. J., MOORE, K., SPILLANE, A. J., BENN, D. E. & BAXTER, R. C. 2013. Breast cancer-associated fibroblasts induce epithelial-to-mesenchymal transition in breast cancer cells. *Endocrine-related cancer*, 20, 1-12.
- SORLIE, T., TIBSHIRANI, R., PARKER, J., HASTIE, T., MARRON, J., NOBEL, A., DENG, S., JOHNSEN, H., PESICH, R. & GEISLER, S. 2003. Repeated observation of breast tumor subtypes in independent gene expression data sets. *Proceedings of the National Academy of Sciences of the United States of America*, 100, 8418-8423.
- SOTIRIOU, C., NEO, S.-Y., MCSHANE, L. M., KORN, E. L., LONG, P. M., JAZAERI, A., MARTIAT, P., FOX, S. B., HARRIS, A. L. & LIU, E. T. 2003. Breast cancer classification and prognosis based on gene expression profiles from a population-based study. *Proceedings of the National Academy of Sciences*, 100, 10393-10398.
- SOUZA, G. R., MOLINA, J. R., RAPHAEL, R. M., OZAWA, M. G., STARK, D. J., LEVIN, C. S., BRONK, L. F., ANANTA, J. S., MANDELIN, J. & GEORGESCU, M.-M. 2010. Three-dimensional tissue culture based on magnetic cell levitation. *Nature nanotechnology*, 5, 291.
- SPITALE, A., MAZZOLA, P., SOLDINI, D., MAZZUCHELLI, L. & BORDONI, A. 2008. Breast cancer classification according to immunohistochemical markers: clinicopathologic features and short-term survival analysis in a population-based study from the South of Switzerland. *Annals of oncology*, 20, 628-635.
- STANTON, S. E., ADAMS, S. & DISIS, M. L. 2016. Variation in the incidence and magnitude of tumor-infiltrating lymphocytes in breast cancer subtypes: a systematic review. *JAMA oncology*, 2, 1354-1360.

- SUNG, K. E., SU, X., BERTHIER, E., PEHLKE, C., FRIEDL, A. & BEEBE, D. J. 2013. Understanding the impact of 2D and 3D fibroblast cultures on in vitro breast cancer models. *PloS one*, 8, e76373.
- SWAIN, S. 2008. Triple-negative breast cancer: Metastatic risk and role of platinum agents.. Presented at the Annual Meeting of the American Society for Clinical Oncology. *Clinical Science Symposium*. Chicago.
- SWARTZ, M. A. & LUND, A. W. 2012. Lymphatic and interstitial flow in the tumour microenvironment: linking mechanobiology with immunity. *Nature Reviews Cancer*, 12, 210.
- TACAR, O., SRIAMORNSAK, P. & DASS, C. R. 2013. Doxorubicin: an update on anticancer molecular action, toxicity and novel drug delivery systems. *Journal of Pharmacy and Pharmacology*, 65, 157-170.
- TAKAI, K., LE, A., WEAVER, V. M. & WERB, Z. 2016. Targeting the cancer-associated fibroblasts as a treatment in triple-negative breast cancer. *Oncotarget*, 7, 82889.
- TAKEUCHI, T., MISAKI, A., CHEN, B. K. & OHTSUKI, Y. 1999. H-cadherin expression in breast cancer. *Histopathology*, 35, 87-88.
- TAMURA, D., HIRAGA, T., MYOUI, A., YOSHIKAWA, H. & YONEDA, T. 2008. Cadherin-11-mediated interactions with bone marrow stromal/osteoblastic cells support selective colonization of breast cancer cells in bone. *International journal of oncology*, 33, 17-24.
- THEVENEAU, E. & MAYOR, R. 2012. Cadherins in collective cell migration of mesenchymal cells. *Current opinion in cell biology*, 24, 677-684.
- TOIVOLA, D., STRNAD, P., HABTEZION, A. & OMARY, M. 2010. Intermediate filaments take the heat as stress proteins. *Trends in cell biology*, 20, 79-91.
- TOYOOKA, K. O., TOYOOKA, S., VIRMANI, A. K., SATHYANARAYANA, U. G., EUHUS, D. M., GILCREASE, M., MINNA, J. D. & GAZDAR, A. F. 2001. Loss of expression and aberrant methylation of the CDH13 (H-cadherin) gene in breast and lung carcinomas. *Cancer research*, 61, 4556-4560.
- TRIVERS, K. F., LUND, M. J., PORTER, P. L., LIFF, J. M., FLAGG, E. W., COATES, R. J. & ELEY, J. W. 2009. The epidemiology of triple-negative breast cancer, including race. *Cancer causes & control*, 20, 1071-1082.
- TYAN, S.-W., KUO, W.-H., HUANG, C.-K., PAN, C.-C., SHEW, J.-Y., CHANG, K.-J., EVA, Y.-H. L. & LEE, W.-H. 2011. Breast cancer cells induce cancer-associated fibroblasts to secrete hepatocyte growth factor to enhance breast tumorigenesis. *PloS one*, 6, e15313.
- VAN DE VIJVER, M. J., HE, Y. D., VAN'T VEER, L. J., DAI, H., HART, A. A., VOSKUIL, D. W., SCHREIBER, G. J., PETERSE, J. L., ROBERTS, C. & MARTON, M. J. 2002. A gene-expression signature as a predictor of survival in breast cancer. *New England Journal of Medicine*, 347, 1999-2009.
- VANNESTE, D., TAKAGI, M., IMAMOTO, N. & VERNOS, I. 2009. The role of Hklp2 in the stabilization and maintenance of spindle bipolarity. *Current Biology*, 19, 1712-1717.

- VARIA, M. A., CALKINS-ADAMS, D. P., RINKER, L. H., KENNEDY, A. S., NOVOTNY, D. B., FOWLER JR, W. C. & RALEIGH, J. A. 1998. Pimonidazole: a novel hypoxia marker for complementary study of tumor hypoxia and cell proliferation in cervical carcinoma. *Gynecologic oncology*, 71, 270-277.
- VINCI, M., GOWAN, S., BOXALL, F., PATTERSON, L., ZIMMERMANN, M., LOMAS, C., MENDIOLA, M., HARDISSON, D. & ECCLES, S. A. 2012. Advances in establishment and analysis of three-dimensional tumor spheroid-based functional assays for target validation and drug evaluation. *BMC biology*, 10, 29.
- VOGEL, C. L., COBLEIGH, M. A., TRIPATHY, D., GUTHEIL, J. C., HARRIS, L. N., FEHRENBACHER, L., SLAMON, D. J., MURPHY, M., NOVOTNY, W. F. & BURCHMORE, M. 2002. Efficacy and safety of trastuzumab as a single agent in first-line treatment of HER2-overexpressing metastatic breast cancer. *Journal of Clinical Oncology*, 20, 719-726.
- WANG, M., ZHAO, J., ZHANG, L., WEI, F., LIAN, Y., WU, Y., GONG, Z., ZHANG, S., ZHOU, J. & CAO, K. 2017. Role of tumor microenvironment in tumorigenesis. *Journal of Cancer*, 8, 761.
- WANG, Y., SHI, J., CHAI, K., YING, X. & P ZHOU, B. 2013. The role of Snail in EMT and tumorigenesis. *Current cancer drug targets*, 13, 963-972.
- WEIGELT, B., LO, A. T., PARK, C. C., GRAY, J. W. & BISSELL, M. J. 2010. HER2 signaling pathway activation and response of breast cancer cells to HER2-targeting agents is dependent strongly on the 3D microenvironment. *Breast cancer research and treatment*, 122, 35-43.
- WELTER, M. & RIEGER, H. 2013. Interstitial fluid flow and drug delivery in vascularized tumors: a computational model. *PloS one*, 8, e70395.
- WHITE, D. E., KURPIOS, N. A., ZUO, D., HASSELL, J. A., BLAESS, S., MUELLER, U. & MULLER, W. J. 2004. Targeted disruption of  $\beta$ 1-integrin in a transgenic mouse model of human breast cancer reveals an essential role in mammary tumor induction. *Cancer cell*, 6, 159-170.
- WIEDERHIELM, C. A., WOODBURY, J. W., KIRK, S. & RUSHMER, R. F. 1964. Pulsatile pressures in the microcirculation of frog's mesentery. *American Journal of Physiology-Legacy Content*, 207, 173-176.
- WIIG, H., REED, R. K. & AUKLAND, K. 1987. Measurement of interstitial fluid pressure in dogs: evaluation of methods. *American Journal of Physiology-Heart and Circulatory Physiology*, 253, H283-H290.
- WU, Y.-D. & ZHOU, B. 2010. TNF- $\alpha$ /NF- $\kappa$ B/Snail pathway in cancer cell migration and invasion. *British journal of cancer*, 102, 639.
- XIA, F. & POWELL, S. N. The molecular basis of radiosensitivity and chemosensitivity in the treatment of breast cancer. *Seminars in radiation oncology*, 2002. Elsevier, 296-304.

- XUE, C., PLIETH, D., VENKOV, C., XU, C. & NEILSON, E. G. 2003. The gatekeeper effect of epithelial-mesenchymal transition regulates the frequency of breast cancer metastasis. *Cancer research*, 63, 3386-3394.
- YANG, L., SHANG, Z., LONG, S., WANG, N., SHAN, G. & ZHANG, R. 2018. Roles of genetic and microenvironmental factors in cancer epithelial-to-mesenchymal transition and therapeutic implication. *Experimental cell research*.
- YASUI, Y., GOTO, H., MATSUI, S., MANSER, E., LIM, L., NAGATA, K.-I. & INAGAKI, M. 2001. Protein kinases required for segregation of vimentin filaments in mitotic process. *Oncogene*, 20, 2868.
- YU, T., LIU, K., WU, Y., FAN, J., CHEN, J., LI, C., ZHU, G., WANG, Z. & LI, L. 2013. High interstitial fluid pressure promotes tumor cell proliferation and invasion in oral squamous cell carcinoma. *International journal of molecular medicine*, 32, 1093-1100.
- YU, T., WANG, Z., LIU, K., WU, Y., FAN, J., CHEN, J., LI, C., ZHU, G. & LI, L. 2014a. High interstitial fluid pressure promotes tumor progression through inducing lymphatic metastasis-related protein expressions in oral squamous cell carcinoma. *Clinical and Translational Oncology*, 16, 539-547.
- YU, Y., XIAO, C., TAN, L., WANG, Q., LI, X. & FENG, Y. 2014b. Cancer-associated fibroblasts induce epithelial-mesenchymal transition of breast cancer cells through paracrine TGF- $\beta$  signalling. *British journal of cancer*, 110, 724.
- ZEISBERG, E. M., POTENTA, S., XIE, L., ZEISBERG, M. & KALLURI, R. 2007. Discovery of endothelial to mesenchymal transition as a source for carcinoma-associated fibroblasts. *Cancer research*, 67, 10123-10128.
- ZHANG, L., HUANG, G., LI, X., ZHANG, Y., JIANG, Y., SHEN, J., LIU, J., WANG, Q., ZHU, J. & FENG, X. 2013. Hypoxia induces epithelial-mesenchymal transition via activation of SNAIL by hypoxia-inducible factor-1 $\alpha$  in hepatocellular carcinoma. *BMC cancer*, 13, 108.
- ZHU, G. G., KAUPPILA, A., RISTELI, L., MÄKINEN, M., STENBÄCK, F. & RISTELI, J. 1995. Immunohistochemical study of type I collagen and type I pN-collagen in benign and malignant ovarian neoplasms. *Cancer*, 75, 1010-1017.
- ZHU, L. & ZHAO, Q. 2017. Hypoxia-inducible factor 1 $\alpha$  participates in hypoxia-induced epithelial-mesenchymal transition via response gene to complement 32. *Experimental and therapeutic medicine*, 14, 1825-1831.
- ZHU, Y.-S., CAI, L.-Q., CORDERO, J. J., CANOVATCHEL, W. J., KATZ, M. D. & IMPERATO-MCGINLEY, J. 1999. A novel mutation in the CAG triplet region of exon 1 of androgen receptor gene causes complete androgen insensitivity syndrome in a large kindred. *The Journal of Clinical Endocrinology & Metabolism*, 84, 1590-1594.
- ZHUANG, J., LU, Q., SHEN, B., HUANG, X., SHEN, L., ZHENG, X., HUANG, R., YAN, J. & GUO, H. 2015. TGF $\beta$ 1 secreted by cancer-associated fibroblasts

induces epithelial-mesenchymal transition of bladder cancer cells through lncRNA-ZEB2NAT. *Scientific reports*, 5, 11924.

ZIELLO, J. E., JOVIN, I. S. & HUANG, Y. 2007. Hypoxia-Inducible Factor (HIF)-1 regulatory pathway and its potential for therapeutic intervention in malignancy and ischemia. *The Yale journal of biology and medicine*, 80, 51.

# Appendices

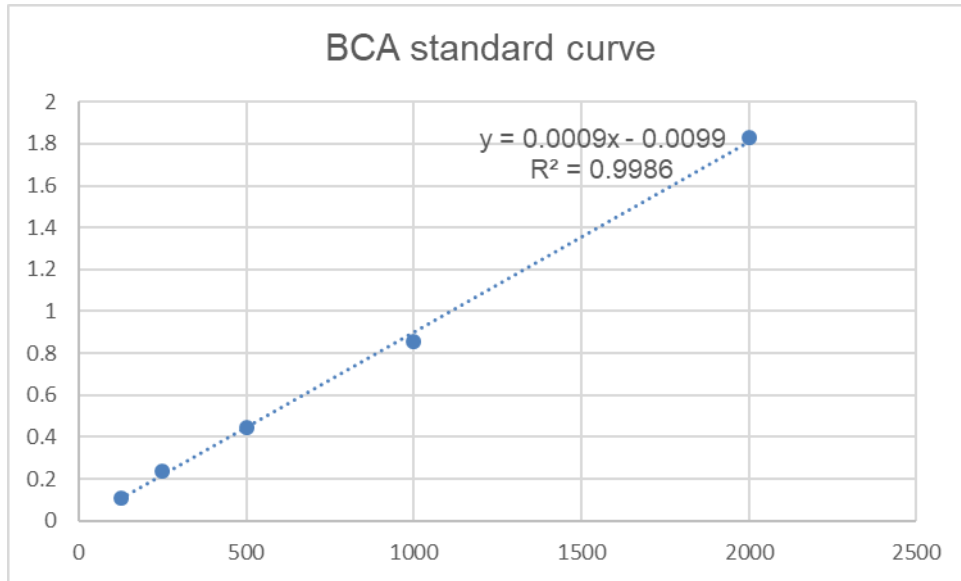
# Appendix 1

## Chemicals used in this project

Chemical	Company and country
Tris base	Sigma Aldrich
Glycine	Sigma Aldrich
Methanol	VWR
Ethanol	VWR
Formaldehyde 4% w/v	Sigma
Tween 20	Fisher Scientific
Sodium Dodecyl Sulphate (SDS)	Sigma
30% Acrylamide/Bis	Sigma
HCl	Thermofisher
TEMED	Sigma
HEPES buffer	Sigma
NaOH	Thermofisher
Hanks Balanced Salt Solution (HBSS)	Sigma
Triton X-114	Sigma
Glycerol	PROLABO
Bromophenol Blue	Plusone
DMSO	Sigma

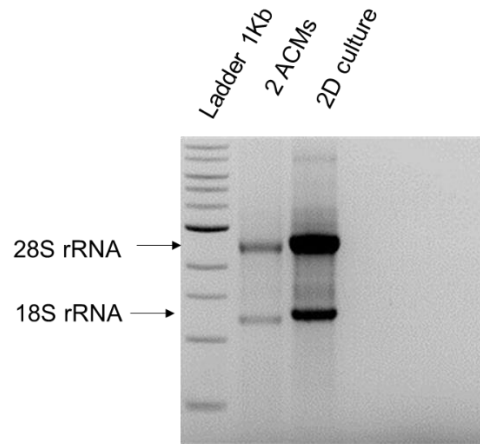
# Appendix 2

## Protein standard curve (BCA assay)

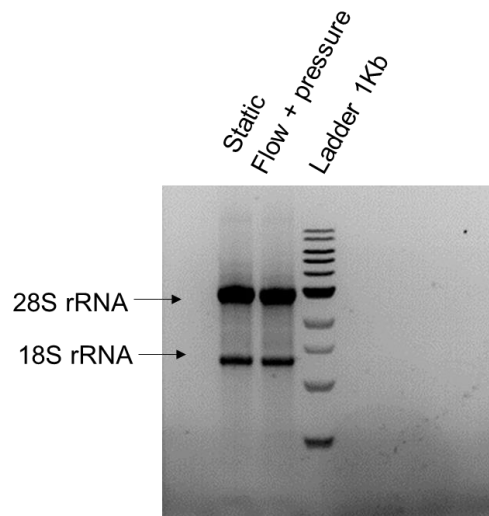


## Appendix 3

### RNA integrity test on 1% agarose gel (2D Vs 3D)

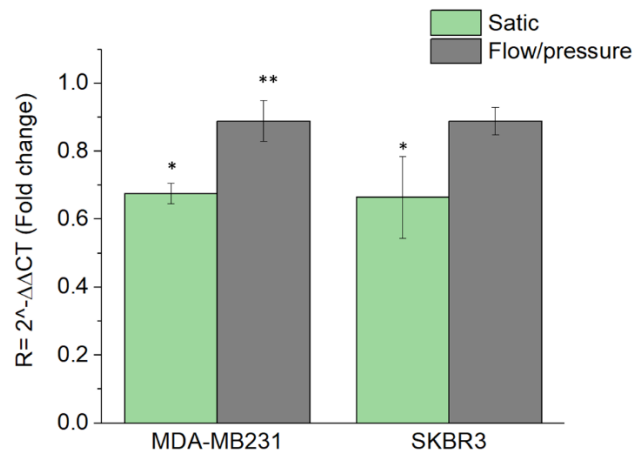


### RNA integrity test on 1% agarose gel (static Vs flow + pressure)



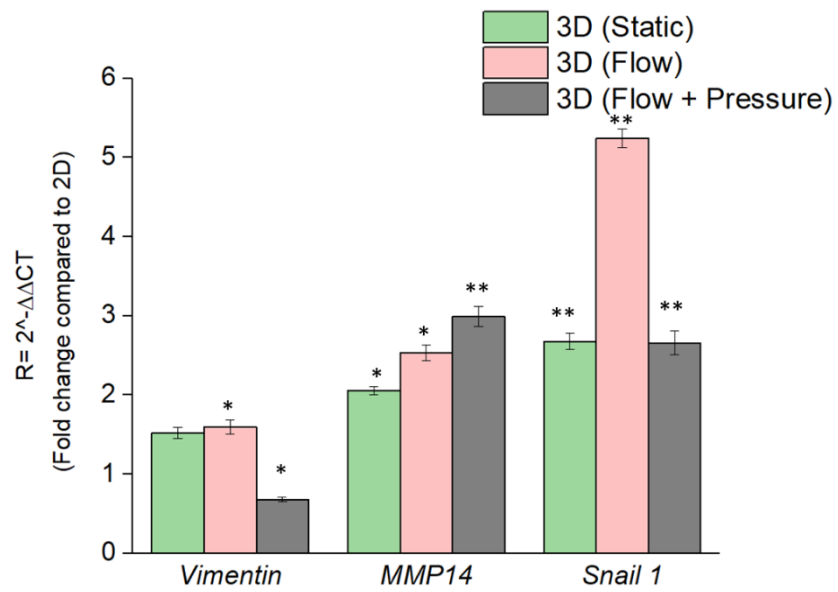
## Appendix 4

### Ki67 mRNA expression in static and flow/pressure conditions compared to 2D culture



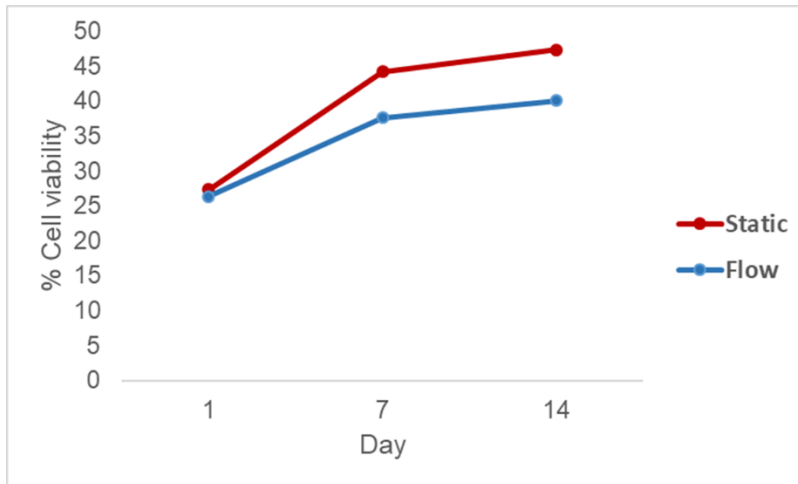
## Appendix 5

### EMT markers mRNA expression in static and flow/pressure conditions compared to 2D culture



## Appendix 6

### Cell viability (static vs flow, 150 $\mu\text{L}/\text{min}$ )



### Cell viability (static vs flow, 550 $\mu\text{L}/\text{min}$ )

